UNIVERSIDAD AUTÓNOMA DE MADRID

DEPARTMENT OF MOLECULAR BIOLOGY

ROLE OF PDS5 PROTEINS IN COHESIN DYNAMICS

Miguel Ruiz Torres

Degree in Biology

Thesis Director: Dr. Ana Losada Valiente

Centro Nacional de Investigaciones Oncológicas (CNIO)

Madrid, 2017

Financiación:

Esta investigación ha sido financiada por los siguientes proyectos del Ministerio de Economía y Competitividad: SAF2010-21517, BFU2013-48481-R, BFU2016-79841-R, CSD2007-00015 INESGEN. Además, Miguel Ruiz Torres ha recibido financiación de una beca del Plan de Formación de Personal Investigador (FPI) con referencia BES-2012-055441 y una beca para la estancia en el extranjero proporcionada por Boehringer Ingelheim Fonds (BIF).

A mis padres, mis hermanos y a Cris

Me gustaría comenzar dando las gracias a Ana Losada. He aprendido muchísimo en estos años en tu laboratorio, no sólo a cómo planear y ejecutar experimentos, si no a cómo interpretarlos, cómo verlos desde una perspectiva crítica y cómo defenderlos. Valoro mucho nuestras discusiones y creo que para mí ha sido fundamental ver cómo has confiado en mi criterio, has tenido en cuenta mis ideas y por supuesto has sabido contradecirme y hacerme reflexionar cuando he estado equivocado. ¡Muchas gracias por todo!

Al final, la tesis es un trabajo global, y he tenido la suerte de tener la ayuda de mucha gente. En primer lugar gracias a María por comenzar el proyecto, con todo el trabajo que conllevó, y por enseñarme todo lo que pudiste durante el tiempo que coincidimos. Gracias a Miry, por hacernos el trabajo más fácil a los demás, por las inmensas curradas en materia de clonajes y por ahorrarme años de trabajo en PCRs. Gracias a Ana Cuadrado por todos los consejos y la ayuda en materia de ChIP, RNA, etc. Gracias enormes a Alek, el hombre detrás de esta maraña de números y overlaps, Hvala! A Magali por sus IPs y por la ayuda recogiendo puntos en estos maravillosos experimentos a las 2 de la mañana que hemos ido haciendo. Y por supuesto gracias a todo el resto de gente con los que he coincidido en Dinámica Cromosómica: Iva, Sam, Carmen, Silvia, Marta y Patri. A nuestros vecinos de Replicación de ADN, en especial a Juan Méndez por los consejos y los reactivos y a Sara por toda la ayuda con las fibras. Pero por supuesto también a Sergio, Marcos, Dani, Karolina, Silvia, Sabe, Silvana, Blanca, Samu, Patri y alguno que me estoy dejando seguro, tanto por la ayuda en el día a día y los consejos en los lab meetings como por el fantástico ambiente de trabajo que hace todo tremendamente más fácil. Además no puedo olvidarme de dar gracias a todo el laboratorio de JM Peters por los tres meses estupendos que pasé allí y al laboratorio de Marcos Malumbres por mis dos años de aprendizaje pre-tesis (y alguna cosa más que me he llevado de ahí).

Si en la tesis es importante la ayuda de un buen grupo de compañeros, también es importante tener cosas fuera que te ayuden a despejar la mente y a tener una vía de escape. Álvaro, Michi, Paty y Jose, sin Maybe Nots esto no hubiera sido lo mismo, muchas gracias por algo tan cojonudo y que he disfrutado tantísimo. Por supuesto también gracias a todos mis demás amigos, tengo suerte de contarlos con las dos manos (y los pies). No voy a convertir esto en una retahíla de nombres, imagino que todos sabéis quienes sois, alcobendenses, blastos, y el resto de gente que ha ido apareciendo por mi vida.

Creo que el lugar dónde te crías y te educas es fundamental para ver en quién te conviertes. Tengo suerte de haber crecido con mis padres y mis hermanos, y les quiero dar las gracias porque son los máximos responsables de que sea una persona responsable y trabajadora (o eso creo), y sobre todo con tantas ganas de saber siempre más cosas, cosa fundamental para un científico. Por supuesto también a todo el resto de mi familia: mis abuelos, mis tíos y mis primos.

Y por supuesto gracias a Cris. Nuestra historia empezó entre el final de una tesis y el principio de otra. Desde chocar la mano todas las mañanas al llegar al laboratorio a recordarme todas las mañanas que no me deje el Tupper han pasado infinidad de cosas, y lo único que me gusta más que recordarlas todas es saber que aún nos falta lo mejor por delante. Has estado ahí durante todos estos años, y eres sin duda el mejor resultado de mi tesis. Gracias Crispi.

Gracias a todos de parte de (elegir lo que convenga):

Miguel, Míguel, Maiki, Mike, Migui, Miki, o Mikaike

Summary

Cohesin is a ring-shaped complex that entraps DNA to mediate sister chromatid cohesion. In recent years, it has also been described as a major organizer of interphase chromatin, being essential for processes that include transcriptional regulation or the organization of replication factories. In order to perform its functions, the association of cohesin to chromatin needs to be tightly regulated. In this work, we have characterized the central role of the cohesin cofactor Pds5 in the regulation of cohesin dynamics and cohesin distribution along the genome, as well as the consequences of its ablation for cell proliferation and gene regulation. Vertebrate cells have two versions of Pds5, Pds5A and Pds5B, whose functional specificity remains unclear. Using Mouse Embryonic Fibroblasts (MEFs) deficient in Pds5A, Pds5B or both, we have demonstrated that Pds5 proteins play a dual role in cohesin dynamics: they allow Smc3 acetylation and Sororin binding during DNA replication to stabilize the fraction of “cohesive” cohesin while, at the same time they cooperate with Wapl to promote cohesin release throughout the cell cycle. The dynamic association of cohesin with chromatin is significantly decreased in cells lacking both Pds5A and Pds5B, leading to aberrant localization of cohesin in axial structures known as *vermicelli.* Cells lacking only Pds5A or Pds5B show mild defects, which suggests an overlapping contribution of both Pds5 proteins to bulk cohesin unloading throughout the genome. We have also found that Pds5 proteins do not dictate cohesin localization at particular genomic locations. However, simultaneous elimination of Pds5A and Pds5B changes genome wide distribution of cohesin in a manner that is different from Wapl depletion. We speculate that this difference might be due to the lack of Smc3 acetylation in Pds5 depleted cells which would restrict cohesin translocation along DNA after loading. The defects in cohesin dynamics and distribution result in transcriptional deregulation. Moreover, cells lacking Pds5 proteins have trouble entering S phase after release from a G0 arrest due to transcriptional alterations and even those that initiate DNA replication display a significant reduction in the replication fork rate, suggesting that cohesin unloading is required to allow replication fork progression. Taken together, our results reveal the importance of Pds5 proteins for cohesin dynamics beyond Wapl-mediated unloading and suggest a clear redundancy of Pds5A and Pds5B for most cohesin functions analysed here.

Resumen

La cohesina es un complejo proteico en forma de anillo capaz de abrazar las cromátidas hermanas para mediar la cohesión. En los últimos años también se ha descrito como un importante organizador de la cromatina en interfase, siendo esencial para procesos como la regulación de la transcripción y la organización de factorías de replicación. Para llevar a cabo estas funciones, la asociación de la cohesina con la cromatina debe estar sujeta a una regulación estricta. En este trabajo hemos caracterizado el papel de las proteínas Pds5 en la regulación de la dinámica de la cohesina y su distribución a lo largo del genoma, así como las consecuencias de su eliminación en la regulación génica y la proliferación celular. En organismos vertebrados hay dos versiones de Pds5, Pds5A y Pds5B, cuya especificidad funcional no está clara aún. Utilizando fibroblastos embrionarios de ratón (MEFs) deficientes en Pds5A, Pds5B o ambas, hemos demostrado que las proteínas Pds5 tienen un papel dual en la dinámica de la cohesina. Por un lado, median la acetilación de Smc3 y la unión de Sororina durante la replicación del ADN para estabilizar la fracción de cohesina “cohesiva”. Por otro, cooperan con Wapl en la disociación de cohesina. La dinámica de asociación y disociación de la cohesina de la cromatina se reduce significativamente en células carentes de Pds5A y Pds5B, lo que favorece la acumulación aberrante de del complejo en estructuras axiales conocidas como *vermicelli*. La eliminación individual de Pds5A o Pds5B tiene un efecto menor, lo que sugiere una contribución redundante de las dos variantes a la disociación de la cohesina. También hemos podido comprobar que la asociación de una u otra proteína Pds5 con la cohesina no es responsable de su localización en sitios concretos del genoma. Sin embargo, la eliminación simultánea de Pds5A y Pds5B cambia la distribución global de la cohesina y lo hace de un modo diferente a la eliminación de Wapl. Esta diferencia podría deberse a la falta de acetilación de Smc3 en ausencia de Pds5, lo que restringiría la capacidad del complejo para desplazarse a lo largo de la fibra de cromatina. Los efectos observados en la dinámica y distribución de la cohesina alteran el trasncriptoma de las células sin Pds5. A su vez, esta alteración provoca defectos en la progresión del ciclo celular, un efecto particularmente notorio cuando se analiza la reincorporación de células quiescente al ciclo celular. Además, las células que sí inician la fase S presentan defectos en la progresión de la horquilla replicativa. Así pues, nuestros resultados ponen de manifiesto la relevancia de las proteínas Pds5 en la dinámica de la cohesina, de manera distinta a Wapl, y sugieren que Pds5A y Pds5B contribuyen de forma redundante a la misma.

Table of contents

Table of contents 1

Abbreviations 5

Introduction 11

1. The cohesin complex 13
2. Dynamic association of cohesin with chromatin throughout the cell cycle 15
    2.1 Cohesin loading and unloading 16
    2.2 Cohesin stabilization or cohesion establishment 18
    2.3 Cohesin dissociation in mitosis 20
3. Cohesin modulates chromatin architecture 20
    3.1 Cohesin distribution and chromatin looping regulate gene expression 20
    3.2 Cohesin in DNA replication initiation and progression 22
4. Contribution of Pds5 proteins to cohesin function 24
    4.1 Two Pds5 proteins in vertebrate cells 24
    4.2 The consequences of Pds5 dysfunction in different organisms 25

Objectives 29

Materials and Methods 33

Results 47

1. Regulation of cohesin dynamics by Pds5 50
    1.1 Pds5 proteins are required for cohesin acetylation and Sororin recruitment 50
    1.2 Pds5 elimination increases chromatin bound cohesin 52
    1.3 An assay to measure cohesin dynamics in Pds5 deficient cells 55
    1.4 Pds5 elimination stabilizes cohesin on chromatin 57
    1.5 Redundant contribution of Pds5A and Pds5B to cohesin dynamics 58
    1.6 Cohesin acetylation does not affect cohesin mobility in G0 59
    1.7 Pds5 deficient cells exhibit *vermicelli* 61

2. Pds5 proteins contribute to determine the distribution of cohesin along the genome 62
2.1 Pds5A and Pds5B localize at the same genomic positions 63
2.2 Distribution of cohesin is restricted in Pds5 DKO cells 66
2.3 Pds5 affects cohesin distribution differently from Wapl 71
2.4 Similar distribution of cohesin in Pds5A KO and Pds5B KO cells 72
3. Transcriptional alterations in Pds5 deficient cells 76
3.1 Pds5 elimination affects transcriptional regulation 76
3.2 Distinct outcomes of Pds5A and Pds5B elimination in transcriptional regulation 78
4. Pds5 elimination affects cell cycle progression 81
4.1 Pds5 elimination blocks cells in G0/G1 81
4.2 Impaired preRC assembly in Pds5 deficient cells 84
4.3 Similar proliferation defects in Pds5A KO and Pds5B KO cells 85
4.4 Fork progression is affected in Pds5 DKO 87

Discussion 93

1. Dual role of Pds5 in the regulation of cohesin dynamics 95
2. Cohesin dynamics determines cohesin distribution 99
3. Gene expression changes upon perturbation of cohesin dynamics and their effect on cell cycle progression 102
4. Defective cohesin dynamics slows down DNA replication 103

Conclusions 109

Bibliography 115

Abbreviations

4-OHT: 4-hydroxy tamoxifen

BrdU: 5-Bromo-2-Deoxyuridine

ChIP: Chromatin Immunoprecipitation

ChIP-seq: Chromatin immunoprecipitation followed by deep sequencing

CldU: 5-Chloro-2'-deoxyuridine

CoAT: Cohesin Acetyltranferase

CoDACs: Cohesin Deacetylases

DAPI: 4',6-diamidino-2-phenylindole

DPC: Days post coitum

DDK: Dbf4-Dependent Kinase

DEG: Differentially Expressed Gene

EdU: ethynyl-29-deoxyuridine

FACS: Fluorescence activated cell sorting

FBS: Foetal bovine serum

FRAP: Fluorescence Recovery After Photobleaching

FPKM: fragments per kilobase million

Gas1: Growth arrest specific 1

gRNA: guide RNA

GSEA: Gene Set Enrichment Analysis

HEAT: Homologous Huntingtin, Elongation factor 3, A subunit and TOR

HID: Helical Insert Domain

HR: Homologous Recombination

IdU: 5-Iodo-2'-deoxyuridine

IF: Immunofluorescence

KO: Knockout

MCM: Minichromosome maintenance

MEFs: Mouse Embryonic Fibroblasts

n.s. non significant

ORC: Origin Recognition Complex

PCH: Pericentric Heterochromatin

PFA: Paraformaldehyde

PI: Propidium Iodide

PP2A: Protein Phosphatase 2A

pre-RC: pre-Replicative Complex

RT-qPCR: Retrotranscription and quantitative PCR

SA: Stromal Antigen

SAC: Spindle Assembly Checkpoint

siRNA: small interfering RNA

Sgo1: Shugoshin 1

SMC: Structural Mainenance of Chromosomes

TAD: Topologically Associating Domain

TIRF: Total Internal Fluorescene

TSS. Transcription starting site

WT: Wild type

Introduction

1. The cohesin complex

Cohesin is a ring shaped complex that belongs to the Structural Maintenance of Chromosomes (SMC) family (Anderson et al., 2002; Nasmyth and Haering, 2005). SMC proteins are around 150 kDa long polypeptides that contain two coiled-coil stretches separated by a flexible globular hinge domain. When folded at this domain, the amino and carboxyl termini of the protein are brought in proximity to create an ATPase head domain (Losada and Hirano, 2005) (Figure I1). There are three different SMC complexes in eukaryotic cells, each one containing a heterodimer of SMC proteins. Cohesin contains Smc1 and Smc3 and mediates sister chromatid cohesion and genome organization, as discussed below. Smc2 and Smc4 are part of condensin, which is important for chromosome condensation. The third complex is Smc5-Smc6 and is involved in processes related to DNA replication and repair (Jeppsson et al., 2014). Bacteria and archaea also possess SMC complexes, in this case forming homodimers, that are essential for chromosome duplication and segregation (Gruber, 2017).

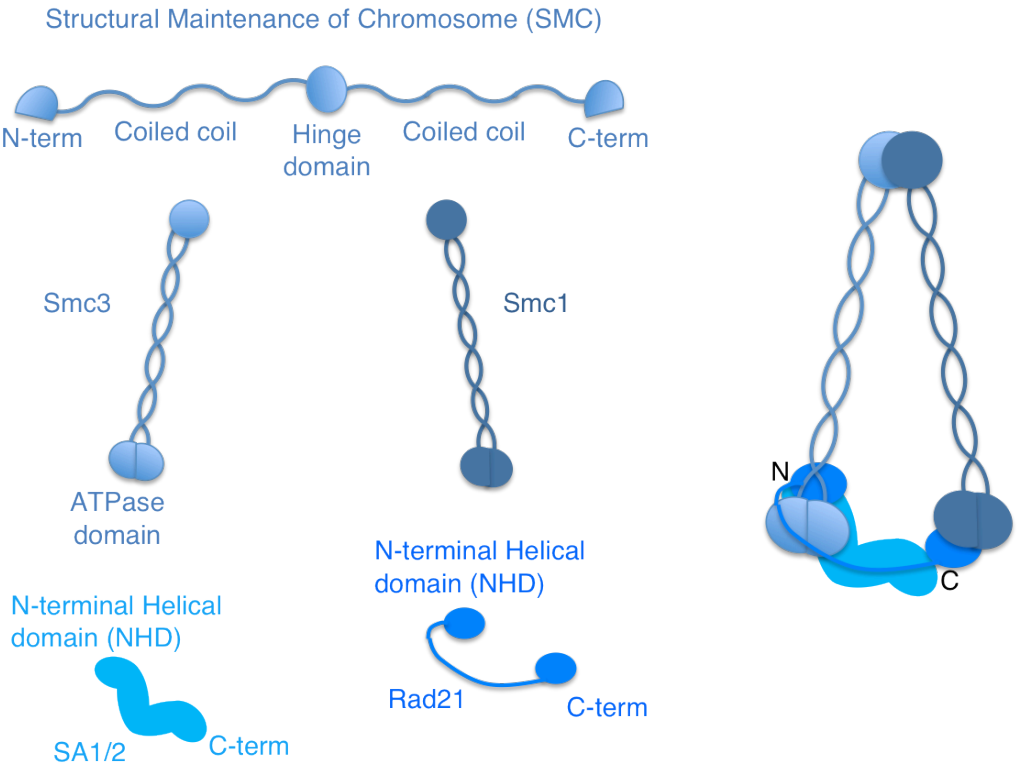

Figure I1. Composition and architecture of cohesin.

Folding of the SMC proteins at the hinge domain connects the C and N terminal regions and creates the ATPase head domain. To form cohesin, the hinge domains of Smc1 and Smc3 associate directly, while the ATPase domains are connected by Rad21. The SA subunit (SA1/2) associates to Rad21 and Smc3.

The Smc1 and Smc3 subunits of cohesin display a stable interaction through their hinge domains (Figure I1). On the other side, the ATPase domains interact with the alpha kleisin Rad21, which acts as a bridge to close the ring. The fourth member of the complex is the Stromal Antigen (SA) protein, which in somatic vertebrate cells can be either SA1 or SA2 (Losada et al., 2000). SA proteins are composed of many homologous huntingtin, elongation factor 3, A subunit and TOR (HEAT) repeats and differ in their C and N terminal regions (Hara et al., 2014). SA1 has been identified as the specific mediator of telomeric cohesion while SA2 mediates centromeric cohesion (Canudas and Smith, 2009; Remeseiro et al., 2012a)

Cohesin was first described as the mediator of sister chromatid cohesion after DNA replication (Guacci et al., 1997; Losada et al., 1998; Michaelis et al., 1997). This process is essential for faithful chromosome segregation in mitosis and meiosis, but also for DNA repair by Homologous Recombination (Nasmyth and Haering, 2009). More recently, cohesin has been shown to perform additional functions related to chromatin architecture that include gene regulation by distal cis-regulatory elements, organization of replication factories and locus rearrangement by recombination (Guillou et al., 2010; Hadjur et al., 2009; Kagey et al., 2010; Seitan et al., 2011).

A number of in vivo and in vitro evidences support a model in which cohesin entraps the chromatin fiber within its ring-shaped structure (Gruber et al., 2003; Haering et al., 2008). In order to perform cohesion, cohesin would hold together two DNA segments in *trans*, the sister chromatids (Figure I2A). For genome organization-related functions, cohesin would entrap two DNA segments in *cis*, i.e. that belong to the same chromatid, likely at the base of a chromatin loop. In both cases, cohesin needs to entrap two different DNA strands at the same time, and different models have been proposed to account for this (Figure I2B). The “two gate” model suggests that one of the strands is held between the Smc coiled coils while the other is located in a pocket created by the flexible central domain of Rad21 and the heads domain of Smc1 and Smc3, which would be interacting. The second model proposes that both strands are held together inside the large pore formed by the coiled-coils when cohesin is a ring-like conformation, as observed by electron microscopy of DNA-free complexes (Anderson et al., 2002). A third possibility is that two distinct cohesin complexes entrapping each a DNA segment are brought together by concatenation or by mediator proteins such as the SA subunit (Barrington et al., 2017; Nasmyth, 2011; Zhang et al., 2008b)

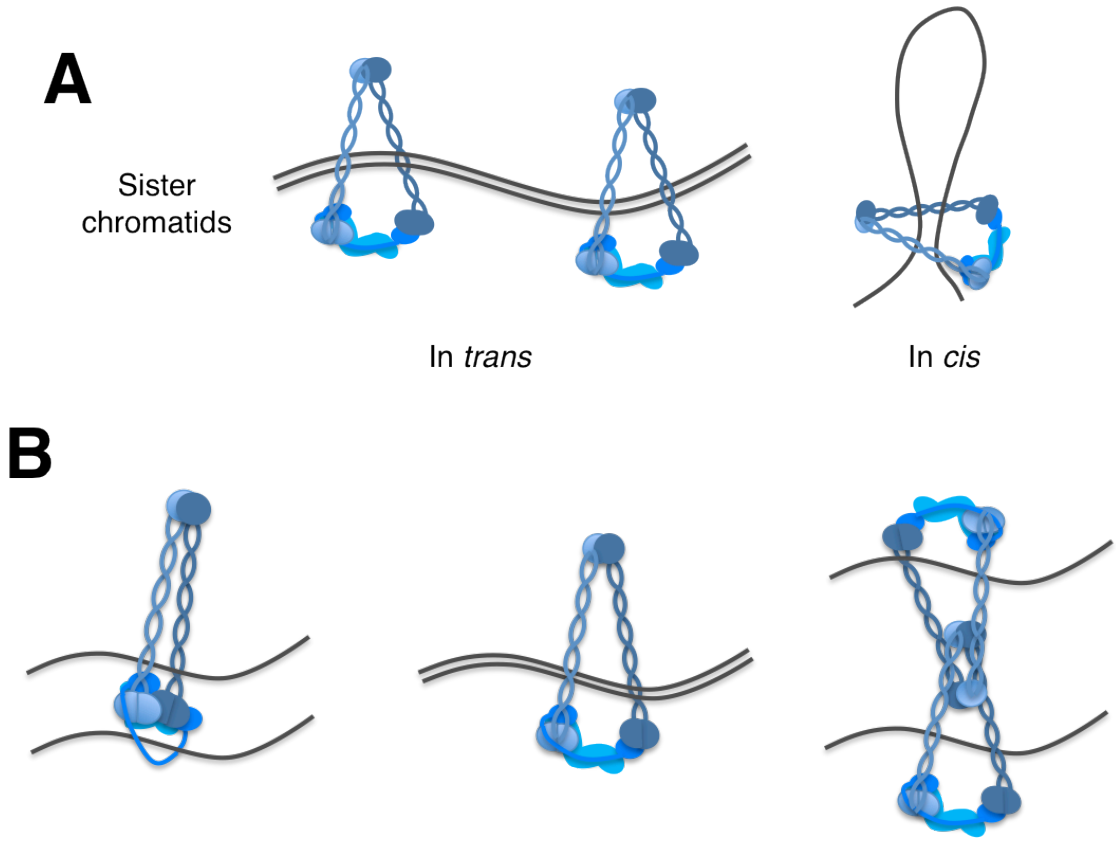

Figure I2. Current model on cohesin-mediated entrapment of chromatin fibers.

A. Cohesin can perform cohesion by embracing two sister chromatids *in trans* and also participate in chromatin organization by entrapping two distal DNA fragments in *cis*. **B.** The current models of cohesin association to chromatin involve the "two gate" model (left), the classical model (middle) and the "handcuff" model (right).

2. Dynamic association of cohesin with chromatin throughout the cell cycle

In cycling cells, several processes determine the association of cohesin with chromatin: cohesin loading, cohesin unloading, cohesin stabilization (or cohesion establishment) and cohesin dissociation (Figure I3). Fluorescence Recovery After Photobleaching (FRAP) studies have shown that a fraction of cohesin remains soluble in the nucleus while another is dynamically associated to chromatin throughout the cell cycle. In addition, from S phase and during G2, a third population of cohesin can be observed whose association with chromatin is very stable and which likely corresponds to cohesive cohesin (Gerlich et al., 2006). The correct balance between these cohesin populations is essential for cohesin function. Three cohesin associated factors known as Wapl, Pds5 and Sororin contribute to regulate the association of cohesin with

chromatin.

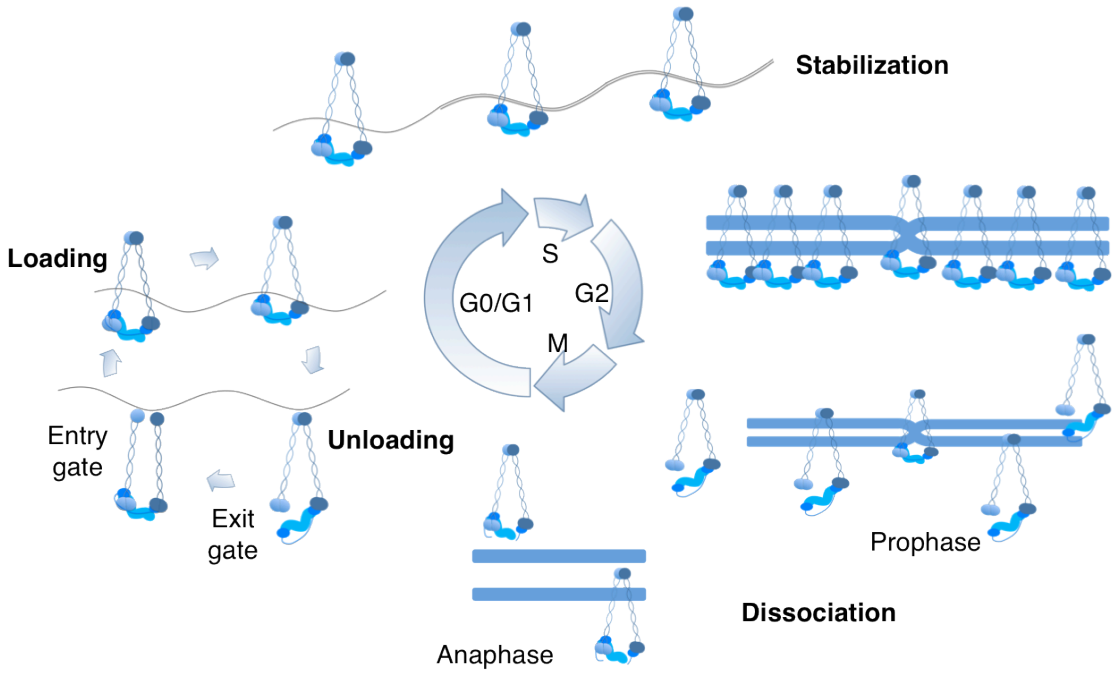

Figure I3. Cohesin dynamics throughout the cell cycle.

Cohesin is loaded at early G1 through the opening of an entry gate. Cohesin association to chromatin is dynamic and the complex is actively released through the exit gate and reloaded at the same site or elsewhere. A fraction of cohesin is stabilized on chromatin after DNA replication and during G2. In prophase, most cohesin is released from chromosome arms, and a small fraction remains at centromeres protected by Sgo1 (not depicted). In anaphase, this centromeric cohesin is cleaved by Separase and sister chromatids can be pulled apart.

2.1. Cohesin loading and unloading

In vertebrate cells, cohesin is loaded on chromatin in early G1 by a heterodimer formed by NIPBL and Mau2 (also known as Scc2 and Scc4, respectively) in a process that requires ATP hydrolysis (Arumugam et al., 2006; Gillespie and Hirano, 2004; Watrin et al., 2006). In vitro experiments suggest that the loader extends the time that cohesin remains bound to DNA before it can convert to a topologically bound conformation (Stigler et al., 2016). NIPBL is mostly composed of HEAT repeats except for a short N terminal region which binds Mau2 (Kikuchi et al., 2016). In vitro, cohesin can associate with DNA on its own, although inefficiently (Murayama and Uhlmann, 2014). Cohesin loading occurs through the opening of an *entry gate* between the hinge domains of Smc1 and Smc3 (Buheitel and Stemmann, 2013; Eichinger et al., 2013; Gruber et al.,

2006). In Xenopus egg extracts, cohesin loading requires the presence on chromatin of the pre-replicative complex (pre-RC) to recruit the Scc2-Scc4 complex through the Cdc7-Drf1 protein kinase (DDK) (Gillespie and Hirano, 2004; Takahashi et al., 2008). In budding yeast, cohesin is loaded independently of the pre-RC along chromosome arms (Uhlmann and Nasmyth, 1998) but the massive loading of cohesin at centromeres also requires Scc2-Scc4 recruitment to kinetochores by DDK (Natsume et al., 2013). In human cells, however, there is no evidence for this requirement (Guillou et al., 2010).

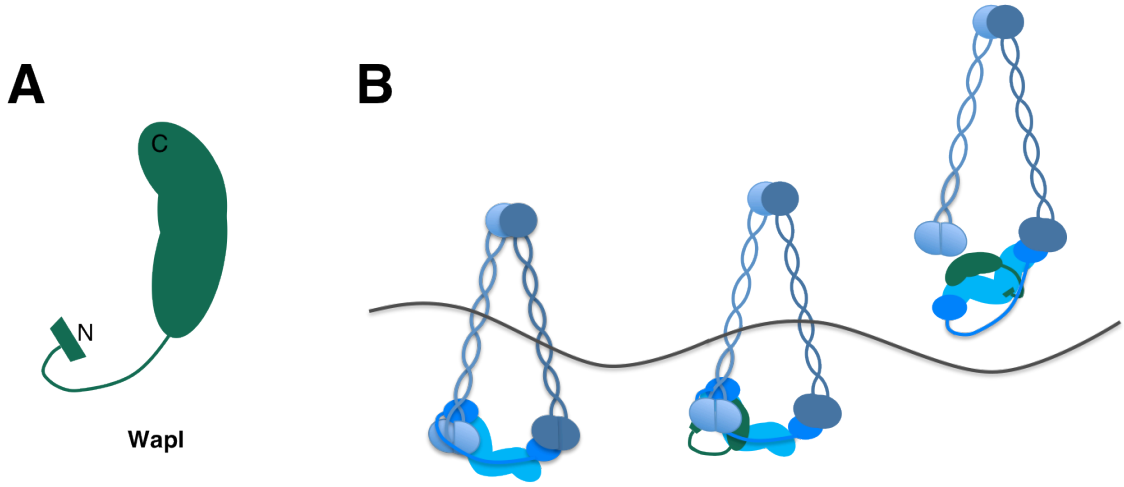

Figure I4. Wapl mediates cohesin release.

A. The structure of Wapl shows a C-terminal region that associates with the core ring and a flexible N-term that binds to the Rad21-SA heterodimer. **B.** Wapl associates to chromatin bound cohesin and promotes the opening of the ring at the Rad21-Smc3 interphase, known as the exit gate.

The association of cohesin to chromatin is unstable. After loading, a factor known as Wapl binds cohesin to actively remove it from chromatin (Gandhi et al., 2006; Kueng et al., 2006). Like the SA cohesin subunit and NIPBL, Wapl is HEAT-repeat containing protein. Eight HEAT repeats are present in its C-terminal region, and are likely to associate with the Smc1-Smc3 heterodimer or other cohesin associated factors. The flexible N-terminal domain of Wapl is able to bind the Rad21-SA heterodimer to mediate cohesin unloading, and has also been described to be important for its interaction with Pds5 (Figure I4A) (Beckouët et al., 2016; Elbatsh et al., 2016; Ouyang et al., 2013a, 2016). Cohesin unloading occurs through an *exit gate* that is different from the *entry gate* mentioned above and that is formed by the interface of Rad21 and the Smc3 coiled coil region next to the Smc3 head (Figure I4B) (Gligoris et

al., 2014). A recent *in vitro* study has proposed that Wapl may also be involved in cohesin loading using this gate (Murayama and Uhlmann, 2015) .

Wapl downregulation in human and mouse interphase cells increases dramatically the residence time of cohesin on chromatin (Kueng et al., 2006; Tedeschi et al., 2013). Elimination of Wapl in G0 arrested cells provokes the accumulation of cohesin in axial structures that resemble condensed chromatin, known as *vermicelli* (worm in Italian). It has been proposed that *vermicelli* could be the result of enhanced cohesin clustering at the base of chromatin loops (Tedeschi et al., 2013). Budding yeast cells lacking Wapl also display increased chromosome condensation both in interphase and mitosis (Lopez-Serra et al., 2013). In cycling cells, Wapl elimination alters transcription, cell cycle progression and chromosome segregation (Gandhi et al., 2006; Haarhuis et al., 2013; Kueng et al., 2006; Tedeschi et al., 2013) All these results point out the importance of Wapl activity during the whole cell cycle.

2.2 Cohesin stabilization or cohesion establishment

Once DNA is replicated, cohesin needs to become cohesive, that is, to hold the sister chromatids together in a stable fashion (Uhlmann and Nasmyth, 1998). The only molecular event during DNA replication that is known to be essential for cohesion establishment in all organisms is cohesin acetylation. In budding yeast, the cohesin acetyltranferase (CoAT) Eco1/Ctf7 acetylates two contiguous lysines (K112 and K113) located in the head domain of Smc3 (Rolef Ben-Shahar et al., 2008; Unal et al., 2008; Zhang et al., 2008a). The substitution of these residues by arginines or mutations affecting Eco1's acetyl-transferase activity generate important cohesion defects and lethality. This phenotype is rescued by the elimination of Wapl (Rowland et al., 2009; Sutani et al., 2009). These results suggest that the function of Eco1 is to counteract Wapl releasing activity. It is possible that Smc3 acetylation provokes a conformational change that reduces affinity of Wapl for the cohesin ring.

In vertebrates, there are two CoATs, Esco1 and Esco2, that can acetylate two lysines (K105 and K108 in humans) in the head domain of Smc3 (Figure I5). Downregulation of one or the other result in partial defects in cohesion (Hou and Zou, 2005). Esco1 acetylates cohesin throughout the cell cycle while Esco2 accumulates in the cell in S phase (Song et al., 2012). Budding yeast Eco1 interacts with PCNA and travels with the replication fork, thereby ensuring that acetylation occurs as the two

sister chromatids emerge from the replisome (Lengronne et al., 2006; Tanaka et al., 2000). In Xenopus egg extracts, where most cohesin acetylation is carried out by Esco2 (xEco2), the CoAT binds to chromatin in a pre-RC dependent manner, same as the cohesin loader, although cohesin acetylation is independent of DNA synthesis (Higashi et al., 2012). Recent results suggest that in human cells Esco1 but not Esco2 is recruited to cohesin by Pds5 (Minamino et al., 2015).

Smc3 acetylation is accompanied by the binding of Sororin in postreplicative cells. In fact, both events are required for cohesion establishment in human cells. Sororin is a 35 kDa protein that was first identified as a substrate of APC/C^{Cdh1} and shown to be essential for cohesion in mammalian cells (Rankin et al., 2005). Sororin recruitment to chromatin-bound cohesin requires Smc3 acetylation (Lafont et al., 2010) and it has been proposed to act by displacing Wapl from its binding site at the Rad21-Smc3 interphase thereby preventing its cohesin unloading activity (Figure I5) (Nishiyama et al., 2010). Sororin depletion reduces the levels of stable fraction of cohesin normally present in G2 cells (Schmitz et al., 2007). Co-depletion of Wapl and Sororin results in the same phenotype as Wapl single elimination, meaning that Sororin is only required if Wapl is present. Besides, it is important to consider that not all cohesin present in the chromatin in G2 cells is stabilized by Sororin, meaning that there is still Wapl-mediated cohesin release in post-replicative cells (Gerlich et al., 2006).

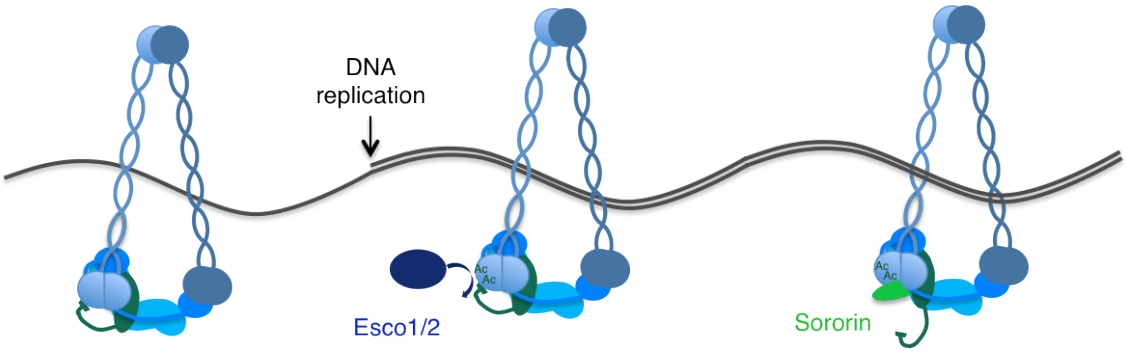

Figure I5. Establishment of sister chromatid cohesion.

Once DNA is replicated, Esco1/2 acetylates Smc3 in two residues of its ATPase head domain. Sororin is recruited and displaces Wapl from its docking site at the Rad21-Smc3 interphase.

2.3 Cohesin dissociation in mitosis

When the cells enter mitosis, cohesin is released from chromatin in two steps in order to ensure proper chromosome segregation (Losada et al., 2000; Waizenegger et al., 2000). The first step occurs in prophase and is driven by phosphorylation. Phosphorylation of SA subunits by Plk1 and release of Sororin upon phosphorylation by CDK1 and Aurora B restore Wapl activity leading to release of more than 90% of cohesin present at chromosome arms (Dreier et al., 2011; Giménez-Abián et al., 2004; Hauf et al., 2005; Losada et al., 2002; Nishiyama et al., 2013). Cohesin dissociation facilitates sister chromatid resolution by metaphase (Haarhuis et al., 2013).

A small fraction of cohesin, enriched around centromeres, resists the prophase dissociation pathway and is essential to hold the sister chromatids together until all the chromosomes establish proper attachments to opposite spindle poles (Toyoda and Yanagida 2006; Liu et al. 2013a). Centromeric cohesin is protected by two mechanisms. One involves Shugoshin (Sgo1) and its binding partner Protein Phosphatase 2A (PP2A) that counteract cohesin phosphorylation (Salic et al., 2004; McGuinness et al., 2005) . Sgo1 also competes out the binding of Wapl to SA-Rad21 (Hara et al., 2014) while PP2A counteracts Sororin dissociation (Liu et al., 2013). The second mechanism involves the inhibitory binding of Securin to Separase, a protease that cleaves Rad21 (Hauf et al., 2001; Uhlmann et al., 1999). When all the chromosomes are properly aligned at the metaphase plate, the Spindle Assembly Checkpoint (SAC) is satisfied and Securin is ubiquitinated by APC/C^{Cdc20} and targeted for proteasomal degradation (Musacchio and Salmon, 2007). Thus, Separase is liberated and able to cleave Rad21, triggering dissociation of the remaining cohesin and allowing the separation of sister chromatids. In yeast, all chromatin bound cohesin is released from chromatin in anaphase by this cleavage pathway (Uhlmann et al. 2000). In order to be reused in the next cycle, all cohesin molecules must be deacetylated by cohesin deacetylases (CoDACs) Hos1 in yeast (Beckouët et al., 2010; Borges et al., 2013) and HDAC8 in human cells (Deardorff et al., 2012).

3. Cohesin modulates chromatin architecture

3.1 Cohesin distribution and chromatin looping regulate gene expression

Cohesin localization along the genome of different model organisms has been mapped using Chromatin Immunoprecipitation (ChIP). In this technique, cells are crosslinked to preserve protein-DNA interactions, and the chromatin is extracted and sonicated to

obtain small fragments of 250-500 base pairs. Incubation of this crosslinked chromatin with specific antibodies isolates DNA fragments bound to the protein of interest that are then identified either by hybridization to microarrays (Chip-on-chip) and more recently, massive sequencing (ChIP-seq). In budding yeast, cohesin accumulates in a 50-kb region around centromeres and at sites of convergent transcription (Glynn et al., 2004; Lengronne et al., 2004). Some experimental evidences suggest that the cohesin ring, after embracing the chromatin fiber, can slide away from the loading site pushed by the transcriptional machinery (Hu et al., 2011; Ocampo-Hafalla et al., 2016). The ability of cohesin to translocate along DNA has been recently demonstrated using Total Internal Reflection Fluorescence (TIRF) microscopyy to visualize the movement of purified cohesin complexes along naked DNA (Davidson et al., 2016; Kanke et al., 2016; Stigler et al., 2016). Thus, it is likely that the dynamic behaviour of cohesin has two components: loading-unloading from DNA and translocation along DNA.

While cohesin and its loader do not colocalize in yeast, they are both found at sites of active transcription in Drosophila (Misulovin et al. 2008). In human and mouse cells, cohesin occupies positions that are also occupied by the architectural protein CTCF (Parelho et al., 2008; Remeseiro et al., 2012b; Rubio et al., 2008; Wendt et al., 2008). The colocalization with Nipbl is also very reduced in these organisms (Busslinger et al., 2017; Kagey et al., 2010; Zuin et al., 2014). Importantly, the presence of cohesin at CTCF binding sites requires that CTCF is also present. When CTCF is depleted, cohesin is still bound to chromatin, but its distribution pattern changes (Busslinger et al., 2017; Wendt et al., 2008). A fraction of cohesin does not colocalize with CTCF but with other transcriptional regulators such as the estrogen receptor-alpha (ER) in breast cells or CEBPA in liver cells (Schmidt et al., 2010).

Chromosome conformation capture (3C) studies suggest that cohesin, together with CTCF or other chromatin bound proteins like transcription factors or Mediator facilitate chromatin looping (Figure I6). These loops regulate gene expression in different ways, e.g. promoting or preventing the interaction between promoters and enhancers, allowing coordinated expression within a gene cluster or generating boundaries (Cuadrado et al., 2015; Hadjur et al., 2009; Kagey et al., 2010; Stedman et al., 2008). Indeed, chromosomes appear to be partitioned into topologically associating domains (TADs) in which interactions between DNA segments within the domain are more frequent than interactions with regions outside the domain (Dixon et al., 2012; Nora et al., 2012; Rao et al., 2014). TAD borders are usually demarcated by CTCF and cohesin and genome editing experiments have shown that eliminating a critical CTCF

binding site can strongly disturb gene regulation by abolishing physical insulation between two separate TADs (Lupiáñez et al., 2015). Mathematical modeling using polymer simulation to try to recreate HiC data suggests that TAD formation is the result of loop extrusion by cohesin until it encounters CTCF proteins bound to sites of inverted orientation (Fudenberg et al., 2016; Sanborn et al., 2015).

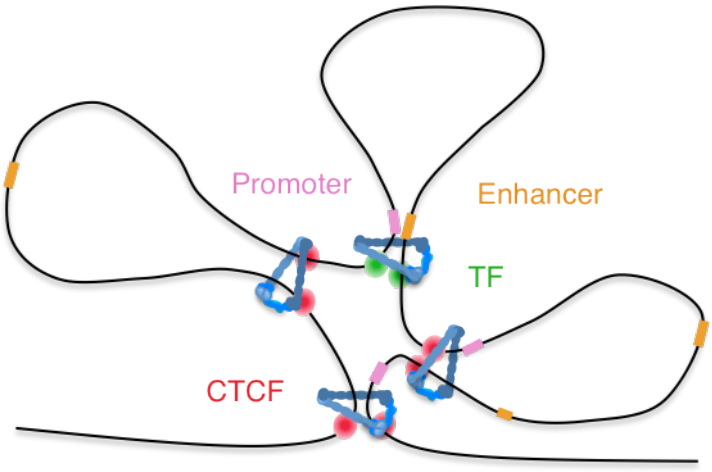

Figure I6. Cohesin mediates DNA looping

Cohesin, together with CTCF (pink ovals) and other regulatory proteins and transcription factors (green ovals), create chromatin loops and regulate gene expression by facilitating enhancer-promoter interactions.

Little is known about the role of cohesin dynamics in the regulation of cohesin distribution throughout the genome. If the presence of cohesin is important for the formation of loops and compartmentalization of the genome in TADs, and to allow proper enhancer-promoter communication, it is likely that the control of cohesin association to chromatin can affect transcriptional regulation. Consistent with this possibility, elimination of Wapl in mouse cells causes major changes in cohesin positioning, and alters gene expression (Haarhuis et al., 2017; Tedeschi et al., 2013). Similarly, downregulation of Esco1 or HDAC8 also alter the transcriptome of human cells (Deardorff et al., 2012; Rahman et al., 2015).

3.2 Cohesin in DNA replication initiation and progression

Some reports in recent years have pointed out the importance of cohesin for DNA replication. Cohesin interacts with components of the pre-Replication Complex and

participates in the spatial organization of DNA replication factories in human cells by organizing them in chromatin loops (Guillou et al., 2010). Downregulation of cohesin has no major impact on fork progression according to this report, but decreases the efficiency of origin firing (Figure I7). Replication origin activation is also related to transcription (Cadoret et al., 2008). Indeed, replication origins have been identified at CpG islands and other gene regulatory elements with open chromatin structure (Cayrou et al., 2015; MacAlpine et al., 2010). A close correlation between replication timing and genome architecture has also been reported (Pope et al., 2014). This suggests that proper regulation of cohesin is important to ensure changes in chromatin structure and initiation of DNA replication.

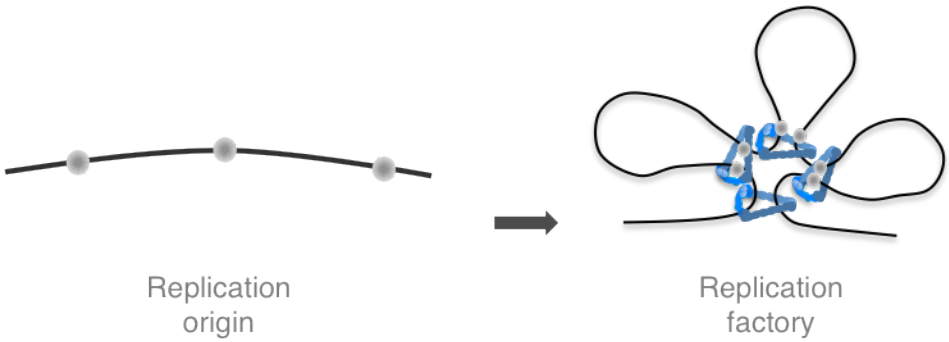

Figure I7. DNA looping by cohesin at replication factories.

Chromatin loops demarcated by cohesin correspond to replicons. Replication origins at the base of the loops (grey circles) are bound by pre-RC component, which associate with cohesin. Clustering of replication origins allows more efficient origin activation.

Once origins are fired and DNA replication is initiated, the replication fork needs to advance through chromatin opening the DNA helix. Some evidences suggest that the presence of cohesin may affect the advance of the replication fork. In human cells, expression of a non-acetylable cohesin reduces fork rate and so does downregulation of either Esco1 or Esco2 or the RFC^{CTF18} clamp loader. This phenotype is rescued if Wapl, and to a lesser extend Pds5A, is also downregulated. However, depletion of Wapl or Pds5A in otherwise normal cells does not alter replication speed (Terret et al., 2009). The authors of this study propose that acetylation switches cohesin from a configuration that obstructs the fork, generated by the tight association of Pds5A-Wapl, to one that permits its advancement. In this scenario, the anti-establishment activity of Pds5-Wapl could be the result of inefficient entrapment of the sister chromatids upon

fork passage. Contrary to these results, elimination of CTF18 or Wapl in budding yeast does not reduce but rather increase replication speed (Lopez-Serra et al., 2013).

Cohesin is also important when replication forks stall, probably to prevent their collapse and to promote its restart by homologous recombination. The genome contains regions that are difficult to replicate and prone to fork stalling, like telomeres, (Gilson and Géli, 2007; Sfeir et al., 2009). Previous work in our group demonstrated that cohesin, in particular cohesin-SA1, is required to allow proper telomere replication (Remeseiro et al., 2012a). In yeast, when DNA synthesis is blocked, cohesin accumulation at replication sites is also critical for the recovery of stalled forks (Tittel-Elmer et al., 2012). Similar experiments in human cells indicate that cohesin associates with BRCA2, a known protector of stalled forks, possibly through Pds5 (Brough et al., 2012; Schlacher et al., 2011).

4. Contribution of Pds5 proteins to cohesin function

4.1 Two Pds5 proteins in vertebrate cells

Pds5 was identified in genetic screen for cohesion factors in yeast (Hartman et al., 2000; Panizza et al., 2000) and found to be homologous to proteins involved in chromosome organization and segregation in fungi (Denison et al., 1993; Holt and May, 1996). Pds5 is evolutionarily conserved but, while there is only one Pds5 protein in yeast, worm and flies, there are two Pds5 proteins in vertebrates, Pds5A and Pds5B (Losada et al., 2005; Sumara et al., 2000). Pds5 proteins are ~1400 amino-acid long polypeptides that show up to 72% sequence homology and differ most in their C-terminal 300 amino acids (Figure I8A). The homology region of Pds5 proteins is composed by a series of 20 HEAT repeats similar to those observed in SA1/2 and Wapl and a helical insert domain (HID), forming a plier-level shaped structure (Ouyang et al., 2016). The C-terminal part of Pds5B contains two AT-hook domains while Pds5A only contains one. Pds5 proteins associate with cohesin through the interaction of its curved domain with the Rad21-Smc3 interphase. The interaction between Pds5 and either Wapl or Sororin occurs at the N-terminal part (Figure I8B) (Ouyang et al., 2016)

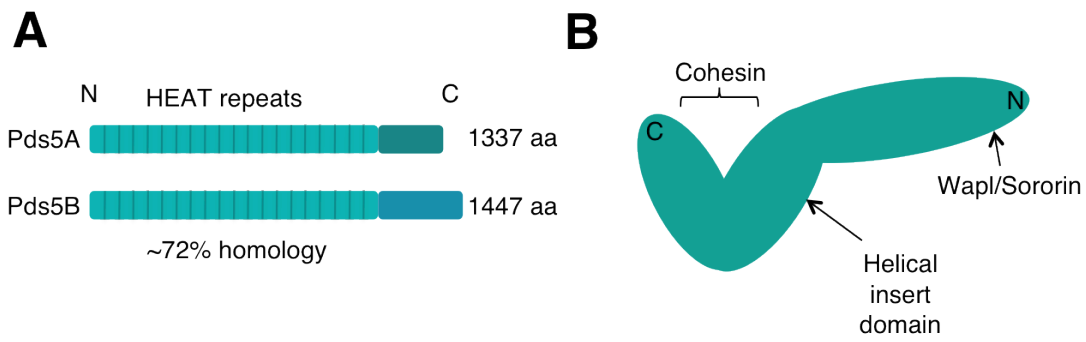

Figure 8. Two Pds5 proteins coexist in vertebrate cells, Pds5A and Pds5B.

A. Schematic representation of the two Pds5 proteins. Both present a series of 20 HEAT repeats in their high homology region and differ in the C-terminal region, which is longer in Pds5B. **B.** 3D structure of the homology region of Pds5. At the N-terminal region there is an interaction site for either Wapl or Sororin. The Helical Insert Domain (HID) is important for the curvature of the protein, which creates an interaction surface for cohesin by bringing to proximity the central domain with the C-terminal region.

4.2 The consequences of Pds5 dysfunction in different organisms

Elimination of BimD6/Spo76, the Pds5 ortholog in *Aspergillus* and *Sordaria* results in cohesion and condensation defects, both in mitosis and meiosis (van Heemst et al., 1999, 2001). In *S. cerevisiae,* Pds5 is an essential gene. It is necessary to establish and maintain sister chromatid cohesion (Hartman et al., 2000; Panizza et al., 2000), since it is required to promote and protect cohesin acetylation (Chan et al., 2012). In fission yeast, Pds5 is also required for cohesin acetylation (Vaur et al., 2012) but its elimination is not lethal unless cells are arrested in G2/M, (Wang et al., 2002). Drosophila Pds5 function is required in early embryonic development and its mutation causes precocious sister chromatid separation and aneuploidy (Dorsett et al., 2005). In *C. elegans* cohesion defects in Pds5 mutants are more important in meiosis than in mitosis (Wang et al., 2003). In HeLa cells, individual downregulation of either Pds5 protein using siRNA produces moderate and somehow different cohesion defects, with Pds5B elimination causing most prominent defects in centromeric cohesion (Losada et al., 2005).

As mentioned in previous sections, Pds5 proteins were also found to be important for facilitating the binding of Wapl and Sororin to cohesin (Nishiyama et al., 2010). Thus, in addition to a major role in cohesion establishment, Pds5 proteins could also facilitate Wapl releasing activity. The seemingly opposing functions of Pds5 in

cohesion were first pinpointed by a study in fission yeast reporting that Pds5 hindered cohesion establishment until counteracted by fission yeast CoAT Eso1p, yet stabilized cohesion once it was established (Tanaka et al., 2001). Similarly, although Pds5 was shown to be required for establishment and maintenance of cohesion in budding yeast, the lethality of yeast *esco1* mutants could be rescued by mutations in either Wapl or Pds5 (Rowland et al., 2009; Sutani et al., 2009). Chromosomes assembled in Xenopus egg extracts displayed subtle centromeric cohesion defects but also increased presence of cohesin on mitotic chromatin, suggesting a defect in cohesion as well as in the prophase dissociation pathway (Losada et al., 2005; Shintomi and Hirano, 2009). In Drosophila salivary glands, Wapl and Pds5 mutations were shown to affect cohesin dynamics in different ways depending on their dosage (Gause et al., 2010).

In order to better understand the contribution of Pds5 proteins to cohesin function, our group generated murine knock out alleles for Pds5A and Pds5B. (Carretero et al., 2013). Embryos homozygous for either one died before birth but Mouse Embryonic Fibroblasts (MEFs) could be extracted at 12.5 dpc and grown in culture. Characterization of these MEFs showed that in the absence of either protein, the amount of acetylated cohesin on chromatin is reduced, but not so the amount of Sororin. We suspect that Sororin is present in limiting amounts so that only a fraction of acetylated cohesin is actually bound to Sororin to make cohesive cohesin at the time of DNA replication. The remaining amounts of cohesive cohesin in Pds5A or Pds5B deficient MEFs appeared to be sufficient to maintain cohesion at telomeres and along chromosome arms. Strikingly, however, we observed that centromeric cohesion was particularly affected in the absence of Pds5B. In Pds5B deficient MEFs, Sororin accumulation at pericentric heterochromatin was defective in the absence of Pds5B. Acetylation of Pericentric Heterochromatin (PCH) depends on Esco2 (Whelan et al., 2012) and we also observed decreased Esco2 staining at PCH. We therefore proposed that acetylation of cohesin and Sororin binding, i.e. cohesion establishment, was impaired around centromeres in Pds5B deficient MEFs, leading to led to chromosome segregation defects and aneuploidy.

Having addressed the importance of Pds5 proteins for chromosome segregation, our next goal was to characterize the contribution of Pds5 proteins to cohesin dynamics and cohesin distribution, as well as the consequences of their ablation in gene regulation and cell cycle progression. Moreover, we asked whether we could identify some specificity for Pds5A and Pds5B in these set of cohesin functions.

Objectives

Objectives

1. To address the relevance of Pds5 proteins in cohesin dynamics and the specific contributions of Pds5A and Pds5B.

2. To assess the contribution of Pds5 proteins to cohesin distribution along the genome.

3. To evaluate the consequences of Pds5 ablation in gene regulation and cell cycle progression.

Objetivos

1. Estudiar el papel de las proteínas Pds5 en la dinámica de la cohesina, así como la especificidad funcional de Pds5A y Pds5B .

2. Caracterizar la contribución de las proteínas Pds5 a la distribución de la cohesina a lo largo del genoma.

3. Evaluar las consecuencias de la eliminación de las proteínas Pds5 en la regulación génica y la progresión del ciclo celular.

Materials and Methods

Antibodies

Sera against Pds5B was obtained from rabbits injected with the peptide NH2-CEEKLGMDDLTKLVQEQKPKGSQRS-COOH (aa1226-1249 of hPds5B). Sera against Wapl was produced by injecting rabbits with His-tag fragment corresponding to the last 352 amino acids of hWapl purified from *E. coli* as an insoluble protein and partially refolded by dialysis in buffer with decreasing amounts of Urea. The full-length cDNA of hWapl was a kind gift of T. Hirano. In both cases, crude sera were affinity purified with the corresponding antigen. Other custom made antibodies used in this study are: Smc1, Smc3, Sororin (Remeseiro et al., 2012a, Remeseiro et al., 2012b); Rad21, Pds5A (Carretero et al., 2013); acetylated Smc3 (a gift from K. Shirahige (Nishiyama et al., 2010); Mcm3 (a gift from J. Méndez; (Alvarez et al., 2015). Additional antibodies from commercial sources are: Pds5B (Bethyl IHC-00381, for immunofluorescence only); CTCF (Millipore 07-729); Aurora B (AIM-1, BD Transduction Laboratories); α-tubulin (Sigma, DM1A); histone H3 (Abcam, ab1791); Mek2 (BD, M24520); Cdc6 (Millipore 05-550); GFP (Roche, 11814460001); BrdU-FITC (BD, 556028) for FACS; ssDNA (Millipore, MAB3034), BrdU, clone B44 (BD, 347580) and clone BU1/75 (ab6326) to detect IdU and CldU, respectively, for DNA fiber analyses.

MEF isolation and culture, RNA interference, chromatin fractionation immunoprecipitation and immunoblotting.

Three mouse lines were used in this study: Pds5A +/- , Pds5 B +/- and Pds5A f/f; Pds5B f/f; Cre-ERT2 (Carretero et al., 2013). Mice were housed in a pathogen-free animal facility following the animal care standards of the institution. All procedures have been revised and approved by the required authorities (Comunidad Autónoma de Madrid). Primary MEFs were isolated from E12.5 embryos. Pregnant females were sacrificed using a CO_2 chamber and uterine horns were removed and transferred to a sterile PBS solution. In a laminar flow hood, embryos were removed from the uterus, fetal liver was excised and a fragment of tissue was taken for subsequent genotyping. The rest of embryonic tissue was minced and treated with 0.25% trypsin-EDTA (Sigma-Aldrich) for 20 min at 37°C. Cells were further disaggregated by pipetting, transferred to 9 mL medium and cultured in DMEM (Lonza) supplemented with 20% FBS (Sigma-Aldrich) at 37 ºC under 90% humidity and 5% CO_2. With the exception of FRAP experiments, all other experiments reported here have been performed in

primary, low passage MEFs.

To ablate Pds5A and Pds5B expression simultaneously, double conditional knock out MEFs (Pds5A f/f; Pds5B f/f; Cre-ERT2) were cultured in medium with 1 μM 4-hydroxy tamoxifen (4-OHT) for at least 5 days and the efficiency of elimination of Pds5A and Pds5B proteins was assessed by western blot. For RNA interference, 100 nM siGENOME SMARTpool against Wapl (M-047528-01, Dharmacon) was introduced in MEFs using the Neon transfection system (Invitrogen) and knock down efficiency was assessed after 72 hours by western blot.

For chromatin fractionation we followed the protocol from (Méndez and Stillman, 2000). Cells were resuspended at $2 \cdot 10^7$ cells/mL in buffer A (10 mM HEPES pH 7.9, 10 mM KCl, 1.5 mM $MgCl_2$, 0.34 M sucrose, 10% glycerol, 1 mM DTT, 1 mM $NaVO_4$, 0.5 mM NaF, 5 mM β-glycerophosphate, 0.1 mM PMSF), and incubated on ice for 5 min in the presence of 0.1% Triton X-100. Low-speed centrifugation (4 min/600 g/4°C) allowed the separation of the cytosolic fraction (supernatant) and nuclei (pellet). Nuclei were washed and subjected to hypotonic lysis in buffer B (3 mM EDTA, 0.2 mM EGTA, 1 mM DTT, 1 mM $NaVO_4$, 0.5 mM NaF, 5 mM β-glycerophosphate, 0.1 mM PMSF) 30 min on ice. Nucleoplasmic and chromatin fractions were separated after centrifugation (4 min/600 g/4°C). Chromatin was resuspended in Laemmli Sample Buffer and sonicated twice for 15 seconds at 20% amplitude.

For immunoprecipitation, asynchronous cells were lysed on ice for 30 min in lysis buffer [0.5% NP-40 in TBS supplemented with 0.5mM DTT, 0.1mM PMSF and 1X complete protease inhibitor cocktail (Roche)] and sonicated. Then NaCl was added to 0.3M and the extract rotated for 30 min at 4ºC. Salt concentration was the lowered to 0.1M NaCl by dilution and glycerol added to 10% final concentration. Extracts were incubated with the specific antibodies for 2h at 4ºC and rotated with 1/10 volume of protein A agarose beads for 1h at 4ºC. The beads were washed 6 times with 20 volume of lysis buffer and eluted in SDS-DTT gel loading buffer for 5min at 95ºC.

SDS-polyacrylamide gels and immunoblotting were performed following standard protocols. Homemade primary antibodies were used at 2 μg/mL for 1 hour/RT, and commercial antibodies following the specifications of the manufacturer. Horseradish peroxidase (HRP)-conjugated secondary antibodies (Amersham Biosciences) were used at 1:5000 dilution in 5% Milk for 1 hour/RT. ECL developing reagent (Amersham Biosciences) was used.

Fluorescence Recovery After Photobleaching (FRAP)

One MEF clone of each genotype was immortalized using SV40 large T antigen and used to generate Rad21-GFP expressing cell lines by CRISPR-mediated homologous recombination, as described (Ladurner et al., 2016; Ran et al., 2013). GFP expressing cells were selected by sorting. A polyclonal population was characterized by immunoblot and immunoprecipitation and used for these studies. For Pds5 DKO MEFs, cells at full confluence were starved in DMEM supplemented with 0.1% FBS for 5 days before performing thee experiment. In Pds5A KO or Pds5B KO MEFs, cells were arrested for 3 days. FRAP experiments were performed in a Leica TCS-SP5 (AOBS) confocal microscope from Germany Leica Microsystems using a 40x/1.2 NA HCX PL APO objective with immersion oil. Cells were kept in a climate chamber at 37ºC with 5% CO2 during the experiment. Image acquisition used the HCSA software in LAS AF 2.7. Cells were photobleached with an argon laser and the recovery was monitored by live-cell imaging taking pictures every minute. Videos were analyzed using FIJI software (Schindelin et al., 2012) and statistical analysis and non-linear regression with GraphPad Prism.

DNA replication analyses

MEFs growing on coverslips or seeded on wells were serum starved for 5 days to arrest them in G0 and then released into rich medium with 10 μM EdU up to 72 hours and coverslips were taken at different time points to monitor entry into S phase. Alternatively, 10 μM BrdU (Sigma) was added for 30 min before collecting cells at the same time points. For EdU detection, coverslips with cells were washed with phosphate-buffered saline (PBS), fixed with 2% paraformaldehyde for 15 min and permeabilized in 0.5% TritonX-100 in PBS for 20 min at room temperature. EdU was detected as described (Salic and Mitchison, 2008). Cells were incubated for 30 minutes with 1mM $CuSO_4$, 100 mM ascorbic acid, 10 μM biotine-azide, 1x PBS, washed with PBS and incubated for 30 minutes with conjugated streptavidin 1/200 in PBS-0,5% Triton X-100. A Leica DM6000 microscope was used to obtain grayscale images, analyzed then using FIJI software. BrdU-pulsed cells were harvested and fixed in ice-cold 70% ethanol overnight at -20ºC. DNA was denatured with 2N HCl for 20 min at room temperature. Cells were blocked with 1%BSA-0.05%Tween20 in PBS. FITC conjugated anti-BrdU was incubated for 1h at 37ºC using a 1:100 dilution. Finally, 50μg/mL of propidium iodide (PI; Sigma) with 10μg/mL RNase A (Qiagen) was added

overnight at 4ºC to stain DNA. FACs data was acquired in a FACS Canto II cytometer (BD, San Jose, CA) and analyzed with FlowJo 10.0.6 (Tree Star, Ashland, OR).

For single molecule analyses of fork progression, exponentially growing MEFs were pulse-labeled with 50μM CldU (20 min) followed by 250μM IdU (20 min). Stretched DNA fibers were prepared as described (Mourón et al., 2013). Labeled cells were harvested and resuspended in cold PBS at $0.25 \cdot 10^6$ cells/mL. 500 cells were lysed in 0.2 M Tris pH 7.4, 50 mM EDTA, 0.5% SDS 6 min at 30°C in a microscope slide into a humidity chamber. Slides were 15° tilted to stretch DNA fibers. DNA spreads were air-dried, fixed in cold 3:1 methanol: acetic acid for 2 min and refrigerated. Slides were treated with 2.5 N HCl for 30 min, washed 3 times with PBS and blocked in 1% BSA, 0.1% Triton X-100 in PBS for 1 h before incubation. For immunodetection of labeled tracks, fibers were incubated with primary antibodies (1:100 dilution) for 1 h at RT and the corresponding secondary antibodies (1:300 dilution) for 30 min at RT, in a humidity chamber. ProLong Gold antifade reagent (Invitrogen) was used as mounting media for IF. DNA was visualized with an anti-ssDNA antibody to assess fiber integrity. Images were acquired in a DM6000 B Leica microscope. The conversion factor used was 1 μm= 2.59 kb. For each clone, at least 300 individual tracks were measured to estimate fork rate. For representation and statistical analyses we used GraphPad Prism.

Immunofluorescence and image analysis.

For regular immunofluorescence, MEFs grown on coverslips were fixed with 4% PFA for 20 min and permeabilized in 0.25% TritonX-100 in PBS for 5 min on ice. Cells were blocked with 3% BSA, 0.05% Tween 20 in PBS for 30 min. Primary and secondary antibodies were diluted in blocking solution and incubated for 1h each. Detection of Sororin required overnight incubation and including 10% normal donkey serum in the blocking solution. DNA was counterstained with 1 mg/ml DAPI. A Leica DM6000 microscope was used to obtain grayscale images, which were later analyzed using FIJI software.

To see *vermicelli*, MEFs kept in starvation for 5 days with or without 4-OHT were released into rich medium without 4-OHT for another 5 days. Cells were pre-extracted with 0.5% Triton X-100 in CSK buffer (10 mM Pipes pH 7.0, 100 mM NaCl, 3 mM $MgCl_2$ and 300 mM sucrose) for 5 min before fixation in 2% paraformaldehyde for 15 min at room temperature. Coverslips were blocked with 3% BSA, 0.05% Tween-20

in PBS for 30 min. Primary and secondary antibodies were diluted in blocking solution and incubated for 1h each at room temperature. DNA was counterstained with 1 mg/ml DAPI. Images were obtained using a TCS-SP5 (AOBS) confocal microscope from Germany Leica Microsystems, using a 63x/1.4 NA HCX PL APO objective with immersion oil. Images were treated using the autoquant deconvolution blind algorithm from Media Cibernetics Inc. in the LAS AF 2.7 software.

ChIP sequencing and analysis

Chromatin immunoprecipitation (ChIP) was performed in asynchronously growing MEFs as described (Remeseiro et al., 2012b). For each condition, two MEF clones were processed independently. Around 5 ng of immunoprecipitated chromatin in each sample were used for library preparation. DNA libraries were applied to an Illumina flow cell for cluster generation and sequenced on an Illumina HiSeq2000. Image analysis, per-cycle base calling and quality score assignment was performed with Illumina Real Time Analysis software. Conversion of Illumina BCL files to bam format was performed with the Illumina2bam tool (Wellcome Trust Sanger Institute - NPG). Alignment of 50-bp long sequences to the reference genome (NCBIm37/mm9, April 2007) was performed using 'BWA' under default settings (Li and Durbin, 2009). Peak calling was performed using MACS2 (version 2.1.1.20160309) (Zhang et al., 2008b). FDR was set <0.05 (for CTCF, Pds5A, Pds5B ChIP in wild type MEFs and Smc1ChIP in Pds5 KOA ad Pds5 KOB MEFs) or < 0.01 (for Scmc1 in WT and Pds5 DKO MEFs). Before the peak calling step, 'macs2 predictd' function was ran in order to estimate the fragment size in each of the experiments. All comparisons used the input tracks as control, and each one of the data sets as treatment. After analyzing the data for the two replicates of each condition separately and confirming that the peak overlap was high, reads from both replicates were pooled and reanalyzed as above. The ChIPseq data of Smc3 in 2 clones each of Wapl +/Δ and Wapl -/Δ MEFs (Tedeschi et al., 2013) were processed in the same way (FDR<0.01). To subsample the reads in Smc1 ChIP of WT MEFs (Figure S3C), we calculated the mean height of the 200 highest peaks in WT and Pds5 DKO and used their ratio (DKO/WT=0.606) as a multiplying factor to decrease the height of all reads in the WT ChIP before running again the peak-calling algorithm.

Genomic interval overlaps required 1-nt overlap and were obtained using BEDTools v2.26 (Quinlan and Hall, 2010). Cohesin occupancy plots were generated using seqMINER v1.3.3e (Ye et al., 2011). BAM files with processed reads, used for the peak calling step, were used to plot mean read density around peak summits in

10kb windows. To check cohesin enrichment at promoters and gene bodies RefSeq gene annotations for NCBIm37/mm9 assembly were downloaded from UCSC browser. Promoter regions were defined as ±2.5 kb from TSS, whereas for the gene bodies the whole length of the genes was considered. Thus, some cohesin positions could be present both at the promoter and at the gene body.

RNA sequencing and analysis

Asynchronous or G0 MEFs (3 clones for each genotype) were harvested and RNA was extracted using RNeasy kit (Qiagen). PolyA+RNA was purified with the Dynabeads mRNA purification kit (Invitrogen), randomly fragmented and converted to double-stranded cDNA and processed through subsequent enzymatic treatments of end-repair, dA-tailing and ligation to adapters as in Illumina's 'TruSeq RNA Sample Preparation Guide' (Part # *15031047 Rev. D*). Adapter-ligated library was completed by limited-cycle PCR with Illumina PE primers and applied to an Illumina flow cell for cluster generation (TruSeq cluster generation kit v5) and sequenced on HiSeq2000 or Illumina HiSeq2500 instrument by following manufacturer's protocols. Differentially expressed genes (DEGs) were obtained using the Nextpresso pipeline (http://bioinfo.cnio.es/nextpresso/). Sequencing quality was analyzed with FastQC (http://www.bioinformatics.babraham.ac.uk/projects/fastqc/); reads were aligned to the mouse genome (GRCm38/mm10) using TopHat-2.0.10 (https://ccb.jhu.edu/software/tophat/index.shtml), Bowtie 1.0.0 (http://bowtie-bio.sourceforge.net/index.shtml) and Samtools 0.1.19.0 (http://samtools.sourceforge.net/); and transcripts assembly, abundance estimation and differential expression were calculated with Cufflinks 2.2.1 (http://cole-trapnell-lab.github.io/cufflinks/). P value was corrected to account for multiple hypotheses testing using Benjamini and Hochberg False Discovery Rate (FDR) adjustment. Genes with FDR ≤ 0.05 and with fpkm≥3 in at least one of the two conditions compared were selected as DEGs. For these genes, we performed GSEA (GSEA Version 2.0.6, http://www.broad.mit.edu/gsea/) following the developer's protocol (Subramanian et al., 2005) and using pathway annotations from Kyoto Encyclopedia of Genes and Genomes (KEGG) databases.

DEGs from Wapl deficient cells, obtained by microarray analysis, were taken from (Tedeschi et al., 2013). We chose data corresponding to Wapl -/fl versus Wapl -/Δ which compares the same MEF clone untreated and treated with 4-OHT, since we think it resembles better our own experiment than the comparison of two different MEF clones, Wapl -/Δ and Wapl +/Δ.

Quantitative RT-PCR and ChIP

For RT-PCR, total RNA extracted as described above was treated with DNaseI (Ambion), and cDNAs were prepared according to the manufacturer's instructions using the Superscript II reverse transcriptase (Invitrogen). qRT-PCR analysis was performed in triplicates using the SYBR Green PCR Master Mix and an ABI Prism® 7900HT instrument (Applied Biosystems®). Quantifications were normalized to endogenous GAPDH, using the ΔΔCt method. Primer sequences are listed in Table S8. For ChIP-qPCR, chromatin immunoprecipitation was performed using chromatin of asynchronously growing MEFs. Fold enrichment of cohesin binding at a given position was calculated over the binding at a nearby position showing few reads in the browser. Chromosome coordinates of the validated peaks and the corresponding primers are listed in Table S7.

Primers for ChIP-qPCR

Chromosome	primer name	primer sequence
chr15	neg15_FWD	CTCGCTGAGGTTCTCCATTC
	neg15_REV	TCTCACACCAAGGACTGCTG
	r1_FWD	AGCGAGTGGTGGCTAAGAAG
	r1_REV	CAGTGTTCTGCAGGCTTTTG
	r2_FWD	CCAGGGTGAACTGAGCCTTA
	r2_REV	AATTCAGACGCCTTTGAGGA
	r3_FWD	TCCGTGTGTAAACCCTCTCC
	r3_REV	GACAGAGTCGCCTGTTGTGA
	r4_FWD	GTGTGTGCAGTACCCACCAG
	r4_REV	GCTGACGCAGGGATTTAGAG

chr9	neg9_FWD	ACATGGAAACAGGCAACACA
	neg9_REV	CAATCATCTGGTGCCAACAC
	r5_FWD	GGAACTGGACTCAGGCCTCT
	r5_REV	CTCGATGTTCTGGCCTTTGT
	r6_FWD	TGGGCTGTCTGTTCATTCCT
	r6_REV	GTCCTCGGATGAAGCCAGTA
	r7_FWD	CCCTAGGTGGAGCCTCAGTA
	r7_REV	CTGGAGCAACGACAAACAGA
chr19	neg19_FWD	GTAGTAGGGCCCCAGTCCTC
	neg19_REV	GCTTTGAAGCTTGCTTTTGG
	r8_FWD	CAGCTCCACGGAAATCAAAT
	r8_REV	CTCCCCACCGAAGTGAGTTA
	r9_FWD	CCAGCCACTGTGGTTCTAGG
	r9_REV	ACCCCCAAATACTGCAAACA
	r10_FWD	ATGCCGTTGACCTGAGAGAA
	r10_REV	CAGTGCTGAACCCAACAAGA
chr5	neg5_FWD	CTTGCAGAGGACCCATGTTT
	neg5_REV	GTTTTCTCCTGCCACTTTGC
	r11_FWD	ATGTGGCAGGGTGTTAAGGA

	r11_REV	CGAATGGCTGAAGTTCCAGT
	r12_FWD	CCACACCCATCTGCATGTAA
	r12_REV	TGTAGAGACAGCCCCTCTGG
chr3	neg3_FWD	CTGCAGAAAACCCACACTGA
	neg3_REV	GACCCCATCATCTCTCCTGA
	r13_FWD	TTGCAGGTGTGAACAACCAT
	r13_REV	ACCACCACCACCACTGGTTA
	r14_FWD	GCCACATCCAGAAGACCCTA
	r14_REV	AGGGCATCTGCCTGAACTAA

Primers for RT-qPCR

gene	**primer name**	**primer sequence**
GAPDH	GAPDH_Fwd	TGCACCACCAACTGCTTAGC
	GAPDH_Rv	GAGGGGCCATCCACAGTCTTC
Mcm3	Mcm3_FWD	TTCCTCAGCTGTGTGTGGTCTG
	Mcm3_REV	TCACCACCCTAGTGGCTTTC
Cdc6	Cdc6_FWD	ACACACTGTTTGAGTGGCCGT
	Cdc6_REV	GCTTCAAGTCTCGGCAGAATTC
Orc1	Orc1_FWD	TGACTTTGAAGCGGATTAGG

	Orc1_REV	GTTGGGAGGGAGGAAATAAA
Cdt1	Cdt1_FWD	TAGTACCCCAGATGCCAAGG
	Cdt1_REV	GTAGGACAAGGCCTGGGAGA
Ccna2 (CycA2)	Ccna2_FWD	AGTACCTGCCTTCACTCACTCATTGCTG
	Ccna2_REV	TCTGGTGAAGGTCCACAAGACAAG
Cdkn1a (p21)	Cdkn1a_FWD	CTAGGGGAATTGGAGTCAGGC
	Cdkn1a_REV	AACAGGTCGGACATCACCAG
Smc3	Smc3_FWD	ATTGGTGCCAAAAAGGATCA
	Smc3_REV	TGAGAATCTGGTGCCGTTGC
NIPBL	NIPBL_FWD	AGTCCATATGCCCCACAGAG
	NIPBL_REV	ACCGGCAACAATAGGACTTG

Results

In order to study the specific contributions of Pds5A and Pds5B to cohesin regulation and function, our group generated mouse models carrying conditional knock out (KO) alleles for both Pds5A and Pds5B (Carretero et al., 2013). Those alleles contain loxP sites flanking exon 6 in Pds5A and exons 4-5 in Pds5B (Figure R1A). Upon expression of a Cre recombinase we induce an efficient excision of the targeted alleles, resulting in an impaired translation of the protein. While heterozygous animals are viable and fertile, constitutive homozygous elimination of either Pds5A or Pds5B from the zygote results in lethality at late stages of embryonic development. However, it was possible to obtain MEFs extracted at day 12.5 of gestation, hereafter known as Pds5A KO and Pds5B KO.

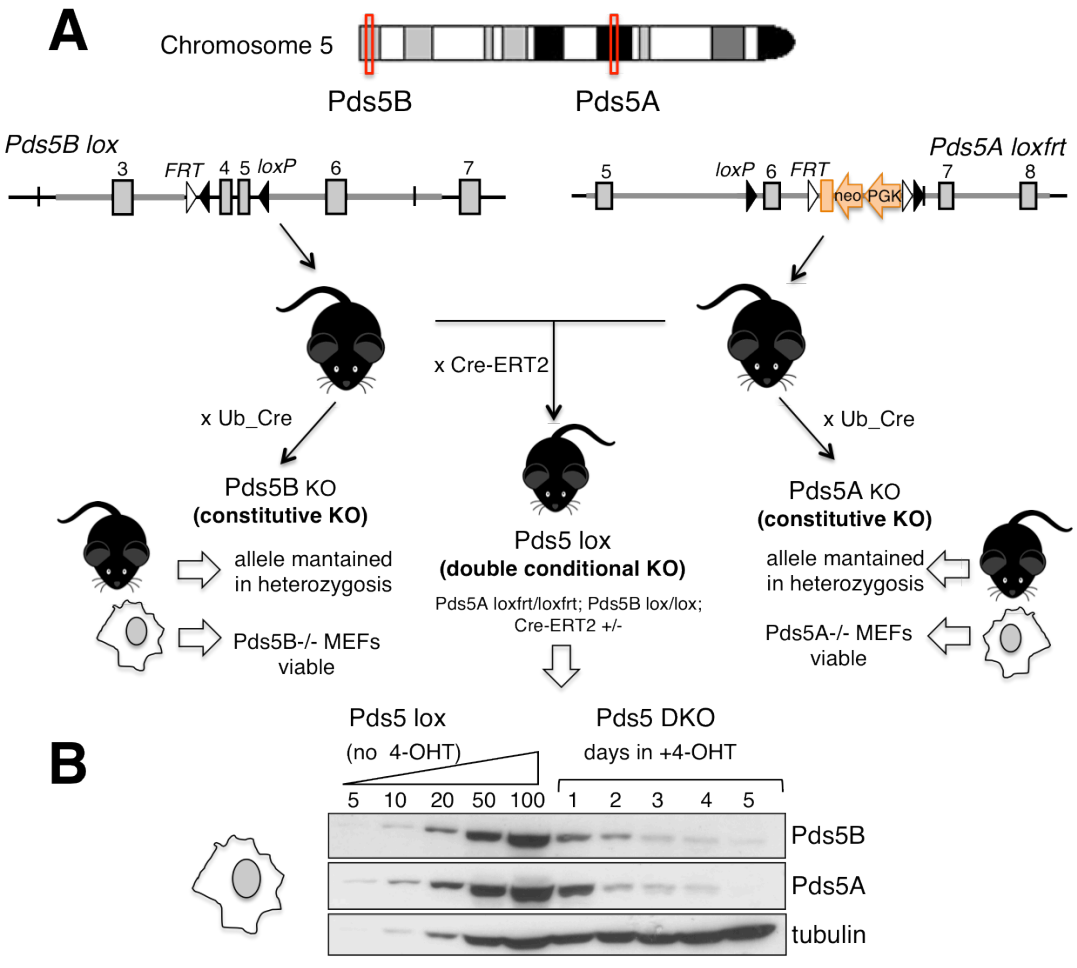

Figure R1. Scheme of the generation of the cells used to study Pds5 functions.

A. Description of the murine KO alleles for Pds5A and Pds5B. **B**. Immunoblot analyses of whole cell extracts from Pds5 lox MEFs cultured for up to 5 days in the absence (left, decreasing amounts of extract were loaded) or presence of 1μM 4-hydroxy tamoxifen (4-OHT) to activate Cre-ERT2 and deplete simultaneously the two Pds5 proteins.

We also generated mice carrying conditional KO alleles for both Pds5A and Pds5B in homozygosis and a Cre-ERT2 transgene. Expression of the Cre recombinase can be induced by tamoxifen. MEFs extracted from these mice, hereafter Pds5 lox, efficiently eliminate both Pds5 proteins after 5 days in culture medium containing 4-hydroxytamoxifen (4-OHT), and generate Pds5 double KO cells, hereafter Pds5 DKO (Figure R1B). We have used these cells to address the dynamics and distribution of cohesin on chromatin, as well as the consequences of these effects on cell function.

1. Regulation of cohesin dynamics by Pds5

The regulation of cohesin dynamics is likely essential for its proper function. Wapl is thought to mediate cohesin release from chromatin while Smc3 acetylation and Sororin binding stabilize the association of cohesin with chromatin. The role of Pds5 in the regulation of these processes was not clear, with evidences for both positive and negative effects of Pds5, at least in yeast, in the interaction of cohesin with DNA. Thus, we decided to evaluate possible changes in cohesin dynamics upon elimination of the Pds5 proteins in MEFs.

1.1 Pds5 proteins are required for cohesin acetylation and Sororin recruitment

As a first approach, we analyzed the levels of Wapl, Sororin and acetylated Smc3 on chromatin upon Pds5 elimination. Chromatin fractionation of Pds5A KO and Pds5B KO MEFs revealed a partial reduction on both Wapl and acetylated Smc3 on chromatin, whereas Sororin levels were not affected (Figure R2A). In contrast, we found a strong reduction in Wapl, acetylated Smc3 and Sororin in Pds5 DKO MEFs (Figure R2B).

Since Sororin binds to cohesin once DNA is replicated, we reasoned that alterations in cell cycle progression might explain the reduced recruitment of Sororin to chromatin in Pds5 DKO MEFs. To address this possibility, we analyzed the presence of Sororin in Pds5 deficient G2 cells by immunofluorescence. To identify cells in G2 phase, we used an antibody against Aurora B, a kinase that accumulates in heterochromatin foci right before mitosis (Figure R2C). Pds5 lox MEFs showed Sororin staining in almost 100% of Aurora B positive cells. In contrast, Sororin could not be detected in at least 70% of Pds5 DKO cells in G2. Therefore, even those cells that progressed through S phase to G2 could not recruit Sororin in the absence of Pds5A and Pds5B, indicating that Pds5 proteins are required for Sororin binding to cohesin.

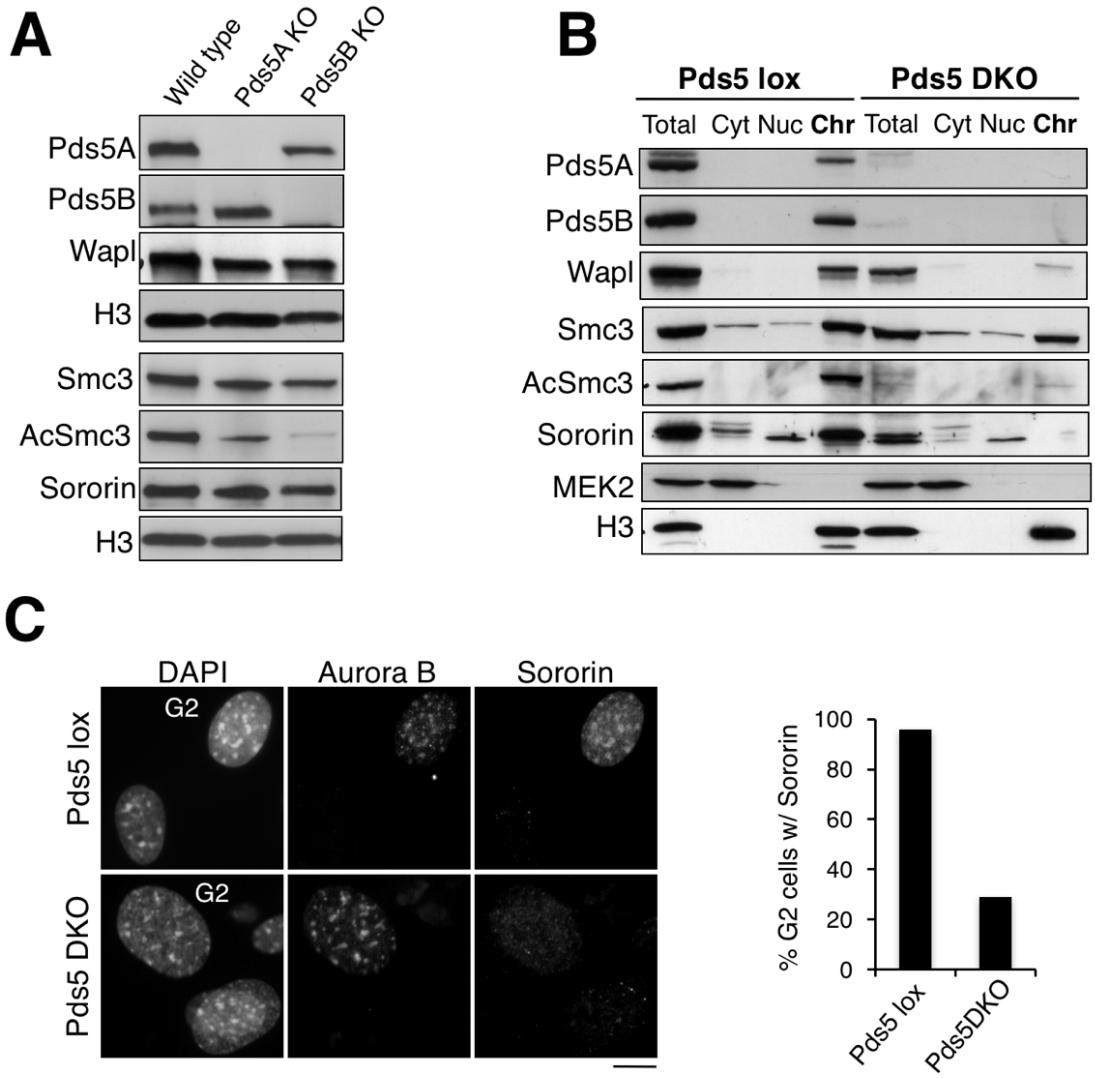

Figure R2. Requirement of Pds5 proteins for cohesin acetylation and Sororin recruitment.

A. Immunoblot analysis of the chromatin fraction of primary MEFs of the indicated genotypes. **B**. Equivalent amounts of total cell extract (Total), Cytoplasmic (Cyt), Nuclear soluble (Nuc) and chromatin enriched (Chr) fractions obtained from Pds5 lox and Pds5 DKO MEFs. The cytoplasmic kinase MEK2 and histone H3 are used as controls for the fractionation procedure. **C**. Pds5 lox and Pds5 DKO cells grown on coverslips were stained with Aurora B and Sororin antibodies and counterstained with DAPI. The percentage of cells labeled by both Aurora B and Sororin was quantified among more than 160 G2 cells from two different clones and plotted in the graph on the right. Scale bar, 10 μm.

Reduction in Smc3 acetylation can be due to defects in cohesin acetylation by CoATs or to increased deacetylation by CoDACs. In budding yeast, Pds5 has been proposed to affect both processes by promoting recruitment of Eco1 and protecting Smc3 from deacetylation by Hos1 (Chan et al., 2013). HDAC8 has been identified as

the Hos1 ortholog in vertebrates (Deardorff et al., 2012). To assess the importance of deacetylation in the absence of Pds5 in MEFs, Pds5 DKO cells were treated with PCI-34051, a specific inhibitor of HDAC8. While HDAC8 inhibition promoted an increase in Smc3 acetylation in Pds5 lox cells both after 8 and 24 hours of treatment, we could not detect a significant increase in acetylated Smc3 levels in Pds5 DKO cells (Figure R3). Thus, it is unlikely that defects in Smc3 acetylation observed in Pds5 DKO are due to defective protection from deacetylation. Instead, they must be the result of an impaired acetylase activity.

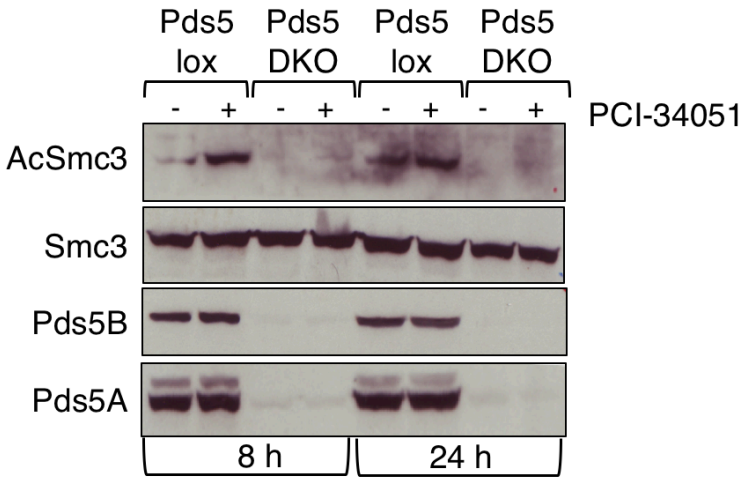

Figure R3. No evidence for increased HDAC8 activity in Pds5 DKO cells

Immunoblot analysis of whole cell extracts from Pds5 lox and Pds5 DKO cells treated or not with the HDAC8 inhibitor PCI-34051 for the indicated times.

1.2 Pds5 elimination increases chromatin bound cohesin

Wapl elimination stabilizes cohesin on chromatin even in the absence of Sororin (Nishiyama et al., 2010; Tedeschi et al., 2013). Given the reduction of Wapl on chromatin observed upon elimination of the Pds5 proteins, we hypothesized that this condition should also increase the stability of cohesin binding to DNA. Unlike reported observations in Wapl KO MEFs, we did not observe a noticeable increase in the levels of cohesin on chromatin in Pds5 DKO MEFs by chromatin fractionation (Figure R2B). Nevertheless, we decided to analyze individual cells by immunofluorescence. Before fixation and staining with cohesin antibodies, cells were treated with detergent to eliminate the soluble population of cohesin in the nucleus and thereby assess the

amount of chromatin-bound cohesin. Single elimination of either Pds5A or Pds5B did not affect the levels of chromatin bound cohesin in interphase cells (Figure R4A, compare wild type with Pds5A KO or PdsB KO). However, simultaneous elimination of both Pds5 proteins led to increased accumulation of cohesin on chromatin (Figure R4A and R4B). A similar increase was observed in MEFs treated with a Wapl siRNA.

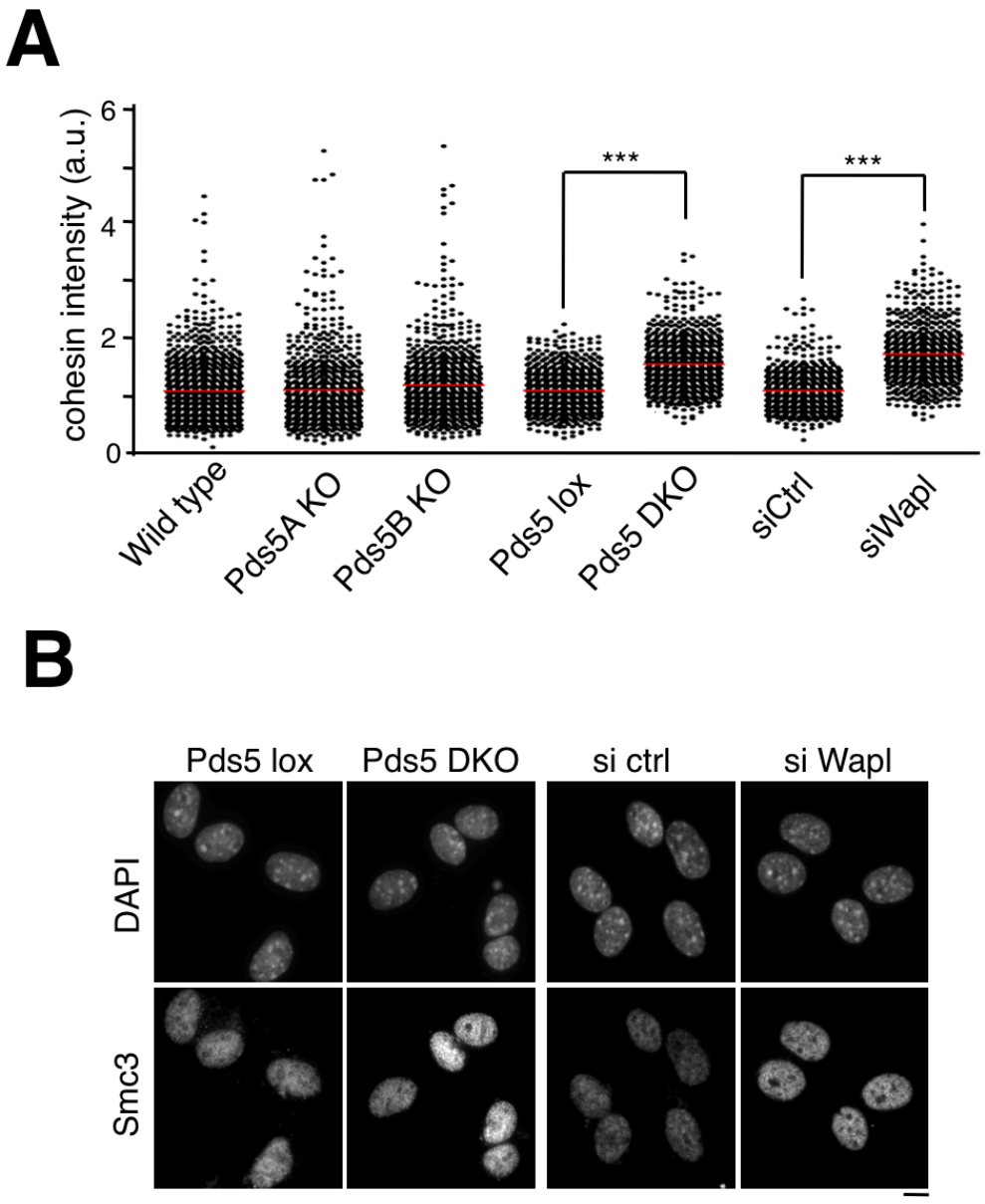

Figure R4. Increased presence of cohesin in interphase chromatin in Pds5 DKO cells.

A. Box plot showing the quantification of cohesin staining (Smc1 or Smc3, in arbitrary units and normalized to the average value obtained in wild type cells) in interphase cells of the indicated genotypes and conditions. The following numbers of cells (n) from several clones (N) were measured: wild type, n=972, N=7; Pds5A KO n= 698, N= 4; Pds5B KO, n=742 cells, N=6; Pds5 lox and Pds5 DKO, n=700 each, N=1; control and Wapl siRNA, n=600 each, N=1. *** P<0.001 (Bonferroni´s multiple comparison test). **B.** Representative images of the cell staining measured in A. Scale bar, 10 μm.

The role of Wapl in cohesin unloading is particularly relevant in early mitosis, when more that 90% of cohesin dissociates from chromatin to allow proper sister chromatid resolution. As a consequence, cohesin can be barely detected in wild type prometaphase cells (Figure R5). In contrast, in Pds5 DKO cells, as in cells treated with Wapl siRNA, cohesin staining could be clearly observed on the condensed chromosomes. Single Pds5A KO or Pds5B KO cells show little staining, similar to wild type cells. Taken together, our observations indicate that Pds5 proteins promote cohesin release from chromatin together with Wapl. Moreover, both Pds5A and Pds5B can perform this function.

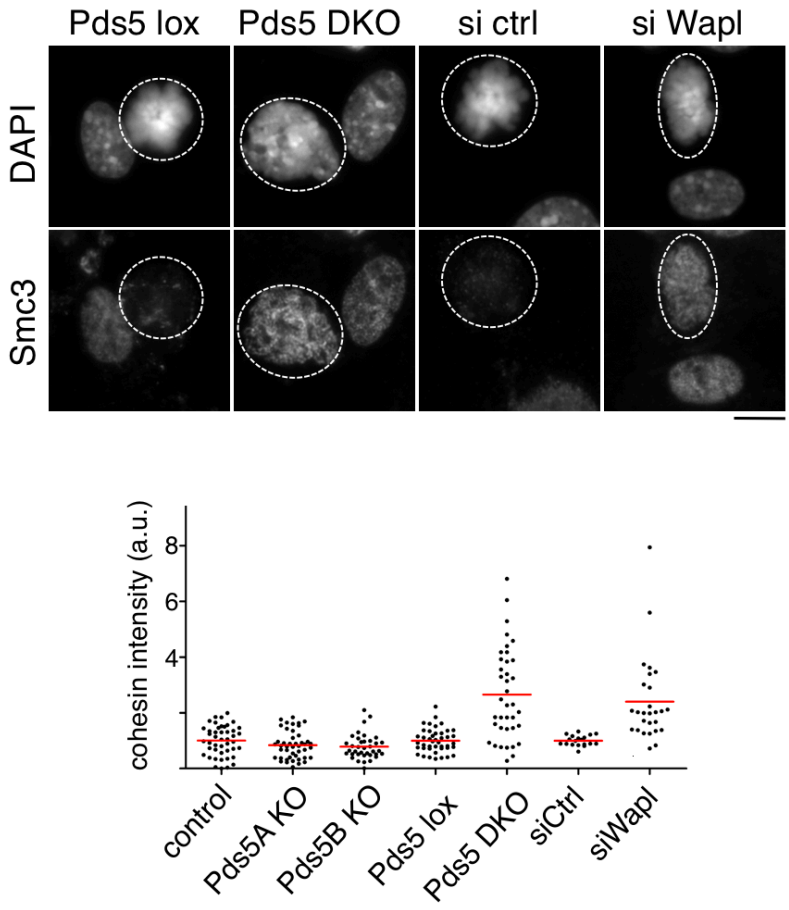

Figure R5. Pds5 proteins are required for the prophase dissociation of cohesin.

Cohesin staining was measured in at least 35 metaphases (surrounded by a dashed white line in the images on top) of each condition. Scale bar, 10 μm.

1.3 An assay to measure cohesin dynamics in Pds5 deficient cells

To better address the role of Pds5 proteins in cohesin dynamics, we decided to use Fluorescence Recovery After Photobleaching (FRAP). This technique is commonly used to evaluate two-dimensional mobility of fluorescently tagged proteins by photobleaching the fluorophores in a specific area and measuring the rate of recovery of fluorescence by time lapse imaging (Figure R6, top). As the photobleaching permanently erases the fluorescence of the affected molecules, the recovery of the fluorescence is due to movement of the fluorophores from the surrounding unbleached region to the bleached area. We used a modification of this technique, termed inverse FRAP (iFRAP) (Dundr et al., 2002). In iFRAP the bleached area is larger, and the time of recovery is estimated by taking into account the redistribution of fluorescence in both the bleached and unbleached regions (Figure R6, bottom). iFRAP is commonly used to analyze molecules bound to an immobile structure for longer periods. We used iFRAP to evaluate chromatin binding stability of cohesin in Pds5 deficient cells.

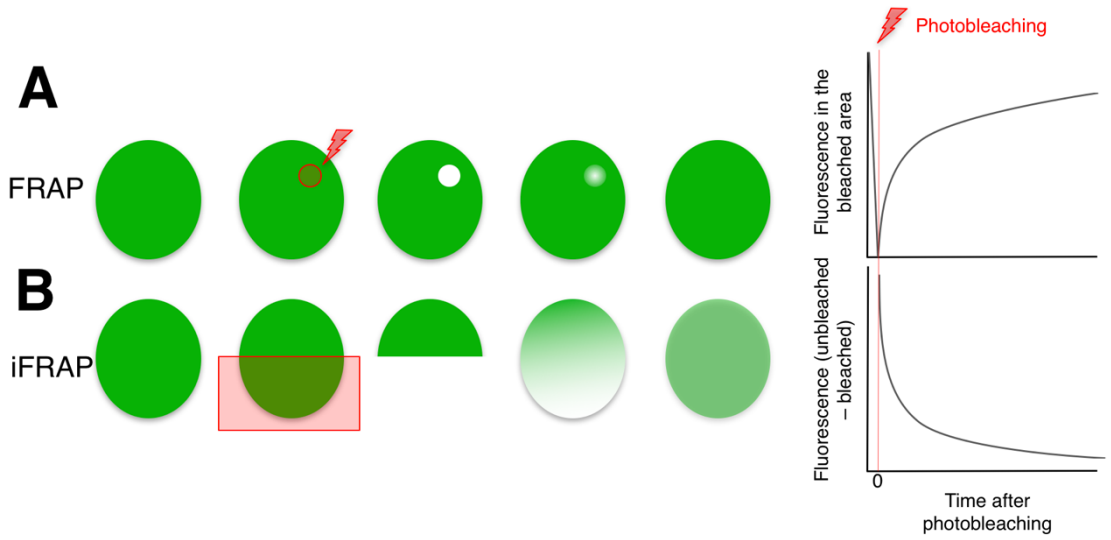

Figure R6. Schematic representation of FRAP and iFRAP experiments

A. Fluorescent molecules present in the cell (green) are irreversibly photobleached in a small area (red circle) with an intense laser beam. Diffusion of the surrounding non-bleached fluorescent molecules into the bleached area leads to recovery of fluorescence, which is measured over time (graph on the right). **B.** In the iFRAP experiments that we performed in this Thesis, half of the cell is bleached (red box) and changes in fluorescence are measured both in the unbleached and the bleached regions.

To that end, we had to generate MEF clones expressing a fluorescent version of cohesin. To facilitate our assays we immortalized a clone each of primary Pds5 lox, Pds5A KO and Pds5B KO MEFs by transducing a retroviral vector expressing the large T antigen of the SV40 virus. We then introduced a GFP tag in the endogenous Rad21 gene using the CRISPR/Cas9 technology. We transfected the immortalized (i)MEFs with a modified version of the *Streptococcus pyogenes* Cas9 that is able to dimerize to recognize two sequences when coupled with a pair of guide RNAs (gRNAs) (Ran et al., 2013). This double nickase was directed to the C-terminal part of the Rad21 gene, inducing the recruitment of the Homologous Recombination (HR) Machinery.

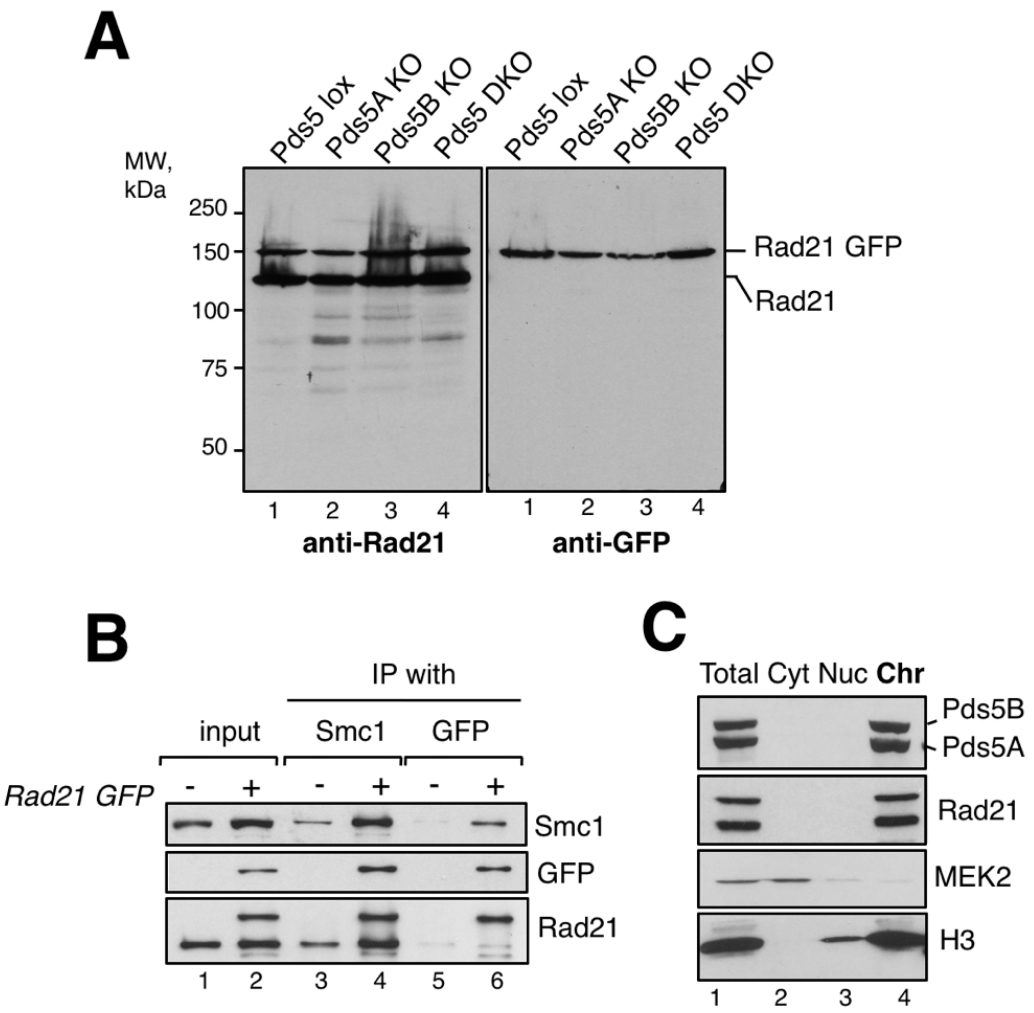

Figure R7. Pds5 proteins are required for the prophase dissociation of cohesin.

A. Immunoblot analyses of total extracts prepared from iMEFs of the indicated genotypes. **B.** Immunoprecipitation reactions with Smc1 and GFP antibodies from iMEFs expressing Rad21-GFP (or not, as control) demonstrate that Rad21-GFP incorporates as well as the untagged Rad21 into cohesin complexes. **C.** Chromatin fractionation shows normal incorporation of cohesin complexes carrying the tagged Rad21 subunit into chromatin. Equivalent amounts of all fractions were analyzed by immunoblot.

To provide a template for the HR, cells were also transfected with a donor plasmid containing the C-terminal sequence of Rad21 fused to GFP. Thus, Cas9 activity triggered the substitution of the endogenous Rad21 with the GFP-tagged version. After transfection, GFP positive cells were selected by cell sorting. To validate the specificity of the GFP insertion and the functionality of the Rad21-GFP protein generated, we analyzed the cells by immunoblot with GFP and Rad21 and confirmed that all the GFP was fused to Rad21 (Figure R7A). We could also confirm by immunoprecipitation that Rad21-GFP forms cohesin complexes containing Smc1 (Figure R7B). Finally, chromatin fractionation indicated that the tagged version of Rad21 is also capable of binding to chromatin (Figure R7C).

1.4 Pds5 elimination stabilizes cohesin on chromatin

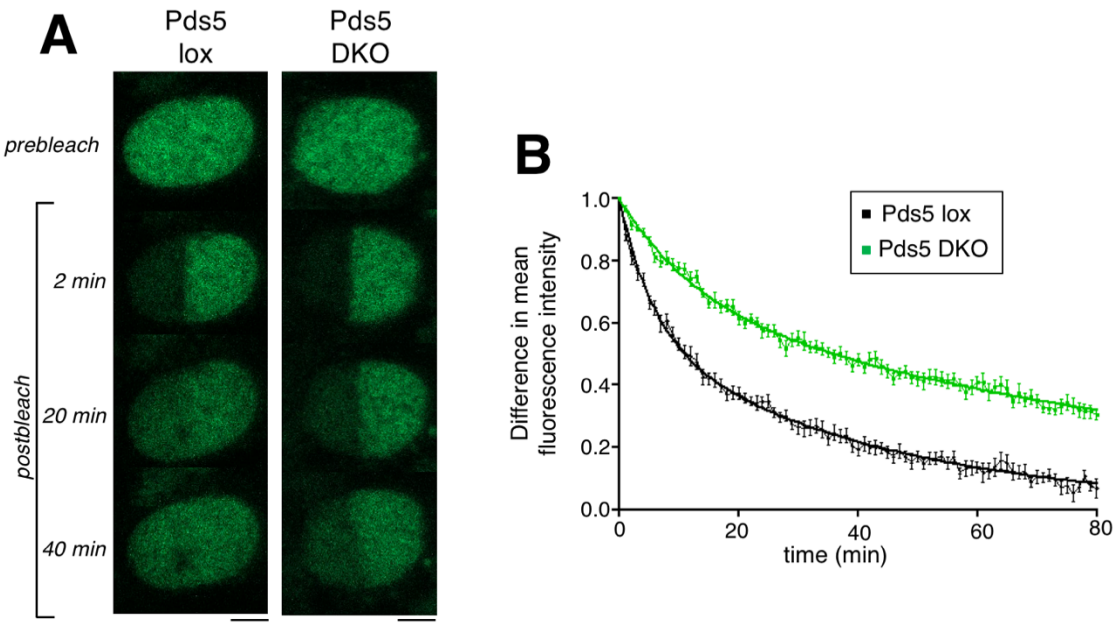

Figure R8. Stabilization of cohesin-DNA interaction in the absence of Pds5 proteins.

A. Still images of a FRAP experiment with quiescent iMEFs expressing Rad21-GFP (green). MEFS were kept in low serum (0.1%) for 5 days in the presence (Pds5 DKO) or absence (Pds5 lox) of 4-OHT. Scale Bar, 5 μm. **B**. Graph plotting the difference in fluorescence intensity between bleached and unbleached regions versus time (mean values and s.d.) Data from at least 12 cells.

We cultured Pds5 lox iMEFs expressing Rad21_GFP in low serum (0.1%) medium without or with 4-OHT to eliminate both Pds5 proteins. In individual cells from these cultures we photobleached half of the nucleus with a high-power argon laser and monitored fluorescence recovery for the following 80 minutes. Pds5 DKO cells showed a significant delay in the recovery of the fluorescence compared with Pds5 lox cells (Figure R8). Despite being arrested in G0, a fraction of stably bound cohesin appeared to be present in the unbleached region. Therefore, we used a bi-exponential curve fitting, commonly used for S/G2 cells, for the analysis of these cells. We calculated a residence time of 127.5 minutes in the slow exchange population in Pds5 DKO cells compared with 29.6 minutes in Pds5 lox cells. This experiment shows that simultaneous elimination of both Pds5 stabilizes cohesin on chromatin.

1.5 Redundant contribution of Pds5A and Pds5B to cohesin dynamics

We next studied the individual contribution of each Pds5 protein to cohesin dynamics. Pds5 lox, Pds5A KO and Pds5B KO iMEFs expressing Rad21_GFP were cultured in low serum for 3 days and analyzed using iFRAP (Figure R9). None of the conditions presented a stably bound cohesin fraction, so we fitted the curve using a single exponential non-lineal regression, commonly used for G0/G1 cohesin. We detected a mild delay in the recovery of the fluorescence in both Pds5A KO and Pds5B KO cells, with residence times of 14 and 15 minutes, respectively, compared to the 8 minutes measured in Pds5 lox MEFs. We can conclude that both proteins act redundantly to promote proper cohesin dynamics.

We also noticed that the curves obtained for Pds5 lox iMEFs were different in the experiments presented in Figures R8 and R9. Since we used the same cells, we speculate that the length of the starvation period (5 or 3 days, respectively) may affect cohesin behavior. We have evidence suggesting that longer periods of starvation provoke general protein degradation and reduce the levels of both Pds5 proteins (data not shown).

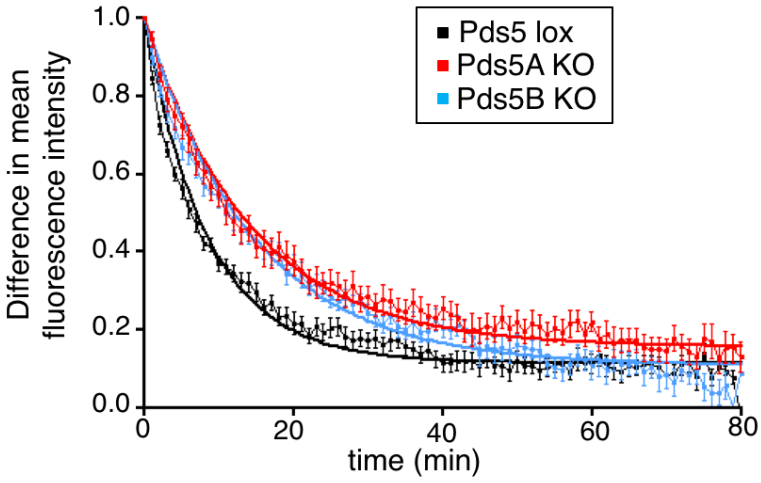

Figure R9. Mild changes in cohesin dynamics in the absence of Pds5A or Pds5B.

iMEFs of the indicated genotypes were culture in low serum (0.1%) for 3 days before imaging. Graph plotting the difference in fluorescence intensity between bleached and unbleached regions against time (mean values and s.d). The curve was fitted using single exponential function. Pds5 lox, n=13 cells; Pds5A KO, n=13; Pds5B KO, n=17.

1.6 Cohesin acetylation does not affect cohesin mobility in G0

Wapl elimination results in a more prominent defect in the recovery of fluorescence in iFRAP experiments compared with Pds5 DKO iMEFs, with the residence time of cohesin increasing to 540±240 min (Tedeschi et al., 2013). We speculate that the conditions of the experiment and the extent of depletion of Wapl and Pds5 proteins in could affect the results of iFRAP analyses. The reported iFRAP in Wapl KO cells was performed after a 10-day G0 arrest in 2% serum, whereas we used 5 days in 0.1% serum. A small amount of Wapl remaining on chromatin in Pds5 DKO cells together with the remaining Pds5 may be sufficient to perform some cohesin unloading.

As shown previously, Pds5 is required for Smc3 acetylation. In contrast, downregulation of Wapl by siRNA does not change the levels of acetylated Smc3 (Figure R10). In yeast, there is no Sororin and cohesin acetylation *per se* appears to be sufficient to stabilize cohesin after DNA replication. It has also been shown that cohesin acetylation occurs also in G0/G1 in vertebrate cells. Thus, an alternative possibility to explain the difference in cohesin dynamics in the experiments that we performed in Pds5 DKO cells and in the experiments reported in Wapl KO was that the

lack of acetylation might limit the stabilization of cohesin after depletion of Pds5 proteins in G0.

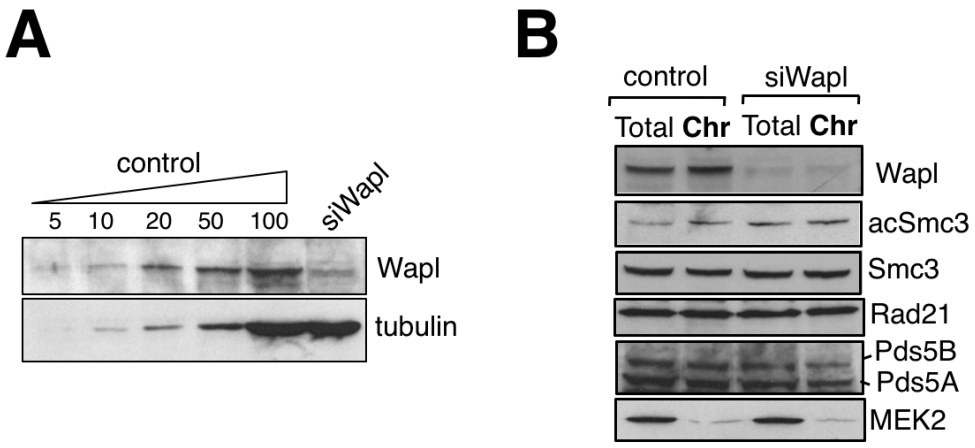

Figure R10. Wapl is not required for cohesin acetylation.

A. Primary Pds5 lox MEFs growing asynchronously were transfected with siRNA against Wapl or mock transfected as control. The extent of Wapl downregulation after 72 hours was assayed by quantitative immunoblotting. Tubulin is used as loading control. **B.** Immunoblot analyses of total cells extracts and chromatin fractions (**Chr**) from the cells in A. MEK2 is a cytoplasmic kinase.

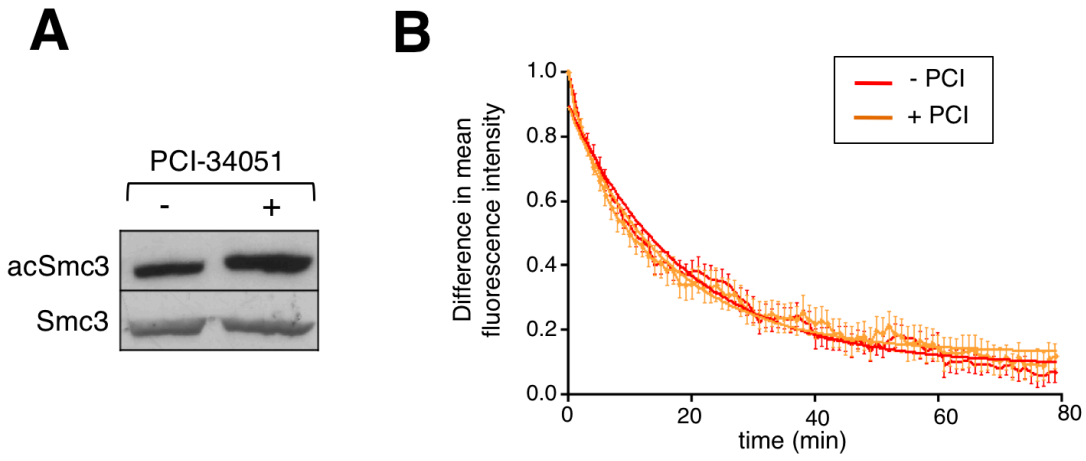

Figure R11. Changes in cohesin acetylation do not alter cohesin dynamics

A. Immunoblot analyses of cells used for the FRAP experiment. Pds5 lox iMEFs were cultured in low serum for 3 days before imaging. To one plate 25 μM PCI-34051 was added to the culture medium for 12 hours before imaging. The observed increase in Smc3 acetylation is around 20%. **B.** Graph plotting the difference in fluorescence intensity between bleached and unbleached regions against time (mean values and s.d). The curve was fitted using single exponential function. Pds5 lox no PCI, n=12 cells; +PCI, n=12 cells.

To test the effect of acetylation on cohesin mobility, we performed iFRAP in G0 arrested iMEFs cells treated with the HDAC8 inhibitor PCI-34051 to increase acetylation. Although the treatment increased acetylated Smc3 levels (Figure R11A), it did not affect the dynamic of fluorescence recovery when compared with the untreated control. It is therefore unlikely that Smc3 acetylation is the reason behind the different behavior of Pds5 DKO and Wapl KO MEFs in the iFRAP experiments.

1.7 Pds5 deficient cells exhibit *vermicelli*

One intriguing feature of Wapl KO cells is the accumulation of cohesin in axial structures resembling prophase-like chromosomes in the nucleus of interphase cells that were called *vermicelli* (Italian for 'little worms'). Although the exact nature of these structures remains to be clarified, it has been speculated that stabilization of cohesin on DNA could promote interactions between cohesin complexes, or enhance intra-chromatid loop formation leading to cohesin clustering. Despite the fact that the dynamic behavior of cohesin was less dramatically affected in Pds5 DKO cells compared to Wapl KO cells, we could clearly observe *vermicelli* in Pds5 DKO cells (Figure R12).

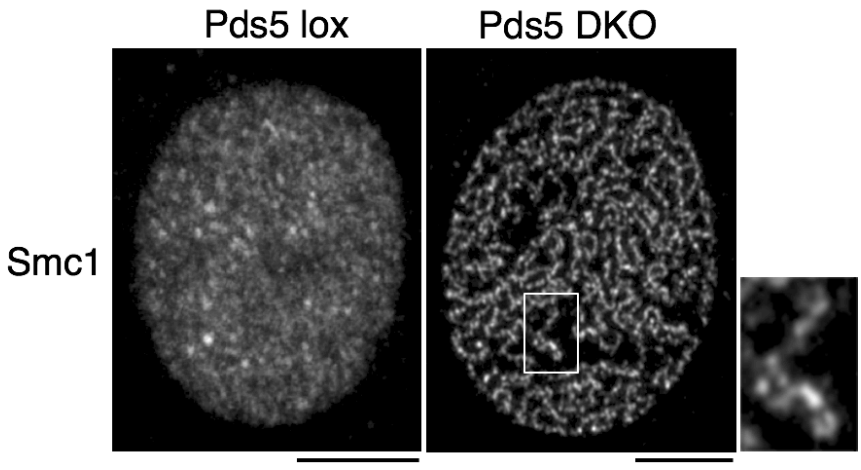

Figure R12. Cells lacking Pds5 proteins display *vermicelli.*

Representative images of interphase Pds5 lox and Pds5 DKO primary MEFs, fixed and stained with anti-Smc1 to reveal *vermicelli* in the absence of Pds5 proteins. The box shows a single *vermicello* that could correspond to a single chromosome. Scale bar, 5 μm.

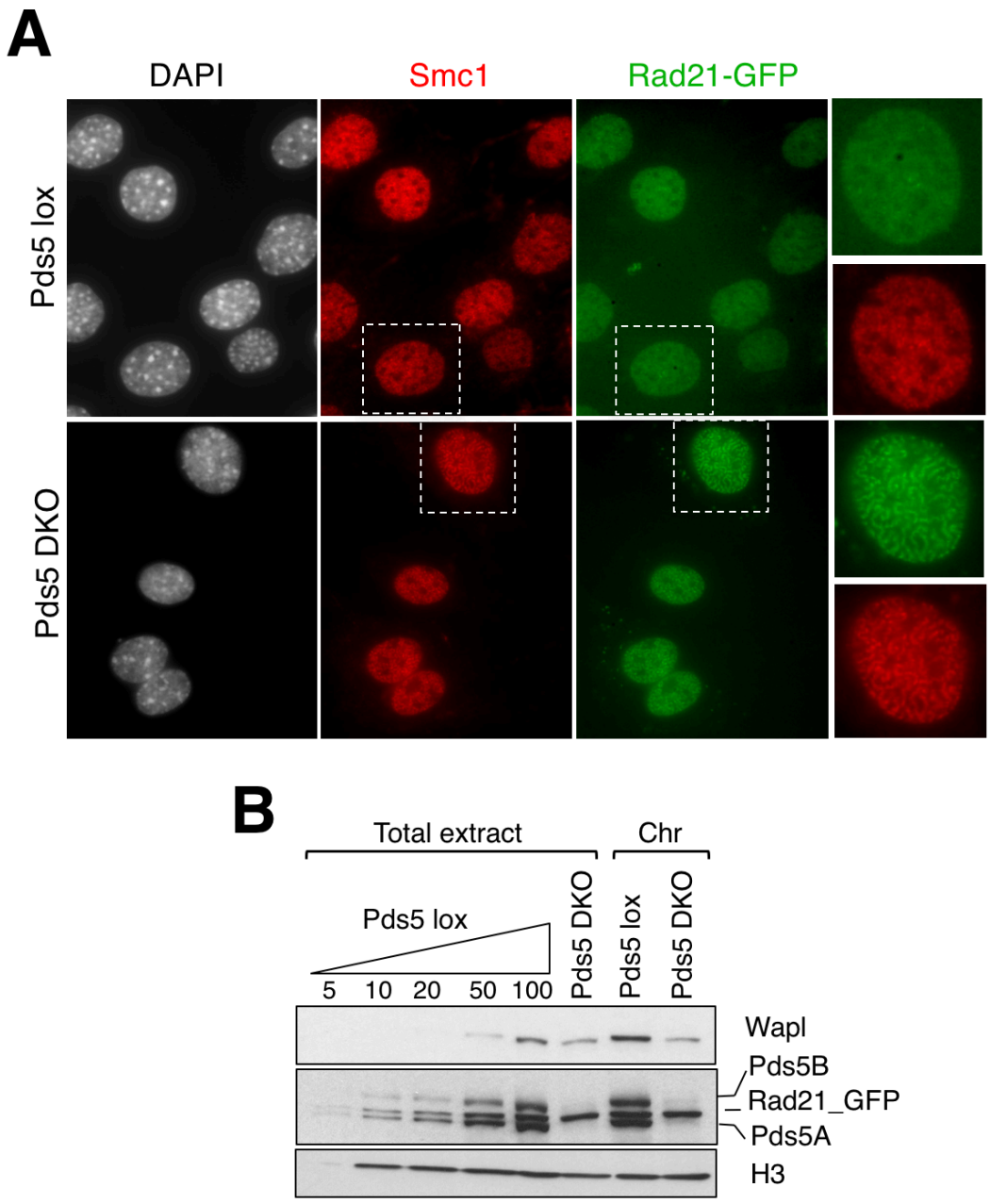

Figure R13. Vermicelli can also be observed in iMEFs expressing Rad21_GFP

A. Pds5 lox iMEFs expressing Rad21-GFP were cultured for 5 days in the presence or absence of 4-OHT and then released in rich medium for another 5 days before fixation and staining with an antibody against Smc1 (red). Vermicelli can be observed in the Pds5 DKO cells also in the Rad21_GFP (green) channel. **B.** The same cells were subject to chromatin fractionation and analyzed by immunoblot.

To rule out that *vermicelli* result from changes in antibody accessibility due to alterations in chromatin condensation we used the Rad21_GFP expressing Pds5 lox iMEFs. Upon treatment with 4-OHT for ten days to eliminate both Pds5A and Pds5B,

vermicelli were evident in the GFP channel (Figure R13A). Unlike Wapl KO cells, which show a clear increase of cohesin on the chromatin fraction, accumulation of cohesin cannot be detected by immunoblot under the same condition used to detect *vermicelli* in Pds5 DKO cells (Figure R13B). A small amount of Wapl can still be detected on chromatin as well. Nevertheless, the absence of both Pds5 proteins impairs cohesin dynamics in such a way that alters chromatin architecture to cause an excessive chromatin compaction, revealing the presence of these worm-like structures.

Together, our results highlight the importance of Pds5 proteins for cohesin dynamics. Elimination of Pds5 proteins reduces Wapl binding to chromatin, and likely prevents its proper function in cohesin release, therefore stabilizing the association of cohesin with DNA. On the other hand, it also causes a drastic reduction in the levels of Smc3 acetylation and Sororin binding, the two main drivers of cohesion establishment and stabilization. Moreover, both Pds5A and Pds5B contribute to cohesin dynamics, with no specific requirement for one or the other. This dual role of Pds5 in cohesin dynamics makes it different to other modulators.

2. Pds5 proteins contribute to determine the distribution of cohesin along the genome

Once we determined the importance of Pds5 for cohesin dynamics, we decided to assess whether Pds5 proteins affect cohesin localization along the genome. Our previous analyses of cohesin distribution by chromatin immunoprecipitation followed by deep sequencing (ChIP-seq) in primary MEFs revealed around 20 thousand positions. The majority of these positions (71%) are coincident with CTCF (Remeseiro et al., 2012b).

2.1 Pds5A and Pds5B localize at the same genomic positions

We first characterized the localization Pds5A and Pds5B along the genome by carrying out ChIP-seq analyses in two different clones of asynchronously growing wild type MEFs with specific antibodies. Peak calling using MACS2 and FDR<0.05 identified 40,524 positions for Pds5A and 48,270 positions for Pds5B, most of them common (Figure R14). Moreover, around 90% of Smc1 positions reported earlier in wild type MEFs (Remeseiro 2012) were among the positions occupied by Pds5 proteins. This

result suggests that the two Pds5 proteins do not occupy or attract cohesin to specific genomic locations.

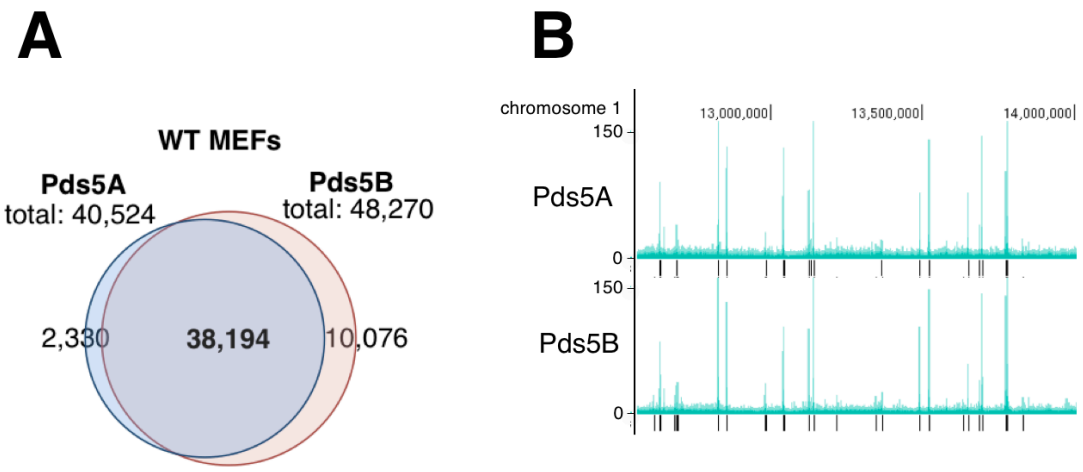

Figure R14. Similar distribution of Pds5A and Pds5B along the genome

A. Venn diagram showing the overlap of genomic positions occupied by Pds5A and Pds5B in wild type MEFs, as obtained from ChIP-seq data with specific antibodies (FDR<0.05). **B.** Snapshot of the browser showing for each data set the aligned reads (green) and called peaks underneath (black lines).

We decided to perform a new ChIP-seq experiment comparing the distribution of Smc1 in Pds5 lox and Pds5 DKO MEFs and sequence more to see if we could increase the number of positions identified. Indeed, this time we obtained 32,567 peaks in wild type (Pds5 lox) MEFs, out of which 18,377 were also present in the previous dataset. We will discuss the results of the ChIP-seq in Pds5 DKO MEFS in section 2.2. We also obtained our own dataset of CTCF positions in primary wild type (Pds5 lox) primary MEFs. We used these data to compare the distribution of cohesin, CTCF and the Pds5 proteins (Figure R15A).

A

overlap with >	Smc1 (32,567 peaks)	CTCF (75,071 peaks)
Pds5A total (40,524)	26,393 (65%)	38,329 (95%)
Pds5A only (2,330)	519 (22%)	1,538 (66%)
Pds5B total (48,270)	27,430 (57%)	43,101 (89%)
Pds5B only (10,076)	1952 (19%)	6,440 (63%)
Pds5A/B common (38,194)	26,368 (69%)	36,791(96%)

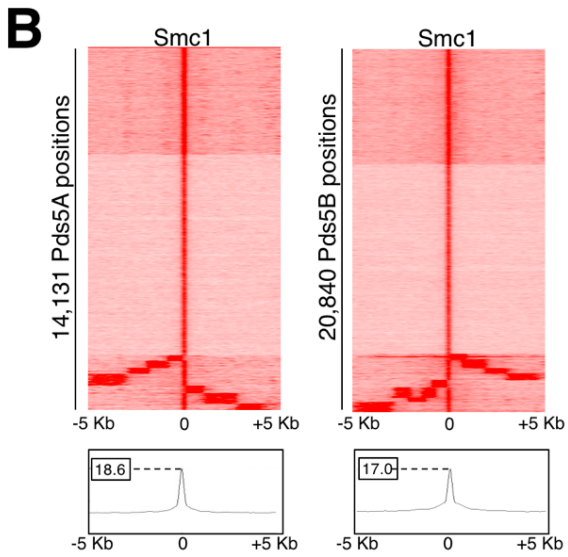

C

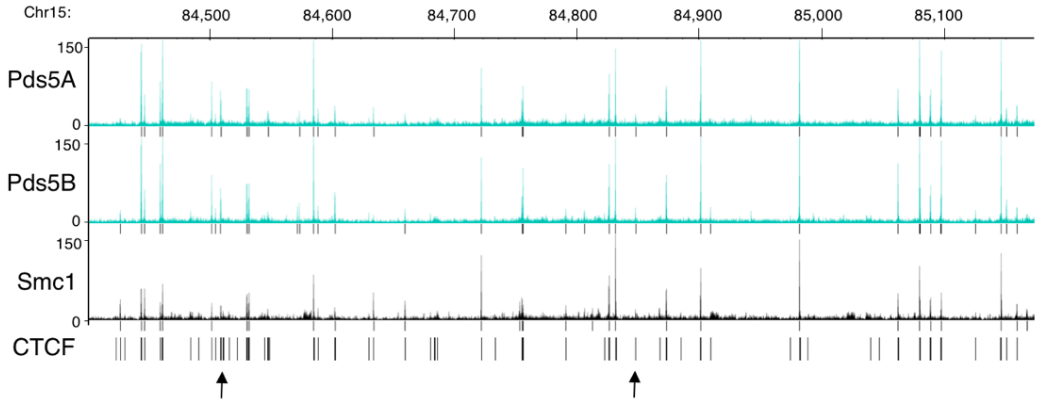

Figure R15. Characterization of Pds5A and Pds5B positions along the genome

A. Table showing the overlaps between the indicated datasets. **B.** Heatmaps (top) and plots of mean read density (bottom) of Smc1 ChIP signals around summits of Pds5A and Pds5B positions that do not overlap with an Smc1 peak. **C**. Snapshot of the browser showing ChIP-seq data tracks (read maps and called peaks) for Pds5A, Pds5B, Smc1, as well as called peaks for CTCF, in wild type MEFS. Arrows point to peaks in which a position containing both Pds5A and Pds5B does not overlap with a called peak for Smc1.

Around 65% of Pds5A positions and 57% of Pds5B positions overlap with Smc1 positions. In the rest of the Pds5A or Pds5B positions, even though there were no called peaks of Smc1, there were Smc1 ChIP-seq reads (Figure R15B; see also the positions marked with arrows in the snap shot of the browser in Figure R15C). It is therefore unlikely that these positions correspond to sites in which Pds5 proteins associate with chromatin independently of cohesin. Additionally, the overlap between Pds5A and Pds5B positions with CTCF is quite high (95 and 89%, respectively) which

suggest that these are *bona fide* cohesin positions. We speculate that the peripheral location of Pds5 proteins in the cohesin ring makes them more accessible to the antibodies compared with the Smc1 antibodies, thereby increasing the efficiency of the ChIP.

We also detected a fraction of sites specific for each Pds5 protein: 2,330 for Pds5A and 10,076 for Pds5B. Those peaks present a lower overlap with CTCF (around 60%) and poor overlap with cohesin (around 20%; Figure R15A). The number of reads in these positions was clearly lower that in the common positions (Figure R16). Thus, we suspect that the presence of cohesin at those sites is more variable in the cell population.

In summary, Pds5A and Pds5 B occupy the same positions in the genome, with only a small fraction of the sites displaying some preference for one or the other. It is therefore unlikely that Pds5A and Pds5B dictate the localization of cohesin at specific sites along the genome.

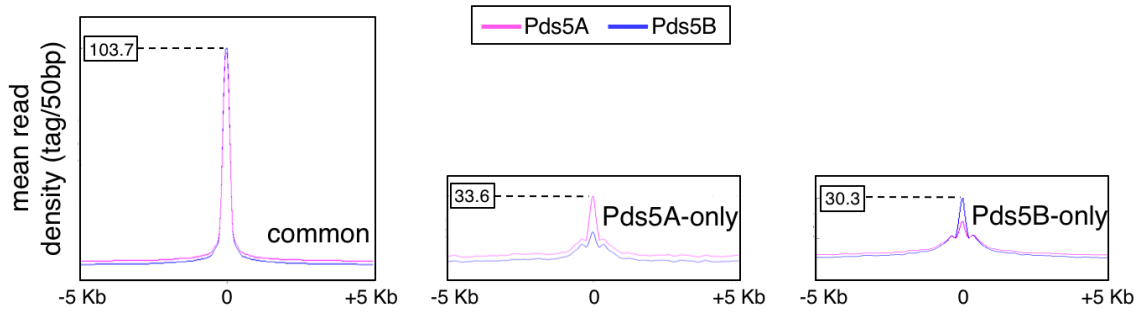

Figure R16. Positions specific for Pds5A or Pds5B are more variable in the population.

Plots of mean read density for Pds5A and Pds5B ChIP signals 5 kb around peak summits of the indicated positions (common, Pds5A-only and Pds5B-only). The boxed values correspond to average read density values.

2.2 Distribution of cohesin is restricted in Pds5 DKO cells

We next compared the distribution of cohesin in the presence of absence of the two Pds5 proteins by comparing the Smc1 ChIP-seq results obtained in Pds5 lox and Pds5 DKO MEFs, the latter treated with 4-OHT for 5 days before fixing the cells. We observed a drastic reduction in the number of cohesin positions in Pds5 DKO cells

(18,607) compared with Pds5 lox cells (32,567), but most of them (85%) were common (Figure R17A).

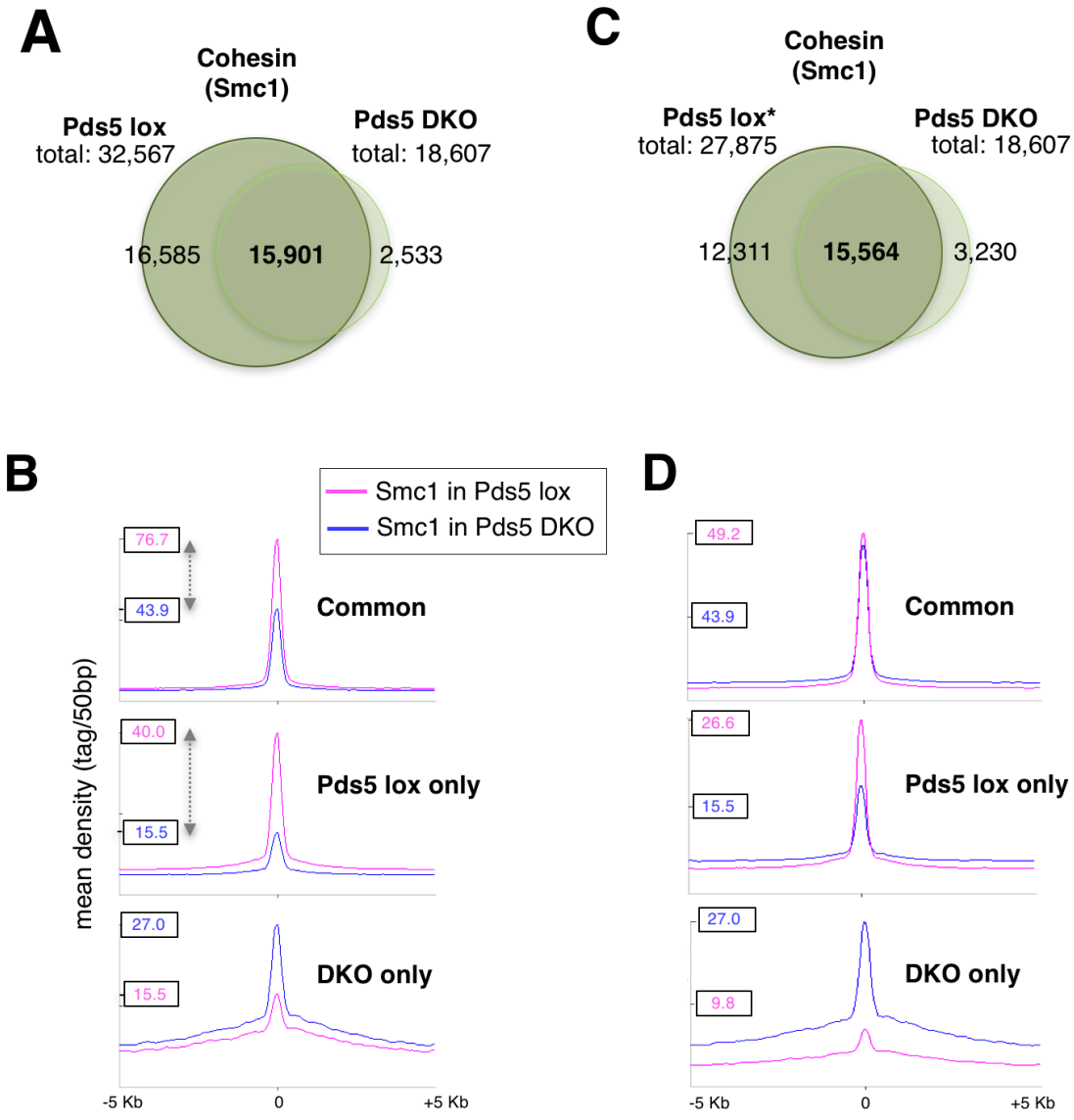

Figure R17. Subsampling of the Pds5 lox peaks does not change the overall result

A. Venn diagram showing the overlap of genomic positions occupied by cohesin (Smc1) in WT and Pds5 DKO MEFs (FDR<0.01). **B.** Plots of mean read density around peak summits of the indicated positions in Pds5 lox and Pds5 DKO MEFs. Arrows expand the difference in average read density between Pds5 lox and Pds5 DKO and show that it is larger in the peaks that disappeared than in the common positions. **C and D.** As in A and B, respectively, but using the cohesin positions in Pds5 lox MEFs obtained after subsampling the original dataset (Pds5 lox*).

We noticed that the average read density was lower in Pds5 DKO than in Pds5 lox cells even in common peaks, raising the possibility that a lower efficiency in the Pds5 DKO ChIP might explain the loss of the less robust cohesin positions (e.g., black

arrows in Figure R18). However, it was unlikely to explain the disappearance of many other strong peaks (e.g., red arrow in Figure R18). The difference in the average read density between Pds5 lox and Pds5 DKO was clearly smaller in common positions than in Pds5 lox only positions (grey arrows in Figure R17B), agains suggesting that a lowe ChIP efficiency could not explain the disappearance of all peaks. Nevertheless, we made a subsampling of the ChIP-seq reads in the Pds5 lox MEFs using the ratio of the average height of the 200 highest peaks in each condition (DKO/lox=0.606) to decrease the height of all reads in the Pds5 lox ChIP before running again the peak calling algorithm. This exercise reduced the number of called peaks in the Pds5 lox to 27,875 (Figure R17C) and eliminated the difference in average read density between the peaks in common in both conditions (Figure 17D). Still, 12,311 were lost in Pds5 DKO MEFs.

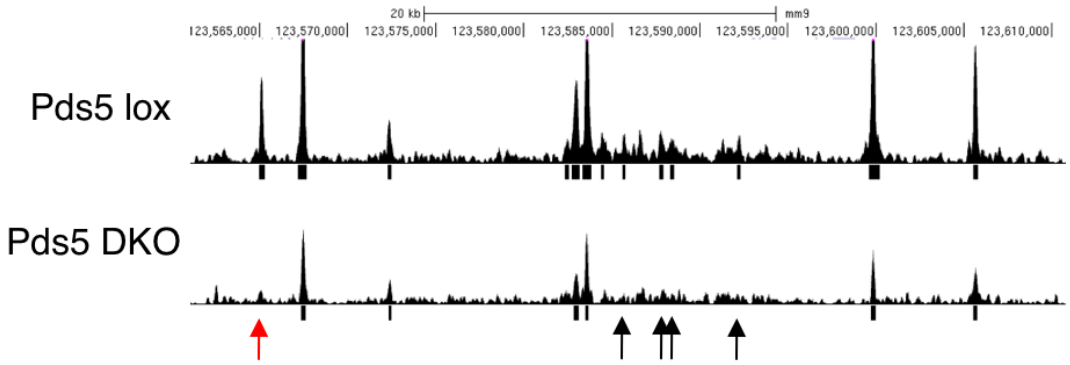

Figure R18. Cohesin positions are lost in the absence of both Pds5proteins.

Snapshot of the browser with ChIP-seq reads and called peaks for Smc1 positions in Pds5 lox and Pds5 DKO MEFs. Arrows points to positions that disappear in the Pds5 DKO MEFs.

To further confirm the disappearance of cohesin positions in Pds5 DKO MEFs compared to Pds5 lox MEFs, we chose five genomic regions were Smc1 peaks lost in Pds5 DKO were next to peaks that were maintained in both conditions, according to ChiP-seq results. By means of quantitative ChIP (ChIP-qPCR) we could validate these results since in all the selected regions we observed the clear decrease in the Smc1 ChIP signal at specific sites in Pds5 DKO MEFs (red arrows in Figure R19), as well as the maintenance of neighboring positions.

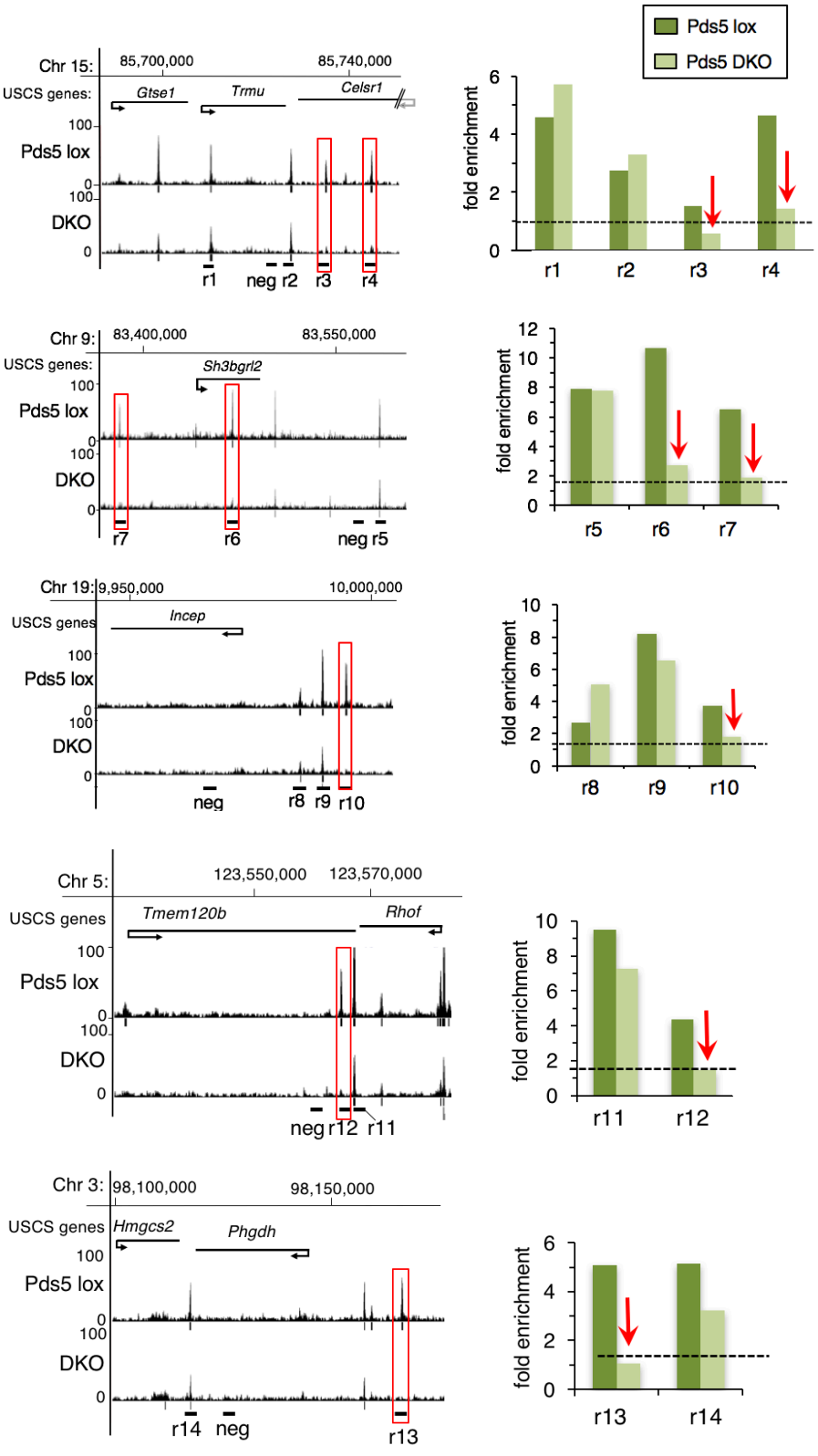

Figure R19. Validation of cohesin positions lost in Pds5 DKO cells.

Snap shots of the browser showing ChIP-seq data (read maps and called peaks) for Smc1 in Pds5 lox and Pds5 DKO cells (DKO) in different genomic regions that were validated by ChIP-qPCR. The peaks that disappear are highlighted. The graphs represent fold enrichment of ChIP signal in each region (r1 to r14) over a neighbor negative region (neg).

Once we validated the ChIP-seq data, we asked whether we could find some feature distinguishing the positions that disappeared and those that remained unchanged in the Pds5 DKO MEFs with respect to Pds5 lox MEFs. We found no differences regarding their localization in genomic features such as promoters or gene bodies (Figure R20A). As for their colocalization with CTCF, it was almost complete (98%) in the positions that remained invariable after Pds5 elimination (Figure R20B), indicating that cohesin-CTCF association is Pds5-independent. Positions only present in Pds5 lox MEFs showed a slight reduction in the overlap with CTCF (79%) compared to common positions. After subsampling, this overlap increased (87%, not shown), suggesting that peaks lost in this process might be weak cohesin positions, variable in the population. In agreement with this, Smc1 signal in the positions present only in Pds5 lox MEFs was lower than in common positions (40 versus 76, Figure R17B). Finally, the number of cohesin binding sites present only in Pds5 DKO cells was rather small (2,625) and displayed the lowest overlap with CTCF (41%, Figure R20B) and a low average read density (Figure R18B). We presume that these positions appear in a low frequency in the cell population, and probably stochastically, in the absence of Pds5 proteins.

A

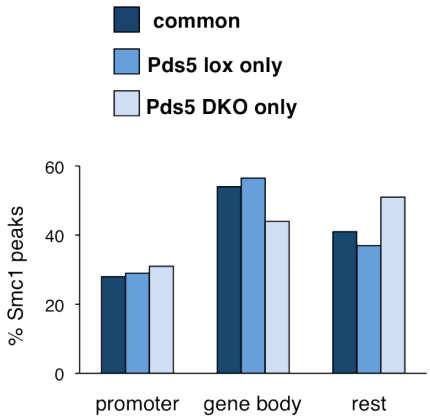

B

Overlap with >	CTCF in Pds5 lox (75,071)
Smc1 in Pds5 lox (32,567)	28,671 (88%)
Smc1 in Pds5 DKO (18,607)	16,641 (89%)
Smc1 in Pds5 lox /DKO common (15,901)	15,5211 (98%)
Smc1 in Pds5 lox only (16,585)	13,109 (79%)
Smc1 in Pds5 DKO only (2,533)	1,042 (41%)

Figure R20. Features of cohesin peaks that change in Pds5 DKO MEFs

A. Percentage of the indicated cohesin peaks present at promoters (±2.5 kb around TSS), gene bodies and intergenic regions**. B.** Table showing the overlap between the indicated categories of cohesin positions and CTCF. Percentages refer to the number of cohesin positions.

We conclude that even though Pds5A and Pds5B do not specify cohesin localization, their simultaneous absence restricts genome-wide distribution of the

complex. The mechanisms that dictate this restriction could be related with the importance of Pds5 proteins for the dynamic behavior of cohesin.

2.3 Pds5 affects cohesin distribution differently from Wapl

As Wapl releasing activity requires Pds5, if the changes in cohesin distribution seen in Pds5 DKO cells are due to impaired regulation of cohesin dynamics, we might expect Wapl elimination to result in similar changes. In fact, it has been reported that the genome wide distribution of cohesin in MEFs changes in the absence of Wapl (Tedeschi et al., 2013). In order to compare the results in Pds5 DKO and Wapl KO cells, we reanalyzed cohesin (Smc3) ChIP-seq raw data from Wapl proficient and Wapl deficient MEFs from *Tedeschi et al.* using the same peak-calling algorithm that we applied for the Smc1 ChIP-seq in Pds5 DKO MEFs. Although Wapl proficient MEFs used in that study were in fact heterozygous (Wapl -/lox), for simplicity here we will refer to them as Wapl WT and use Wapl KO for Wapl -/Δ MEFs.

Our analysis identified 44,750 and 57,243 cohesin (Smc3) peaks in Wapl WT and Wapl KO MEFs, respectively, out of which 29,681 (66% of the smaller dataset) were present in both conditions, similar to the proportion reported in the original analysis (Figure R21A). Around 90% of cohesin (Smc1) positions in Pds5 lox MEFs coincided with cohesin (Smc3) positions in Wapl WT MEFs, which supports the robustness of the data (Figure R21B, green colored cell). Importantly, the 15,069 peaks that disappeared and the 28,577 peaks that appeared after Wapl elimination were quite different from those changing in Pds5 DKO MEFs. Moreover, half of the positions that were lost in Pds5 DKO cells were retained in the absence of Wapl (Figure R21B, pink colored cell), including most of the peaks absent in Pds5 DKO MEFs that were validated by ChIP-qPCR in Figure R19. This result points to the different contributions of Wapl and Pds5 to cohesin distribution along the genome. We speculate that cohesin acetylation, which is dramatically decreased only in the absence of Pds5 proteins could underlie this different behavior. We based our hypothesis in a recent study showing that, at least *iin* vivo, Smc3 increases the translocation of cohesin along DNA (Kanke 2016).

A

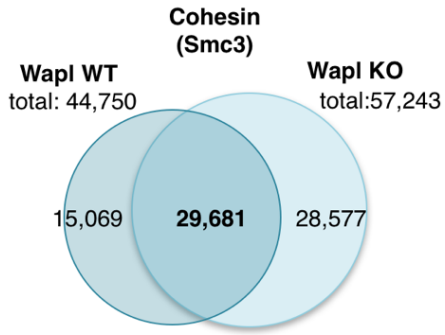

B

	Smc3 Wapl WT (44,750)	Smc3 gone Wapl WT (15,069)	Smc3 new Wapl WT (28,577)	Smc3 invariable (29,681)
Smc1 Pds5 lox (32,567)	29,311 (90%)	5,724 (18%)	1,062 (3%)	24873 (76%)
Smc1 gone DKO (16,585)	12,709 (77%)	4,708 (28%)	769 (5%)	8049 (48%)
Smc1 new DKO (2,533)	649 (26%)	65 (3%)	372 (15%)	586 (23%)

Figure R21. Different contributions of Wapl and Pds5 to cohesin distribution

A. Venn diagram showing the overlap of genomic positions occupied by cohesin (Smc3) in Wapl WT (-/lox) and KO (-/Δ) MEFs after reanalysis of data from Tedeschi et al. (2013), FDR <0.01.**B.** Comparison of the indicated subsets of cohesin positions coming from Smc1 and Smc3 ChIP-seq data in Pds5 lox and Pds5 DKO (DKO) and Wapl WT and Wapl KO MEFs. Percentages refer to Smc1 positions.

2.4 Similar distribution of cohesin in Pds5A KO and Pds5B KO cells

Next, we asked if the absence of either Pds5A or Pds5B also altered cohesin localization at specific sites. To answer that question, we performed ChIP-seq of cohesin (Smc1) in Pds5A KO and Pds5B KO MEFs and identified 17,973 positions and 19,332 positions, respectively. Both conditions showed a very similar although not identical distribution of cohesin (Figure R22A). All positions presented a high overlap with CTCF, 97% in those present in both Pds5A KO and Pds5B KO cells, and a bit lower (86%) in those specifically found in either one (Figure 22C). Overlap with Smc1 was also high, above 90%. However, many peaks were also lost, as in Pds5 DKO cells.

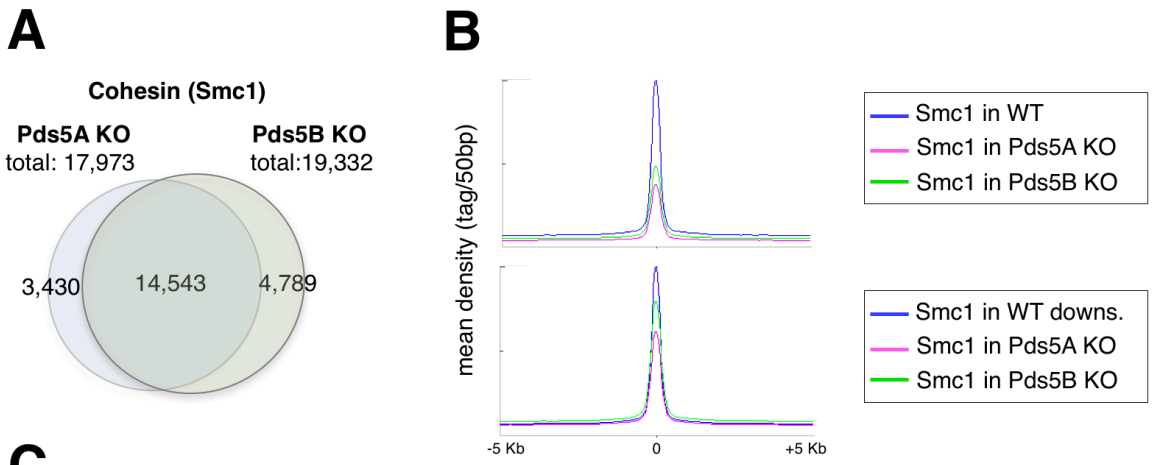

C

overlap with >	CTCF (75,071 peaks)	Smc1 (32,567 peaks)	Smc1 downsampled (27,875 peaks)	Smc1 in Pds5 DKO (18,607 peaks)
Smc1 in Pds5A KO total (17,973)	16,993 (95%)	16,882 (94%)	16,356 (91%)	13,030 (80%)
Smc1 in Pds5B KO total (19,332)	18,111 (94%)	17,996 (93%)	17,438 (93%)	13,293 (76%)
Smc1 in Pds5A/B KO common (14,543)	14,115 (97%)	14,264 (98%)	14,119 (97%)	11,765 (83%)
Smc1 in Pds5A KO only (3,430)	2,965 (86%)	2,606 (76%)	2,243 (65%)	1,285 (57%)
Smc1 in Pds5B KO only (4,789)	4,099 (86%)	3,776 (79%)	3,303 (69%)	1,535 (46%)

Figure R22. Cohesin distribution in Pds5A KO and Pds5B KO MEFs.

A. Venn diagram showing the overlap of genomic positions occupied by Smc1 in MEFs deficient for one or the other Pds5 protein (FDR<0.05). **B.** Plots of mean read density around peak summits of Smc1 in positions common for Pds5 lox (complete, top; downsampled, bottom), Pds5A KO and Pds5B KO MEFs. **C.** Table showing overlaps between the indicated categories of genomic positions. Percentages refer to the number of Smc1 positions shown in the column on the left.

A fraction of cohesin positions may be lost due to experimental reasons. For the ChIPs of cohesin in Pds5A KO and Pds5B KO MEFs we obtained 33 and 44 millions of valid reads, respectively, while we had 57 million reads for Pds5 lox cells. Although we could observe a 98% overlap between our ChIP-seq in Pds5 lox and the common positions identified in both Pds5A KO and Pds5B KO MEFs, there were clear differences in the height of those peaks (Figure R22B). The positions with less robust peaks, i.e. those that are more variable in the population, may not reach statistically significant enrichment when a lower number of reads is used for peak calling. When we

compared cohesin positions in Pds5A KO and Pds5B KO MEFs with the positions obtained after subsampling the cohesin positions in Pds5 lox MEFs (as in Figure R17C), we obtained more comparable average read densities of Smc1 signals (Figure R22B). The use of this dataset instead of the total number of cohesin positions in Pds5 lox MEFs barely altered the overlap with positions in Pds5A KO and Pds5B KO, supporting our hypothesis that we might be missing those peaks with less robust cohesin signals (Figure R22C).

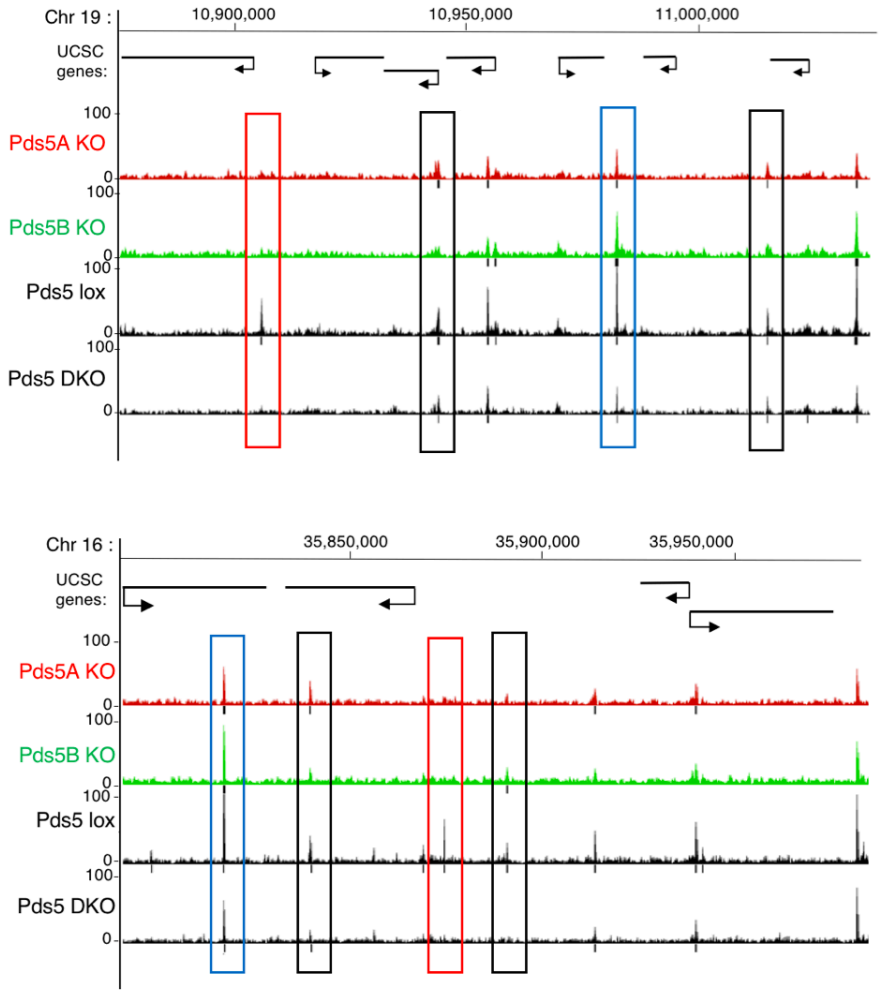

Figure R23. Some cohesin positions are sensitive to Pds5 dosage

Snap shots of the browser in two different genomic regions showing ChIP-seq data (read maps and called peaks below) for Smc1 in Pds5A KO, Pds5B KO, Pds5 lox and Pds5 DKO. Examples of peaks that disappear in all three KOs are indicated with red rectangles, and are located close to peaks maintained in all conditions (blue rectangles). Smaller peaks that are reduced in all three KOs are called or not by the peak calling algorithm (black rectangles).

Close inspection of the browser showed that some cohesin positions in Pds5 lox MEFs were clearly lost in either Pds5A KO, Pds5B KO or Pds5 DKO MEFs (e.g., red rectangles in the regions shown in Figure R23). For other positions to disappear, however, simultaneous elimination of Pds5A and Pds5B was required. For example, of the 14,115 cohesin peaks present in both Pds5A KO and Pds5B KO MEFs, only 11,765 remain in Pds5 DKO (Figure R22C). In other cases, the Smc1 ChIP signals were reduced in all three KOs compared to Pds5 lox, but whether the peak was still called or not depended on the surrounding signals (e.g., black rectangles in Figure R23).

Similarly, among the peaks from five genomic regions validated by ChIP-qPCR in Figure R19, we observed that 2 of the 7 peaks that were lost in Pds5 DKO, were also lost in Pds5A KO and Pds5B KO cells (r7 and r13); r6 was lost only in Pds5 DKO cells and for the other 4 peaks the behavior was different in Pds5A KO and Pds5B KO cells. Of note, these peaks in which the two KOs behaved differently were similarly occupied by Pds5A and Pds5B in wild type cells (Figure R24).

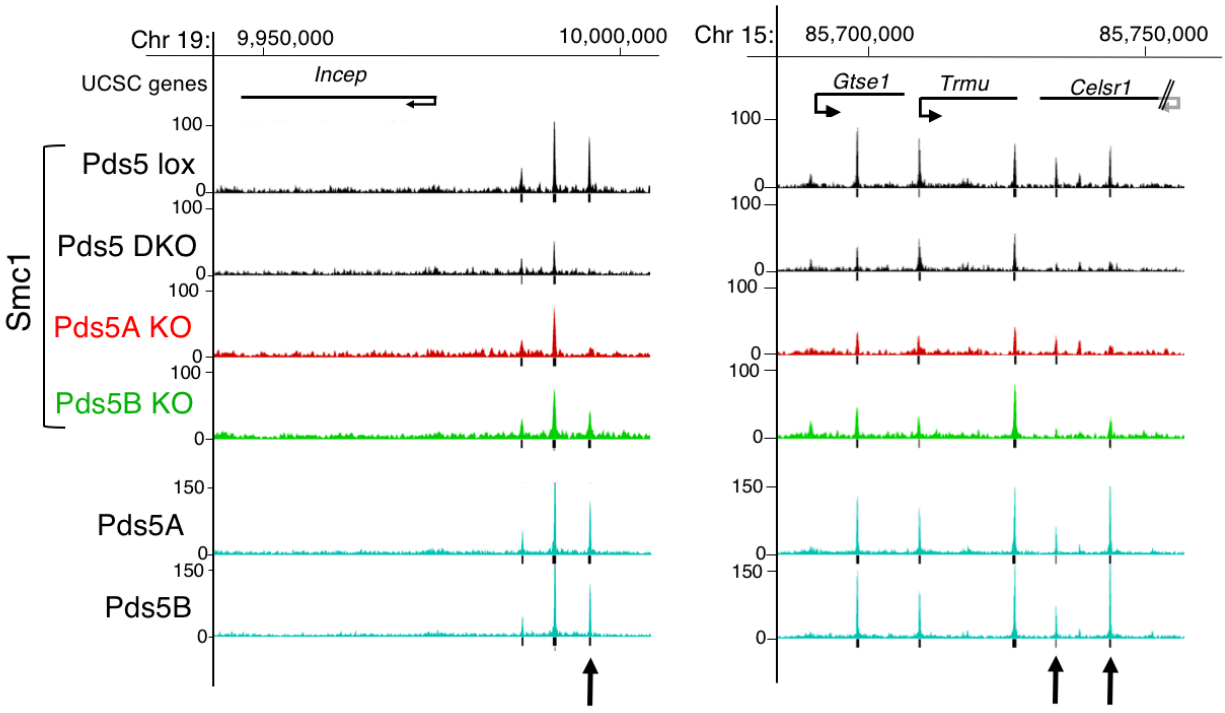

Figure R24. No clear preference for Pds5A or Pds5B at positions that disappear specifically in either Pds5A KO or Pds5B KO MEFs

Snap shots of the browser in two of the regions validated by ChIP-qPCR in Figure R19 showing cohesin ChIP-seq tracks for cells of the indicated genotypes as well as the tracks for Pd5A and Pds5B distribution in wild type MEFs. The arrows point to positions that are lost in Pds5 DKO MEFs and in which a different behavior is observed for Pds5A KO and Pds5B KO MEFs.

Overall, we conclude that there are cohesin positions in the genome that are particularly sensitive to lower dosage of Pds5 proteins while in others the presence of one of the Pds5 proteins is sufficient. Given the almost identical distribution of Pds5A and Pds5B along the genome, it is unclear why some positions disappear specifically in the absence of one or the other protein.

3. Transcriptional alterations in Pds5 deficient cells

Having determined the effect of Pds5 proteins in cohesin distribution and dynamics, we set out to assess the consequences of Pds5 elimination in cohesin functions beyond cohesion establishment. As mentioned in the introduction, one such function is the regulation of gene expression.

3.1 Pds5 elimination affects transcriptional regulation

We first compared the transcriptome of cells with and without both Pds5 proteins. For that, we performed RNA sequencing (RNA-seq) in three clones of Pds5 lox MEFs growing asynchronously in media with or without 4-OHT. Applying an FDR<0.05 and a threshold of fragments per kilobase million (fpkm)>3 in at least one of the two conditions compared, 364 differentially expressed genes (or DEGs) were identified, with 219 genes upregulated and 145 downregulated in Pds5 DKO MEFs (represented in red in Figure R25A). The extent of the deregulation corresponded to log2 fold change between -4 and +6.3. Gene Set Enrichment Analysis (GSEA) showed “Cell Cycle” and “DNA replication” pathways among those most significantly downregulated in the absence of the two Pds5 proteins (Figure R25B).

To assess if these gene expression changes correlated with the changes in cohesin distribution identified by ChIP-seq analyses, we compared cohesin occupancy around the Transcription Start Sites (TSSs) of the DEGs. Around half of the DEGs had cohesin peaks close to the TSS. Average signal density for Smc1 at TSSs appeared to decrease more in the downregulated genes than in upregulated or invariant genes (Figure R26), suggesting that the presence of cohesin in the downregulated genes could contribute directly to promote their transcription.

A

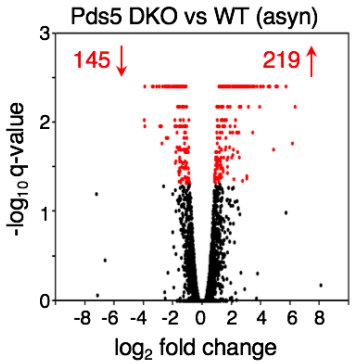

B

Downregulated	Upregulated
Ribosome	Olfatory transduction
Cell Cycle	Cytokine/cytokine receptor interaction
DNA Replication	Retinol Metabolism
Pyrimidine metabolism	Neuroactive Ligand/receptor interaction
Purine metabolism	Oxidative phosphorylation
Adherens junction	Alzheimer's disease

Figure R25. Gene expression changes in Pds5 deficient cells

A. Volcano plot representation of gene expression changes in asynchronously growing Pds5 proficient and deficient MEFs after RNA-seq analyses. RNA was obtained from 3 clones growing asynchronously for 5 days ± 4-OHT. Significant deregulated genes (FDR<0.05) appear in red. **B.** KEGG pathways most significantly deregulated in Pds5 DKO MEFs according to GSEA.

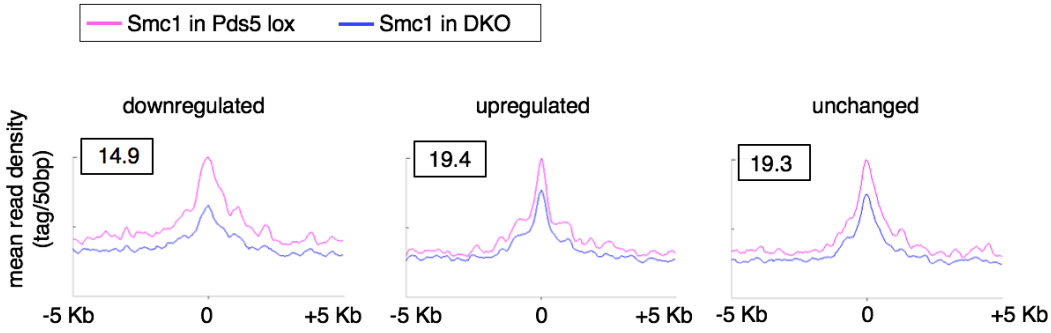

Figure R26. Cohesin occupancy around promoters of DEGs

Plots of cohesin (Smc1) mean read density in Pds5 lox and Pds5 DKO MEFs around the TSSs of genes that are downregulated, upregulated or invariant after elimination of Pds5 proteins.

Cell cycle analysis by flow cytometry revealed a higher percentage of G1 cells and a reduced S phase population in Pds5 DKO cells (Figure R27A). It was therefore possible that some of the gene expression changes observed were an indirect consequence of the different cell cycle profiles in the Pds5 lox and Pds5 DKO MEFs. To eliminate this possibility, we repeated the RNA-seq analyses in cells arrested in G0 (Figure R27B). In this case 306 DEGs were identified, out of which 206 were upregulated and 100 were downregulated in Pds5 DKO MEFs (Figure R28A). The

extent of deregulation was narrower, with log2 fold change ranging from -3.2 to +3.1. Around one third of the DEGs (96) were found both in asynchronous and G0 arrested cells (Figure R28B). The downregulation of cell cycle and DNA replication pathways could still be observed in this condition although with lower statistical significance. Among the genes affected only in G0-arrested cells we found several genes involved in cancer pathways like Wnt and p53 signaling (Figure R28C).

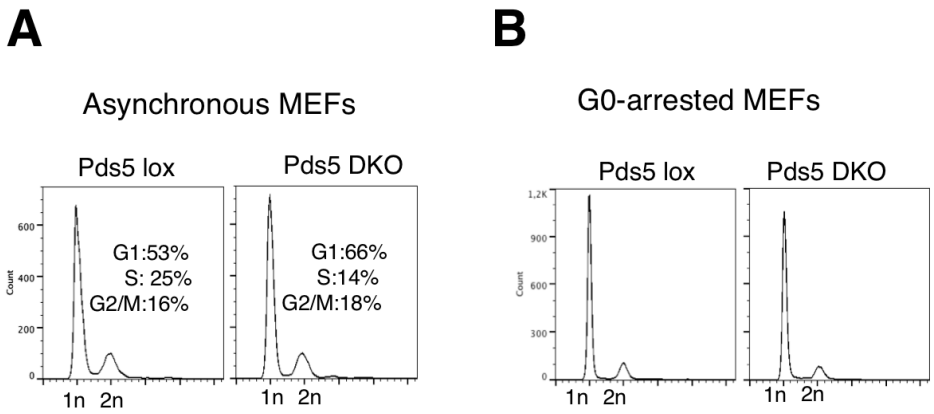

Figure R27. Cell cycle profiles of Pds5 lox and Pds5 DKO cells

Cell cycle profiles obtained by fluorescence-activated cell sorting (FACS). Percentages of each cell cycle phase in (A) were calculated using Flow Jo software. The 2n population in G0 arrested cells, kept for 5 days in confluence and 0.1% serum, most likely corresponds to polyploid cells.

Wapl depletion also affects gene expression (Tedeschi et al., 2013). We compared our results with those from microarray analyses for Wapl WT and Wapl KO MEFs arrested in G0 in which 300 DEGs were identified, 163 downregulated and 138 upregulated Interestingly, only 20 genes were changed in both conditions (Figure R28D). Thus, consistent with the different distribution of cohesin in Pds5 and Wapl deficient cells, their gene expression profiles are different as well.

3.2 Distinct outcomes of Pds5A and Pds5B elimination in transcriptional regulation

To explore the contribution of each Pds5 protein to transcriptional regulation, we also performed RNAseq in three independent clones of asynchronously growing Pds5A KO, Pds5 BKO and wild type MEFs. We found 2,563 DEGs in Pds5A KO cells (1,193 up

and 1,370 downregulated) and 1,080 DEGs in Pds5BKO (662 up and 418 downregulated), out of which 497 were common (Figure R29A). The number of DEGs in Pds5A KO or Pds5B KO MEFs is therefore much bigger than in Pds5 DKO MEFs. One reason may be that, in the case of Pds5 DKO, the same clone of MEFs is treated or not with tamoxifen for 5 days to induce deletion of Pds5 genes so we can see early defects caused directly by Pds5 protein elimination. Pds5 single KOs are constitutive knockouts, and we are comparing cells from different embryos, so we might be observing changes in gene expression due to the accumulation of errors and the adaptation to the lack of a particular Pds5 isoform.

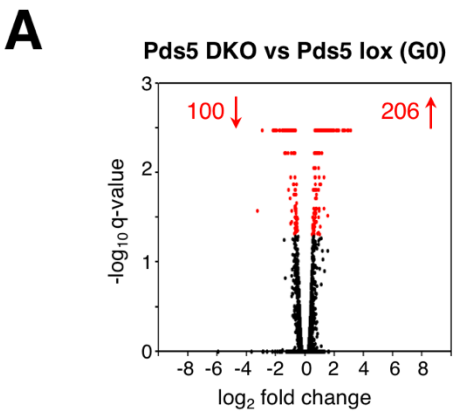

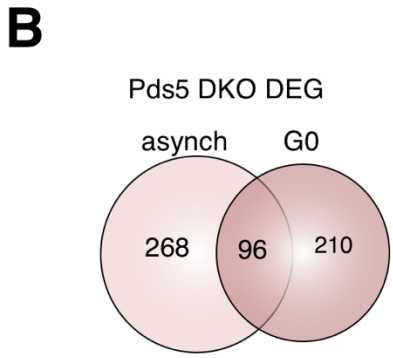

C

Downregulated	Upregulated
Pathways in cancer	Ubiquitin mediated proteolysis
ECM receptor interaction	Lysosomes
Base excision repair	Proteasome
Dilated cardiomiopathy	Parkinsons disease
Focal adhesion	Axon guidance
Hypertrophic cardiomiopathy	Oxidative phosphorylation

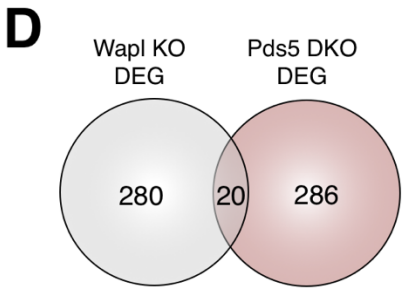

Figure R28. Gene expression changes in quiescent cells lacking Pds5 or Wapl

A. Vulcano plot representation of gene expression changes between Pds5 lox and Pds5 DKO MEFs arrested in G0 for 5 days ± 4-OHT. Significant deregulated genes (FDR<0.05) appear in red. **B**. Venn diagram showing the overlap between DEGs found in asynchronous or G0-arrested condition. All common genes changed in the same direction except one (Ptx3). **C**. KEGG pathways most significantly deregulated in quiescent Pds5 DKO MEFs according to GSEA. **D.** Venn diagram showing the overlap between DEGs found in G0-arrested Pds5 DKO MEFs and Wapl KO MEFs.

We found that 230 Pds5A KO DEGs and 107 Pds5B KO DEGs were also among Pds5 DKO DEGs, and 71 were common in the three conditions (Figure R29B). Around 25% of Pds5DKO DEGs are deregulated neither in Pds5A KO nor in Pds5B KO MEFs, suggesting some redundancy in the regulation of these genes. GSEA of Pds5A KO deregulated genes revealed many commonalities with the most significantly downregulated pathways in Pds5 DKO MEFs, including "Cell Cycle" and "DNA Replication" (Figure R30A). Among the affected genes, we found reduced transcription of master cell cycle regulators such as c-Myc and E2f4 and increased transcription of repressors such as the suppressor Rb. In contrast, cell cycle genes were not deregulated in Pds5B KO MEFs, although we could identify alterations in individual genes involved in control of the cell cycle, such as the upregulation of the tumor suppressor Growth arrest specific 1 (Gas1). Among the upregulated pathways there were some previously found also in Pds5 DKO cells, like "Retinol metabolism" or "oxidative phosphorylation" (Figure R30B). Moreover, cell cycle regulators found among Pds5A KO DEGs (c-Myc, E2f4 and Rb) showed noticeable deregulation in Pds5 DKO MEFs, although the changes were above FDR=0.05. Gas1 was found to be significantly upregulated both on Pds5 DKO and Pds5B KO MEFs.

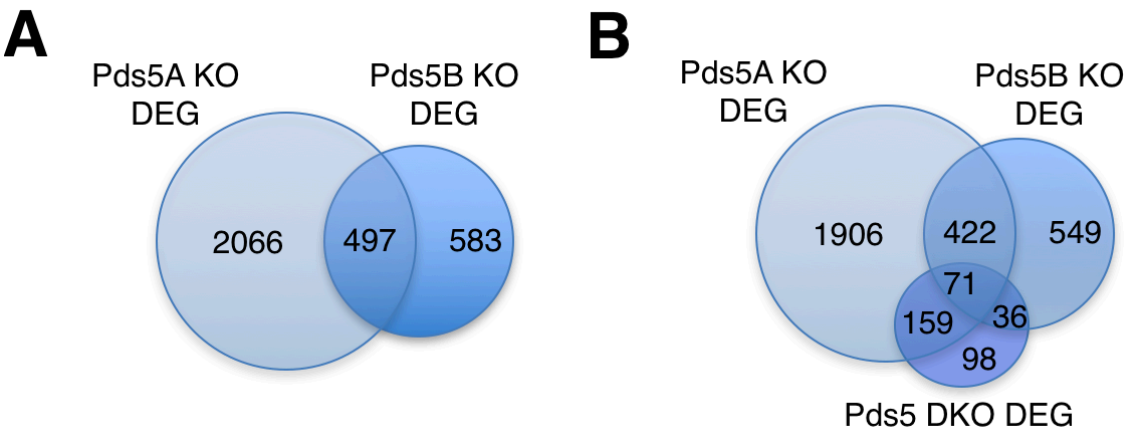

Figure R29. Gene expression changes in the absence of Pds5A or Pds5B

Venn diagrams showing the overlap between DEGs identified for the indicated genotypes. RNA was obtained from 3 clones each of Pds5A KO, Pds5B KO and wild type MEFs growing asynchronously.

Thus, many of the gene expression changes observed in Pds5 DKO MEFs might result from the combination of independent effects of the absence of Pds5A and Pds5B. This is in contrast with the findings reported in the previous sections showing

the similar distribution of Pds5A and Pds5B along the genome and the similar effect of depleting one or the other Pds5 protein on cohesin distribution. It is possible that the role of Pds5 proteins on gene expression is not strictly related to the regulation of cohesin distribution but with the regulation of its dynamic association to chromatin.

A

Pds5A KO

Downregulated	Upregulated
Ribosome	Cell adhesion molecules
Cell Cycle	Autoimmune thyroid disease
DNA Replication	Asthma
Pirimidine metabolism	Glycan Structures
Mismatch Repair	Arachidonic acid metabolism
Nucleotide excision repair	Drug metabolism cytochrome p450

B

Pds5 BKO

Downregulated	Upregulated
Biosynthesis of steroids	Drug metabolism cytochrome p450
C21 steroid hormone metabolism	Ribosome
Thyroid cancer	Metabolism of xenobiotics by cytochrome p450
Caffein metabolism	Retinol metabolism
VEGF signaling pathway	Oxidative phosphorylation
ERBB signaling pathway	Parkinson disease

Figure R30 Gene expression changes in the absence of Pds5A or Pds5B

KEGG pathways most significantly deregulated in Pds5A KO and Pds5B KO MEFs according to GSEA.

4. Pds5 elimination affects cell cycle progression

4.1 Pds5 elimination blocks cells in G0/G1

Our transcriptome analyses together with cell cycle profiles of asynchronous cells pointed to cell cycle progression defects in Pds5 DKO cells. In order to study the first cell cycle without the two Pds5 proteins, we decided to eliminate both Pds5A and Pds5B in G0 arrested cells and follow their re-entry in the cell cycle. Pds5 lox MEFs were seeded on plates and once they had reached confluency, serum was withdrawn for 5 days to while 4-OHT was added to induce Pds5 deletion (Figure R31A). At the time of release into rich medium, the extent of depletion of the two Pds5 proteins was assessed by immunoblot (Figure R31B).

To monitor entry in S phase, cells were incubated for 30 minutes with 5-Bromo-2-Deoxyuridine (BrdU) before collecting them at different times after serum stimulation and the incorporation of the thymidine analogue was then measured by flow cytometry (Figure 32A). We found a clear reduction in the percentage of BrdU positive cells in Pds5 DKO cells at all times (Figure 32B).

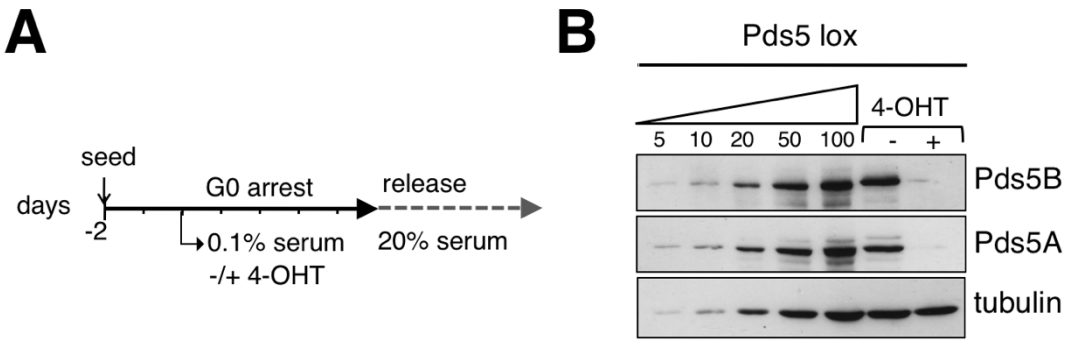

Figure R31. Protocol to examine cell cycle re-entry without Pds5 proteins

A. Scheme of the experiment to deplete both Pds5 proteins in conditions of G0 arrest (confluence and low serum) before releasing them into rich medium (20% serum) to analyze their progression through S phase. **B**. Immunoblot analyses to estimate the extent of depletion of Pds5A and Pds5B at the time of release in the cells treated with 4-OHT (Pds5 DKO cells). Decreasing amounts of an extract of Pds5 lox cells were loaded for comparison. Tubulin, loading control.

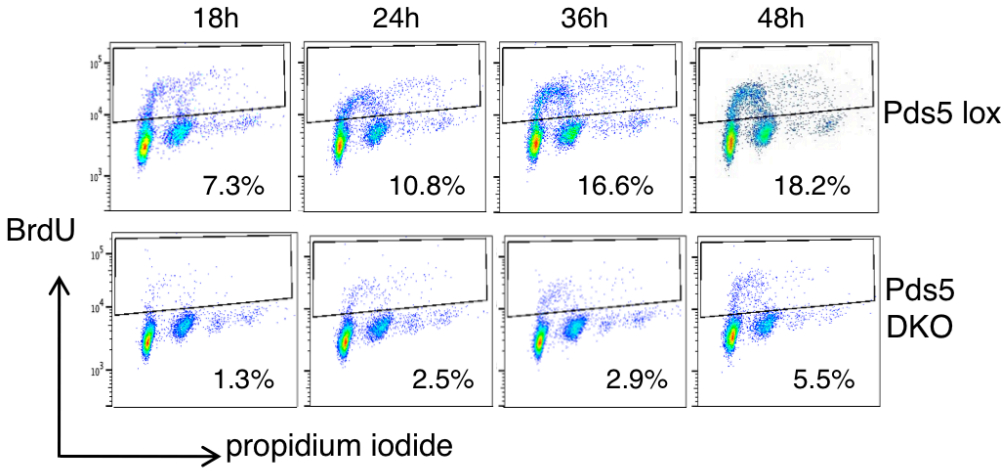

Figure R32. Impaired entry in S phase in the absence of Pds5 proteins

BrdU incorporation profiles at different time points in Pds5 lox and Pds5 DKO MEFs after release from G0 arrest. The percentage of cells that incorporated BrdU during a 30-min pulse is indicated.

As an alternative approach to assess progression into S phase, quiescent MEFs growing on coverslips were released into 20% serum in the continuous presence of ethynyl-29-deoxyuridine (EdU), a thymidine analog that is incorporated in replicative cells. Coverslips were collected at several times after release, immunostained and EdU

positive cells counted under the microscope to estimate the cells in S phase in each timepoint (Figure R33A). Using this assay, we calculate the ability of the population to enter at least once in S phase during the first three days after G0 release. Pds5 lox MEFs entered in S phase almost immediately after G0 release, with the vast majority going through replication at least once within the first 48 hours (Figure R33B). In contrast, Pds5 DKO cells showed a clear defect in S phase entry, with less than 40% of the cells showing some EdU staining 72 hours after release. We thought that the Pds5 DKO cells that entered S phase might have some remaining Pds5 proteins. We co-stained the cells with a mixture of Pds5A and Pds5B antibodies while developing the EdU signal but could not find a clear correlation between cells with higher levels of Pds5 and EdU signals (Figure R33C).

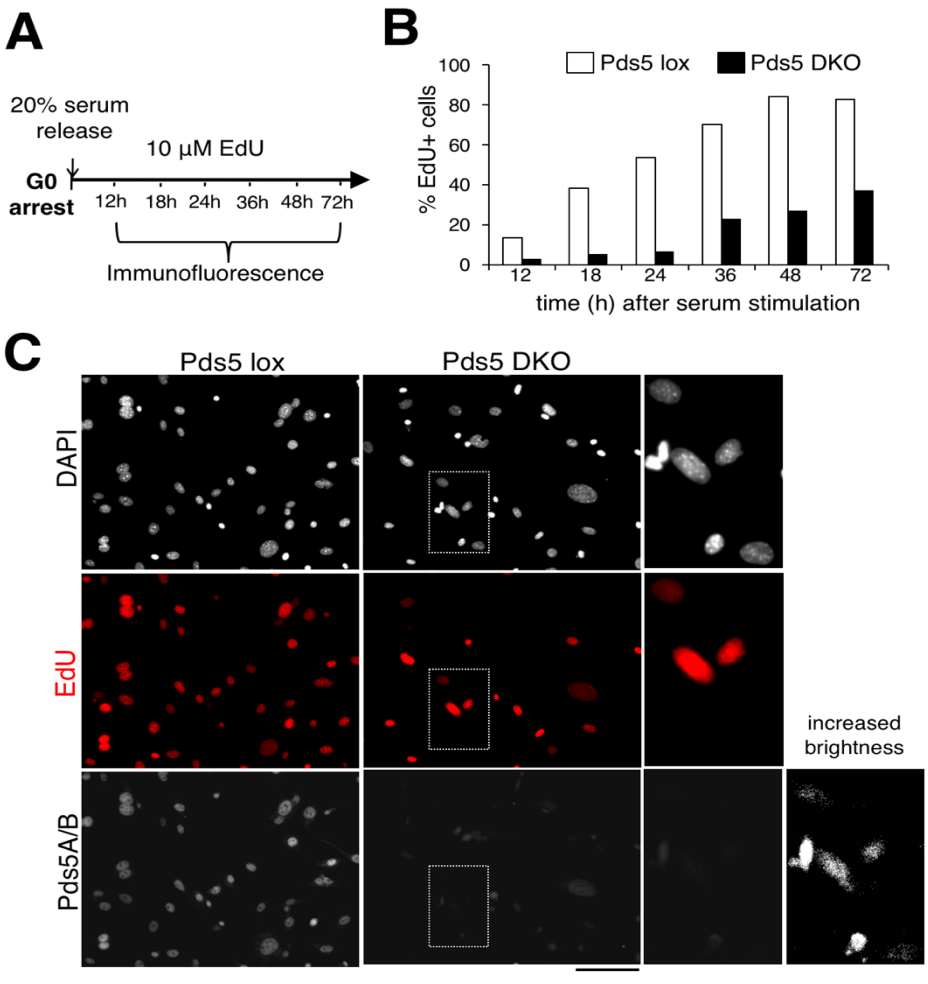

Figure R33 Impaired entry in S phase in the absence of Pds5 proteins

A. Scheme of the experiment. **B**. The fraction of EdU positive cells was assessed by microscopy; 500 cells were counted per time point. **C.** Images of cells taken 72 h after serum stimulation. EdU detection (red) was combined with immunostaining with a mixture of Pds5A and Pds5B antibodies (Pds5, lower panels). Scale bar, 100 μm.

4.2 Impaired preRC assembly in Pds5 deficient cells

Initiation of DNA replication requires assembly of the pre-replicative complex (preRC) at the origins and its subsequent licensing. PreRC consist of the origin recognition complex (ORC), Cdc6, Cdt1 and minichromosome maintenance (MCM) proteins. As Pds5 DKO cells failed to enter in S phase, we asked whether assembly of preRC on chromatin was affected under this condition. We used chromatin fractionation followed by immunoblot to analyze the proteins bound to chromatin at different times after release from a 5-day G0 arrest (Figure R34). Two components of the preRC, Mcm3 and Cdc6, showed an impaired binding to chromatin in Pds5 DKO compared to Pds5 lox cells. Interestingly, levels of these proteins in whole cell extracts were also very reduced, suggesting a defect in their synthesis. We also observed, as mentioned previously, that levels of both Pds5 proteins in wild type (Pds5 lox) cells are significantly reduced at the time of release compared to their levels after 30 hours in high serum (compare lane 1 and 6 in Figure R34).

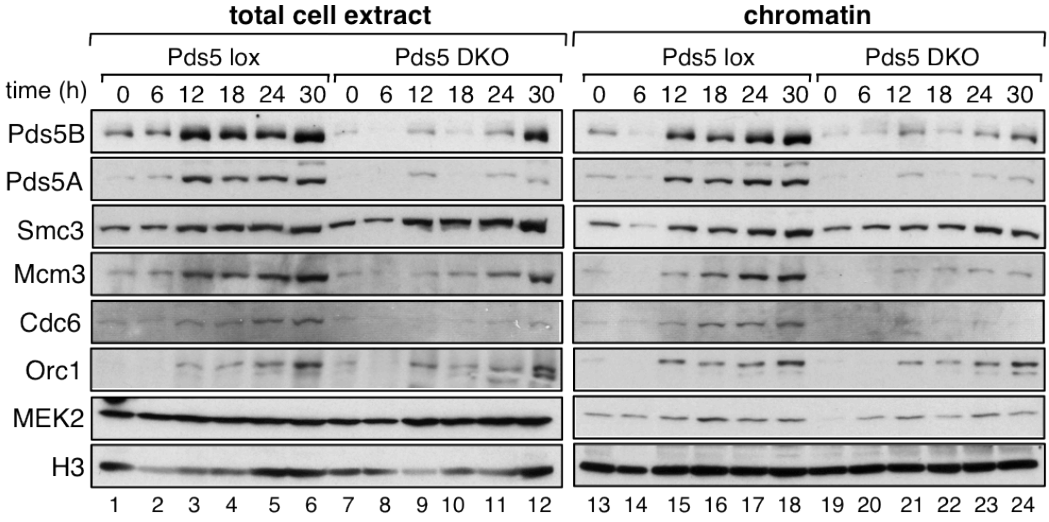

Figure R34. Impaired preRC complex assembly in Pds5 DKO cells

Immunoblot analyses of total cell extract and chromatin fractions of Pds5 lox and Pds5 DKO MEFs at the indicated time points after serum stimulation. Components of the preRC appear in red. MEK2 is a cytoplasmic kinase. Histone H3 is an abundant component of chromatin

To assess if the lower levels of preRC components in the Pds5 DKO cells were the results of transcriptional downregulation, we analyzed transcript levels of the corresponding genes at early time points after release from G0 arrest by quantitative PCR (Figure R35). Levels of Mcm3, Cdc6, Cdt1 and Orc1 as well as Cyclin A2, used

as a control of cell cycle progression, were clearly lower in Pds5 lox cells than in Pds5 DKO cells, while transcript levels of cohesin Smc3 or the cohesin loader NIPBL were similar in both conditions. We thus conclude that the absence of the two Pds5 proteins alters transcription and therefore re-accumulation of preRC components after the G0 arrest, which in turn impairs entry into S phase.

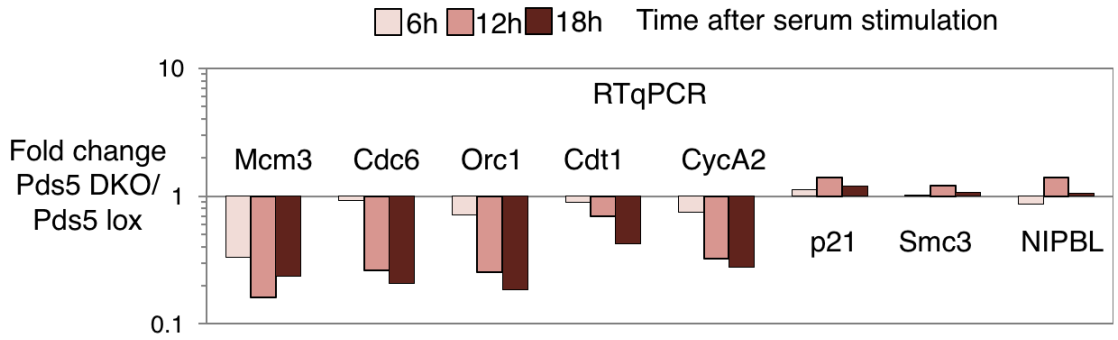

Figure R35. Transcriptional reactivation of genes encoding preRC components is delayed in Pds5 DKO cells

Quantitative PCR analyses of the mRNA levels of genes encoding replication initiator proteins, cell cycle regulators (CycA2 and p21) and cohesin (Smc3) and its loader (NIPBL). Bars represent the fold change in Pds5 DKO over Pds5 lox cells at three time points after release from G0.

4.3 Similar proliferation defects in Pds5A KO and Pds5B KO cells

The results described in Section 3 suggested that cell cycle defects in Pds5 DKO cells could be mainly due to the lack of Pds5A. If so, re-entry in S phase after G0 arrest would be more severely impaired in Pds5A KO MEFS than in Pds5B KO MEFs. To test this hypothesis, we first analyzed the fraction of replicating cells after releasing Pds5A KO and Pds5B KO MEFs in high serum containing EdU. Contrary to our expectations, we found defects in the two conditions when compared with MEFs from wild type littermates, although a slightly stronger defect could be measured in the cells without Pds5A (Figure R36A). The observed defects were milder than those observed in Pds5 DKO MEFs. Similar conclusions were obtained using 30-minute BrdU pulses, which revealed a reduced fraction of replicating cells in both Pds5A KO and Pds5 BKO MEFs compared with wild type MEFs in every time point examined (Figure R36B).

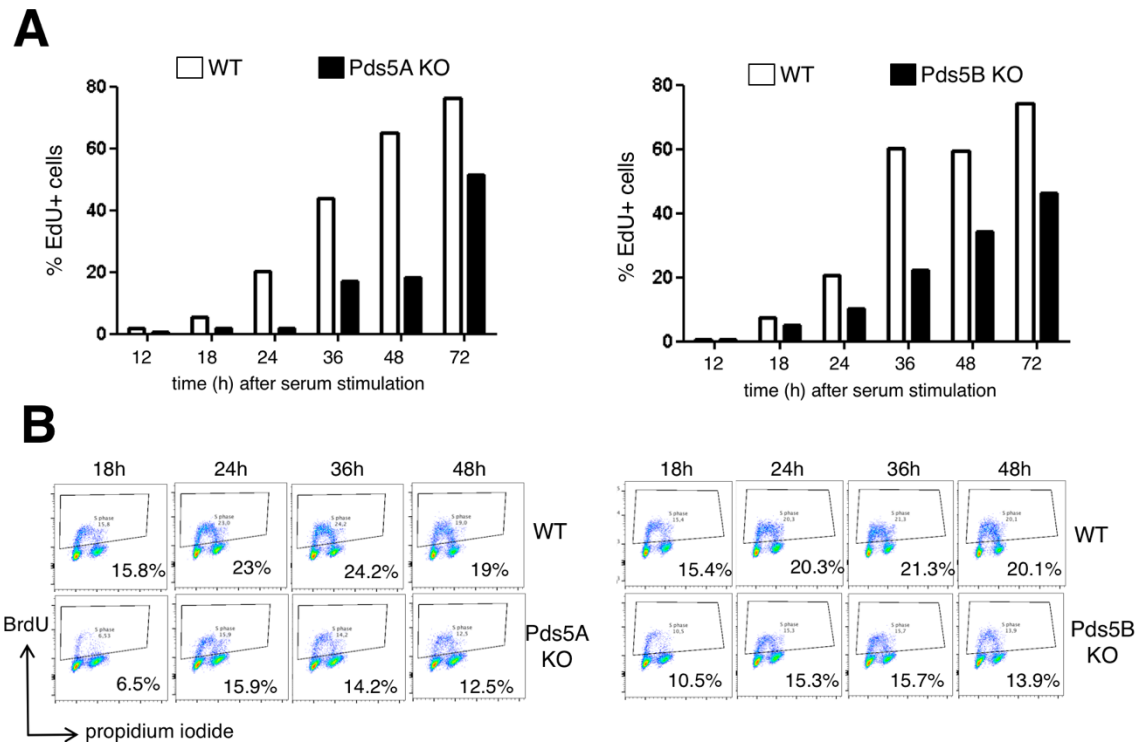

Figure R36. Delayed entry in S phase in Pds5A KO and Pds5B KO MEFs

A. MEFs of the indicated genotypes were starved for 3 days and released in rich medium containing EdU. Incorporation of the analog was analyzed at different time points by microscopy; 500 cells were counted per time point in each condition. **B**. BrdU incorporation during 30-min pulses obtained by flow cytometry at different time points after release from G0 arrest. The percentage of cells that incorporated the nucleotide analog is indicated.

We asked if there were defects in accumulation and assembly of preRC on chromatin also in these cells but the results were not very conclusive. Immunoblot analyses showed decreased levels of Mcm3 in whole cell extracts from both Pds5A KO and Pds5B KO MEFs, but its association to chromatin appeared reduced only in Pds5A KO cells (Figure R37A). Analysis of mRNA levels of genes encoding DNA initiators by quantitative PCR at different time points after release from the G0 arrest suggested larger defects in Pds5B KO cells, with Pds5A KO cells recovering transcription of Mcm3, Orc1 and CycA2 by the 18 h time point (Figure R37B). Further analyses will be required to understand the mechanisms behind delayed entry in S phase in cells lacking Pds5A or Pds5B, but they could be different in each condition. Of note, we also observed that depletion of a single Pds5 protein was sufficient to cause a significant loss of acetylated Smc3 under the conditions of the experiment.

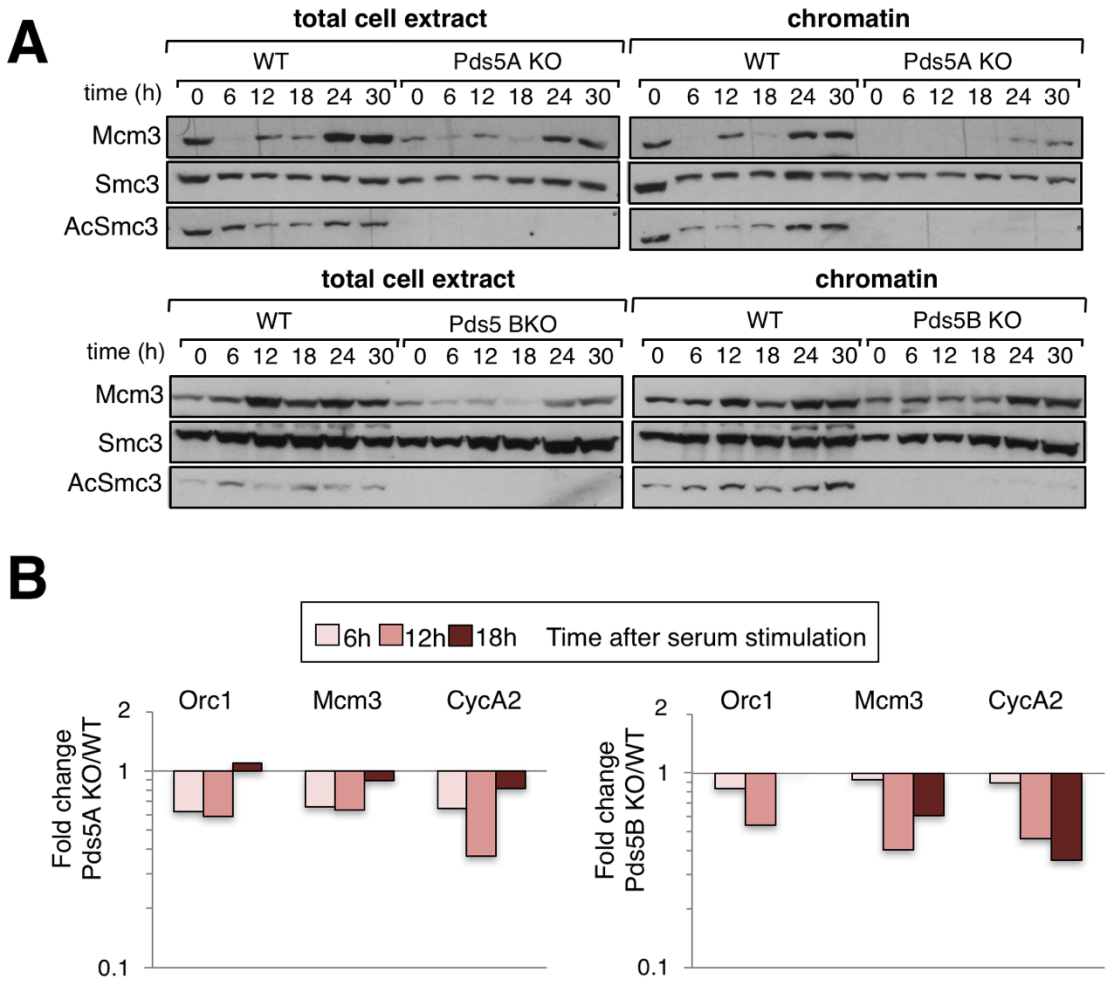

Figure R37. Delayed entry in S phase in Pds5A KO and Pds5B KO MEFs

A. Immunoblot analyses of total cell extract and chromatin fractions of the indicated MEFs at different time points after serum stimulation. **B**. Quantitative PCR analyses of the mRNA levels of genes encoding replication initiator proteins Orc1 and Mcm3 and cell cycle regulator CycA2. Bars represent the fold change in Pds5A KO (left) or Pds5B KO (right) over the corresponding WT MEFs at three time points after release from G0.

4.4 Fork progression is affected in Pds5DKO

We next asked if besides perturbing the initiation of DNA replication, the absence of Pds5 proteins had any effect in replication fork progression. A previous report had proposed that during DNA replication cohesin must switch from a configuration that obstructs the fork to one that permits its advancement, and that this switch involved Pds5A and Wapl (Terret et al., 2009). We therefore used single-molecule analysis of

DNA replication by means of stretched DNA fibers to measure fork progression in Pds5 deficient cells. In this technique, cells are sequentially incubated with two thymidine analogs, CldU and IdU, and then they are lysed and spread on a coverslip and immunofluorescence is used to detect CldU, IdU and DNA. Fork speed is calculated measuring the length of green tracks that follow a red track (Figure 38A, top). Analysis of three independent clones of Pds5 lox after 5 days in the absence or presence of 4-OHT revealed a significant reduction of fork speed upon Pds5 elimination (graph in Figure 38A).

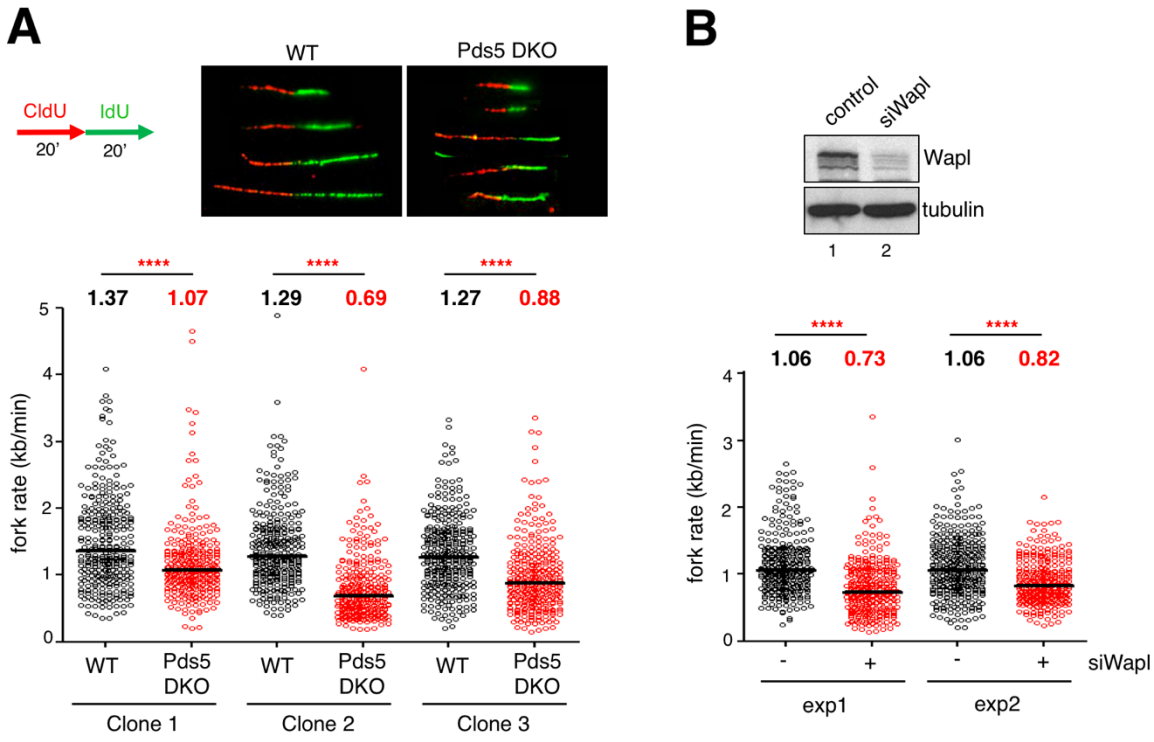

Figure R38. Pds5 proteins speed up the replication fork

Single-molecule analyses of DNA replication using stretched DNA fibers after two consecutive pulses with CldU and IdU were carried out in 3 different clones of WT and Pds5 DKO MEFs (A) and in two clones of untransfected and siWapl MEFs (B) growing asynchronously. The length of more than 300 green tracks preceded by a red track (as in the images above the graph) was measured in each clone. The median values (red horizontal line) for fork rates are indicated above. ****$P < 0.0001$ (Mann-Whitney test).

We reasoned that this effect could be due to impaired cohesin release during S phase hindering the progression of the replication machinery. To explore this possibility, we performed DNA fiber analysis in Pds5 lox MEFs treated with a siRNA against Wapl (Figure 39A, top). Consistent with our hypothesis, we found that the absence of Wapl also slowed significantly fork progression (graph in Figure 38B).

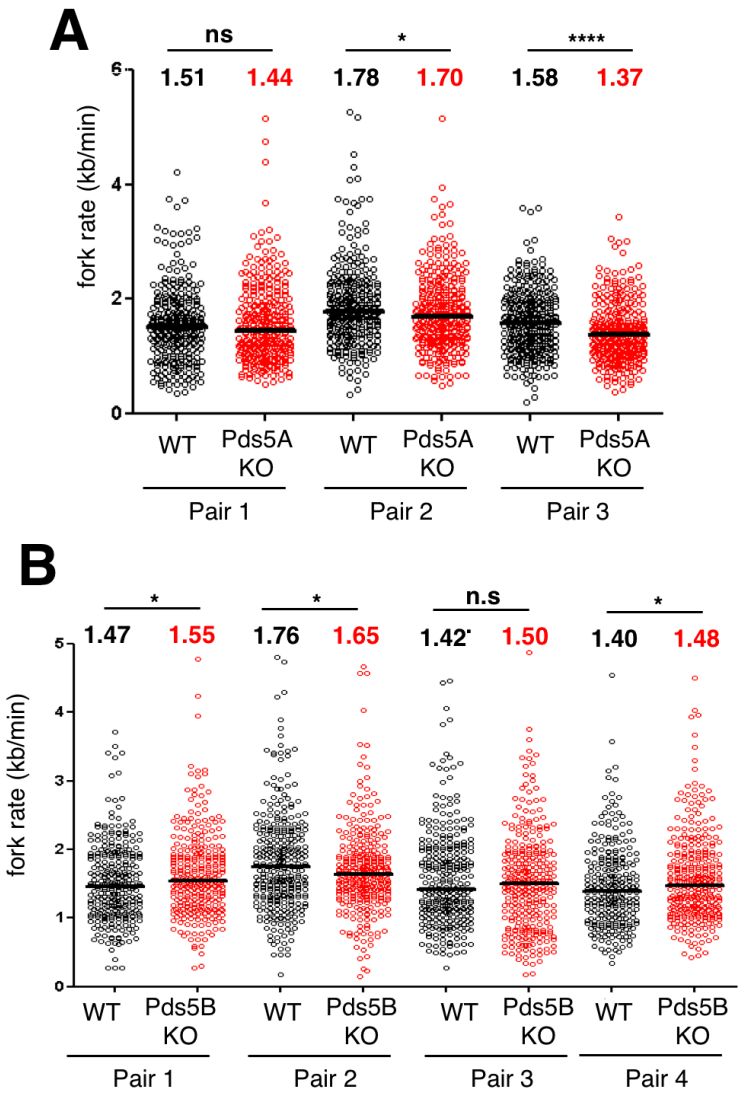

Figure 39. A single Pds5 protein is sufficient for proper fork progression

Single-molecule analyses of DNA replication using stretched DNA fibers after two consecutive pulses with CldU and IdU (20 min each) were carried out in 3 pairs of primary MEFs from Pds5A KO embryos and wild type littermates (**A**) or 4 pairs MEFs from Pds5B KO embryos and wild type littermates (B), all of them growing asynchronously. At least 300 green tracks preceded by a red track were measured in each clone. The median values (black horizontal line) for fork rates are indicated above. *n.s.*, not significant; **P* < 0.1, *****P* < 0.0001 (Mann-Whitney test).

According to the FRAP experiments reported in Section 1 of Results, cohesin unloading is only marginally affected in the absence of a single Pds5 protein. Thus, we would expect fork progression to be similar in wild type, Pds5A KO and Pds5B KO MEFs. Single molecule analyses of replicating cells showed that replicating forks progressed more slowly also in Pds5A KO cells (Figure 39A). Although the changes appeared to be statistically significant, they were unlikely to be biologically relevant

since the reduction in average fork rate was less than 15% in all three clones analyzed (Técher et al., 2013). In Pds5B KO MEFs, three out of four pairs of clones showed a tendency towards increased fork speed while it decreased in the fourth. In all cases, the changes were less than 10% (Figure 39 B). We therefore conclude that fork progress normally in the absence of either Pds5A or Pds5B.

To sum up, Pds5 proteins are important for cell cycle progression. In their absence, cells present severe difficulties to re-enter the cell cycle after a prolonged G0 arrest, and those cells that are able to initiate DNA replication show decreased replication fork rates. Similar defects in fork speed are observed upon Wapl elimination, suggesting that cohesin unloading is required for proper movement of the replisome.

Discussion

As a chromatin organizer, cohesin affects many processes including gene expression, genome duplication and chromosome segregation. Two important aspects of cohesin behaviour are essential for its function, its genomic distribution and its dynamic association with chromatin. What determines the fate of a cohesin ring after loading remains to be understood. However, we have learnt in recent years that postraslational modification of cohesin, most remarkably Smc3 acetylation, and cohesin-associated factors Pds5, Wapl and Sororin are essential for the dynamic behaviour of the complex. In this Thesis, we have focused on understanding the relevance of Pds5 proteins for the regulation of cohesin dynamics. Pds5-Wapl is often considered a complex, also called “releasin" (Buheitel and Stemmann, 2013; Cunningham et al., 2012; Nasmyth, 2011). We here have shown that Pds5 proteins are indeed required to unload cohesin from DNA together with Wapl, as previously show in yeast (Chan et al., 2012; Vaur et al., 2012) and Drosophila (Gause et al., 2010). However, they have additional functions that explain that the consequences of eliminating Pds5 are not the same as those observed after eliminating Wapl.

Another important goal of this work was to address the functional specificity of Pds5A and Pds5B, the two versions of Pds5 present in vertebrate cells. Our previous work analyzing cohesion related functions in mouse cells deficient for either Pds5A or Pds5B revealed that the latter could be specifically involved in cohesion establishment and maintenance at centromeres (Carretero et al., 2013). Here we have failed to identify distinct functions for Pds5A and Pds5B in cohesin dynamics or cohesin distribution, although we observed differential deregulation of gene expression in Pds5A null and Pds5 B null cells. We tentatively conclude that, regarding the regulation of cohesin association to chromatin, maintenance of a pool of total Pds5 is more important than the presence of a specific Pds5 isoform.

1. Dual role of Pds5 in the regulation of cohesin dynamics

Wapl promotes cohesin unloading and in its absence there is an excess of cohesin on chromatin and chromosome organization is altered, both in interphase and mitosis (Haarhuis et al., 2013, Lopez-Serra et al., 2013, Tedeschi et al., 2013). The role of Pds5 is less clear for it has seemingly opposite effects on cohesin stability: it contributes to cohesion establishment during S phase through cohesin acetylation and Sororin binding but it also participates in cohesin unloading (Figure D1).

We have shown that Smc3 acetylation is dramatically reduced upon elimination of the two Pds5 proteins in MEFs. Pds5 proteins mediate Esco1 binding to cohesin in HeLa cells (Minamino et al., 2015). However, Smc3 acetylation during S phase by Esco2 does not depend on Pds5 proteins in those cells. It is possible that cohesin acetylation in the reduced fraction of cells in S phase present in asynchronous cultures of Pds5 deficient MEFs is under the threshold of detection of the antibody, which is admittedly not very sensitive. It is also possible that Esco2 contribution to cohesin acetylation is much larger in rapidly proliferating, transformed HeLa cells than in primary MEFs.

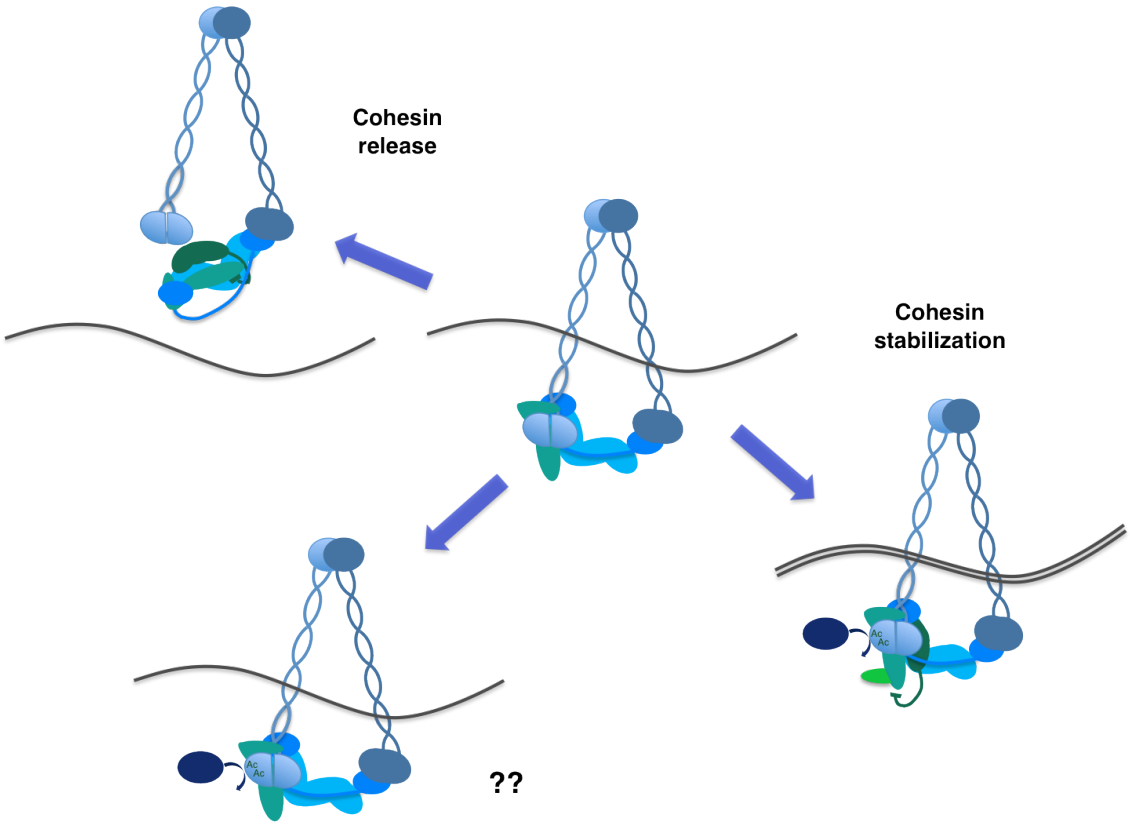

Figure D1. Model of the regulation of cohesin dynamics by Pds5.

Once cohesin is loaded on chromatin, Pds5 and Wapl associate to the ring and can promote cohesin unloading (left). Upon DNA replication, cohesin acetylation by Esco1/2 likely provokes a conformation change in cohesin that promotes Sororin binding to Pds5, displacing Wapl and stabilizing a fraction of cohesin embracing the two sister chromatids (right). Whether acetylation of cohesin is able to alter cohesin dynamics in pre-replicative chromatin is still not fully understood.

Scm3 acetylation also depends on Pds5 in yeast (Chan et al., 2013; Vaur et al., 2012). A study in *S. cerevisiae* reported that Pds5 not only promotes *de novo* acetylation by Eco1 but it also prevents deacetylation by Hos1 (Chan et al., 2013). In contrast, Pds5 deficient MEFs do not show increased Smc3 acetylation after inhibition of HDAC8 and similar observations have been reported in HeLa cells (Minamino et al., 2015). Thus, we conclude that Pds5 proteins are important to establish acetylation *de novo* in cooperation with Esco1. They are also required for Sororin recruitment. Wapl and Sororin compete for binding the same domain in the amino terminal region of Pds5, and this binding requires Pds5 association with cohesin (Ouyang et al., 2016; Tedeschi et al., 2013). As a consequence, Pds5 deficient cells fail to recruit Sororin to chromatin in G2, indicating that Pds5 is essential for cohesin stabilization after DNA replication (Figure D1, top right). Single elimination of Pds5A or Pds5B results in partial decrease of acetylated Smc3 levels while no major reduction is observed in Sororin recruitment. This result suggests that only a fraction of acetylated cohesin complexes actually bind Sororin in S phase (Carretero et al., 2013).

We have also shown that Pds5 is required for Wapl-mediated cohesin unloading (Figure D1, top left). The dynamic association of cohesin to chromatin, measured in FRAP experiments, is significantly decreased in cells lacking both Pds5A and Pds5B. Much milder effects are observed in cells lacking only one Pds5 protein, which implies an overlapping contribution of both isoforms to bulk cohesin unloading throughout the genome. Wapl and Pds5 can associate with cohesin independently, with the HEAT repeats of Pds5 binding Rad21 and the N terminal region of Wapl binding the SA subunit (Ouyang et al., 2013b; Shintomi and Hirano, 2009). However, in vitro experiments with purified components show little association of Wapl or Pds5 separately with the cohesin tetramer, and it is therefore likely that they bind cohesin coordinately and once cohesin is on chromatin (Murayama and Uhlmann, 2015). Pds5 and Wapl interact with each other and they associate with cohesin close to the Smc3-Rad21 interface, i.e. cohesin's exit gate (Huis in 't Veld et al., 2014). Recent structural data suggest that Pds5 plays an active role in cohesin unloading by stabilizing a transient, open state of the complex that facilitates its release from chromosomes (Ouyang et al., 2016). This stabilization occurs once Pds5 is bound at the same time at cohesin and Wapl, acting as a bridge that would facilitate Wapl association to cohesin and therefore trigger cohesin release. However, there is no clear evidence that Wapl is actually the effector of the releasing activity. One alternative mechanism would be that Pds5 is actually inducing cohesin release, with Wapl acting as a cofactor that activates

this function. Once DNA replication occurs, Pds5 would facilitate cohesin acetylation and Sororin recruitment, which would displace Wapl from its Pds5 binding site. This change in the Pds5 cofactor might be responsible for the switch between a pro-releasing activity to cohesin stabilization to maintain sister chromatid cohesion.

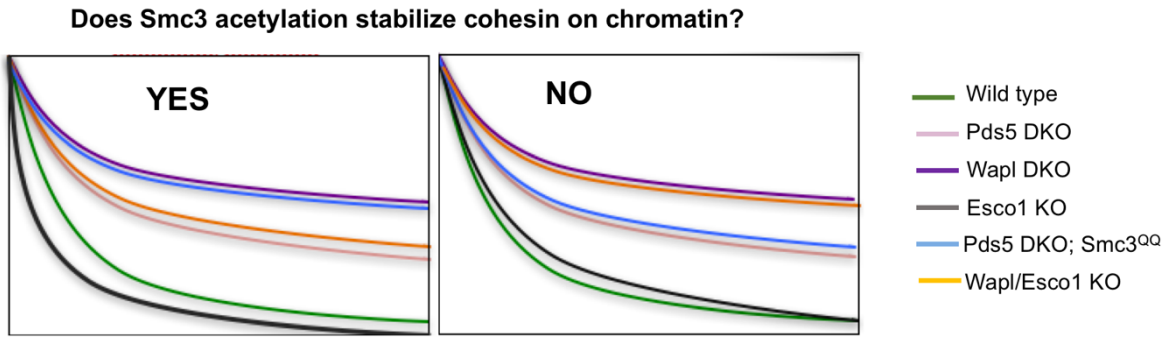

Figure D2. FRAP experiments to evaluate the effect of Smc3 acetylation on cohesin dynamics

If Smc3 acetylation hinders cohesin release, Esco1 elimination would accelerate recovery of fluorescence and combined with Wapl depletion would permit a faster exchange, more similar to that observed in Pds5 DKO MEFs. Conversely, introduction of the $Smc3^{QQ}$ would stabilize cohesin on chromatin and, if combined with Pds5 deletion could result in a curve similar to the Wapl KO MEFs. If Smc3 acetylation does not affect cohesin dynamics, however, the proposed combinations would not alter the rate of fluorescence recovery of Wapl KO and Pds5 DKO MEFs.

Our FRAP results in Pds5 deficient MEFs are similar to those reported for Wapl deficient MEFs (Tedeschi et al., 2013), but Wapl elimination causes a more prominent defect in the recovery of fluorescence. Results similar to ours have been reported in HeLa cells after downregulation of the two Pds5 proteins (Ouyang et al., 2016). Since our experiments require simultaneous elimination of two Pds5 proteins instead of one, it is possible that Wapl depletion is more quantitative and causes a more profound effect. In fact, a small amount of Wapl is present in the chromatin of Pds5 DKO MEFs that, together with the remaining Pds5A/B, could perform some cohesin unloading. We have also observed that the population of soluble cohesin does not change in Pds5 DKO MEFs, while it is dramatically reduced in Wapl KO MEFs (Busslinger et al., 2017; Tedeschi et al., 2013). This can also contribute to slow down the exchange of cohesin complexes in Wapl KO cells. A third possibility, not mutually exclusive with the previous ones, is that cohesin acetylation, which occurs in Wapl KO but not in Pds5 DKO cells, also contributes to cohesin stabilization even in the absence of Sororin. We addressed

this possibility by inducing increased acetylation in wild type MEFs by HDAC8i treatment but failed to observe clear changes in fluorescence recovery. In agreement with our findings, cells carrying an Smc3 acetyl-mimic mutant that substitutes two Glutamines for the two Lysines that are acetylated, $Smc3^{QQ}$, do not display differences in the residence time of cohesin on chromatin, neither in G1 nor G2 (Ladurner et al., 2016). These results indicate that Smc3 acetylation cannot counteract Wapl-mediated releasing activity in the absence of Sororin, at least to an extent measurable in the FRAP assays. One caveat of this experiment is that the $Smc3^{QQ}$ mutant would cause a constitutive acetylation-like status of cohesin, and we might miss the importance of the balance between acetylation, deacetylation and Wapl activity. To further analyze the role of Smc3 acetylation in cohesin dynamics it would be useful to check if deletion of Esco1 in Wapl KO MEFs results in a FRAP curve similar to that of Pds5 DKO cells or if expression of $Smc3^{QQ}$ mutant in Pds5 DKO cells recapitulate the behavior of Wapl deficient cells (Figure D2).

Interestingly, elimination of the two Pds5 proteins results in a worm-like staining of cohesin in interphase cells, previously described in Wapl depleted cells and named *vermicelli* (Tedeschi et al., 2013). *Vermicelli* resemble prophase chromosomes and have been observed also after downregulation of Pds5A and Pds5B in HeLa cells (Ouyang et al., 2016). Unlike Wapl deficient cells, Pds5 deficient cells do not display increased amount of chromatin-bound cohesin. Thus, *vermicelli* are not the consequence of an aberrant accumulation of cohesin on chromatin but of a less dynamic cohesin leading to chromatin compaction. Nevertheless, a certain threshold amount of cohesin on chromatin would be required to produce them, since co-depletion of Wapl and the cohesin loader abolishes *vermicelli* (Haarhuis et al., 2017). It is tempting to speculate that one major difference between cohesin and condensin, the SMC complex involved in chromosome condensation, may be a less dynamic behavior of the latter which may be required to preserve loops for longer time and/or to make longer loops (Goloborodko et al., 2016; Haarhuis et al., 2017).

2. Cohesin dynamics determines cohesin distribution

Here we have addressed the importance of Pds5 proteins for genome-wide cohesin localization by ChIP-seq. We have shown that Pds5A and Pds5B occupy virtually the same genomic positions, and conclude that they do not dictate cohesin localization at specific sites. This conclusion is also consistent with the observation of very similar

distribution of cohesin in Pds5A KO and Pds5B KO MEFs. However, simultaneous depletion of both Pds5 proteins results in loss of almost half of cohesin positions detected in wild type (Pds5 lox) cells, as well as the appearance of a reduced number of new sites. Cohesin positions that do not change upon elimination of Pds5 proteins are also maintained in Wapl deficient cells, suggesting that these are robust cohesin peaks, not sensitive to alterations in cohesin dynamics, and present in most cells in the population. In contrast, only 28% of cohesin binding sites lost in Pds5 deficient MEFs are also lost upon Wapl elimination. In addition, while only a small amount of new positions are detected in Pds5 DKO MEFs compared to Pds5 lox MEFs, in Wapl KO MEFs there are over thirty thousand new cohesin positions, a number larger than that of positions lost. Thus, Pds5 and Wapl regulate cohesin distribution differently.

In addition to cohesin loading and release from on chromatin, a second mechanism initially described in yeast is becoming important for the correct understanding of cohesin dynamics: cohesin translocation (Ocampo-Hafalla and Uhlmann, 2011). It consists in the lateral movement of the ring once it is loaded on chromatin and explains why cohesin and its loader do not colocalize in yeast (Glynn et al., 2004; Lengronne et al., 2004; Ocampo-Hafalla et al., 2016) or vertebrate cells (Busslinger et al., 2017; Kagey et al., 2010; Zuin et al., 2014). Unlike cohesin release and reload, this movement occurs within neighboring genomic regions, and is not detected by FRAP. Single-molecule imaging experiments have demonstrated the ability of purified cohesin to diffuse along naked DNA (Stigler et al., 2016) and showed that DNA bound proteins such as CTCF constrain this diffusion (Davidson et al., 2016). Cohesin localization along the genome is likely influenced by its ability to efficiently translocate along chromatin until it encounters certain obstacles such as CTCF. Consistent with this hypothesis, CTCF depletion changes cohesin distribution favoring occupancy of active TSSs (Busslinger et al., 2017). Interestingly, these active TSSs coincide with NIPBL binding sites, which would imply that they act as secondary boundaries in the absence of CTCF. Alternatively, it can also mean that, in the absence of CTCF, cohesin cannot translocate after being loaded onto chromatin.

Experimental evidences from different organisms suggest that acetylation may affect the conformation of the cohesin ring, the binding of cohesin associated factors and the ATPase activity of the Smc heads (Chan et al., 2012; Ladurner et al., 2014; Murayama and Uhlmann, 2015). Recently, another *in vitro* study showed that cohesin acetylation enhances its translocation ability (Kanke et al., 2016). Thus, the correct balance between cohesin loading, cohesin release and cohesin acetylation likely

contributes to cohesin distribution. Indeed, increased cohesin acetylation due to impaired activity of HDAC8 results in decreased occupancy of cohesin at several sites (Deardorff et al., 2012). In Wapl deficient MEFs there is deficient cohesin release but acetylation still happens and as a consequence, there is a massive accumulation of acetylated cohesin on chromatin (Busslinger et al., 2017). This highly mobile and release-resistant cohesin may translocate further away from its loading sites and reach positions not reached in wild type cells (Figure D3, right). The height of the peaks present only in WT or Wapl KO cells is clearly lower than in unchanged positions, supporting the variable nature of these sites.

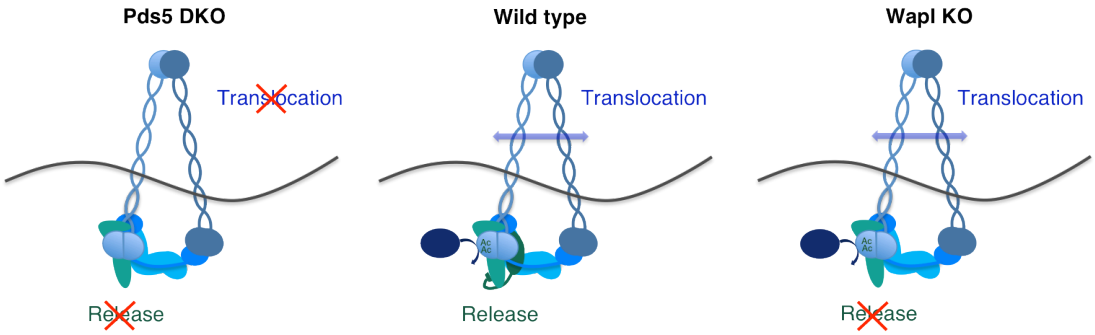

Figure D3. Different consequences of Pds5 or Wapl elimination in cohesin dynamics.

In both situations cohesin release is compromised, but only in Pds5 DKO cells the lack of acetylation affects cohesin translocation.

In Pds5 DKO cells, despite impaired cohesin release, we do not detect increased chromatin bound cohesin. While it is possible that this is the consequence of a less thorough depletion of the Pds5 proteins, as commented in the previous section, it is also possible that cohesin loading is reduced in the absence of Pds5 proteins. It has been proposed that Pds5 and NIPBL compete for binding to Rad21 and this competition facilitates disengagement of cohesin of its loader upon binding of Pds5, thus freeing the loader which is then capable of loading another cohesin complex (Kikuchi et al., 2016). Also in vitro, addition of Pds5 prevents loading of cohesin on DNA by NIPBL (Murayama and Uhlmann, 2015). Reduced loading efficiency may therefore balance the reduced release of cohesin in Pds5 deficient cells. Importantly,

the loaded cohesin cannot be acetylated, which would reduce its translocation ability, and thereby restrict its distribution (Figure D3, left). We hypothesize that the cohesin positions that disappear in Pds5 DKO MEFs but not in Wapl KO MEFs should be also lost in Wapl KO cells if acetylation is prevented. We are currently performing ChIPqPCR analyses of these positions in MEFs treated with siRNA against Wapl and Esco1.

3. Gene expression changes upon perturbation of cohesin dynamics and their effect on cell cycle progression

The ability of cohesin to form chromatin loops in association with CTCF and other transcriptional regulators facilitates or restricts the long range interaction between enhancers and promoters and contributes to regulate gene expression (Hadjur et al., 2009; Kagey et al., 2010; Schmidt et al., 2010). According to the loop extrusion model, once entrapping DNA topologically, cohesin would generate a chromatin loop by extruding DNA until being stopped by boundary elements, such as CTCF, or being released from chromatin by the action of Pds5-Wapl (Nichols and Corces, 2015; Sanborn et al., 2015). Indeed, HiC analyses have shown that Wapl elimination increases the size of chromatin loops and allows interactions between nearby TADs leading to gene deregulation (Haarhuis et al., 2017).

We have demonstrated that elimination of the two Pds5 proteins causes changes of the expression of more than 300 genes both in cells growing asynchronously or arrested in G0. Wapl ablation alters gene expression of a similar number of genes (Tedeschi et al., 2013). However, there are few genes in common between the two datasets. We speculate that this is due, at least in part, to the lack of acetylation on Pds5 deficient cells but not in Wapl deficient cells. Esco1 has been proposed to repress transcription, probably through cohesin acetylation (Rahman et al., 2015). In quiescent Pds5 DKO cells, two thirds of the genes whose expression changes are upregulated while in Wapl KO downregulation is more common. These results hint at a relevant role of cohesin dynamics in transcriptional regulation. We could not find a clear link between the deregulated genes and the presence of cohesin nearby. The changes observed may be indirect, i.e. the consequence of changing the levels of a transcription factor, or result from impaired interactions with distal enhancers or repressors.

Intriguingly, while we have not found major changes in cohesin dynamics and distribution in Pds5A KO and Pds5B KO MEFs, we have observed clear differences in their transcriptomes, both with respect to wild type MEFs and between them. A fraction of the genes deregulated in Pds5 DKO cells come from combining genes deregulated in Pds5A KO and Pds5B KO cells, suggesting that Pds5 proteins make some specific contribution to the regulation of transcription. One possibility is that at least some of these changes are indirect and follow alterations in cellular functions in which one or the other Pds5 protein participates. For example, asynchronous cultures of Pds5A KO MEFs show a larger fraction of G1 cells (Carretero et al., 2013), which may cause downregulation of pathways related to DNA replication, Cell cycle (see table Figure R30). We are currently exploring the interactomes of Pds5A and Pds5B by proteomics to search for specific interactors of either protein that can help explain the consequences of depleting one or the other protein in cellular function.

Among the genes deregulated in Pds5 DKO MEFs we identified several cell cycle-related genes as well. Asynchronously growing Pds5 DKO MEFs display an enrichment in the G1 population more notorious than Pds5A KO MEFs, mentioned above. Moreover, these cells have serious troubles to progress to S phase after release from a prolonged arrest in G0. Although deregulation of cell cycle genes, particularly those involved in DNA replication and mitosis, can be a consequence of impaired cell proliferation, we find a tendency towards the downregulation of cell cycle regulators that are active in G1 and promote the G1/S transition, such as E2f4 and c-Myc, and the upregulation of tumor suppressors that block cell proliferation, like Rb1. We and others have previously reported the importance of cohesin for c-Myc expression and its reintroduction in Wapl deficient MEFs partially rescued their block in S phase entry (Tedeschi et al., 2013; Remeseiro et al., 2012b). Thus, we hypothesize that defects observed in cell cycle progression in Pds5 DKO cells are due to the deregulation of the expression of a small subset of master regulators whose expression might be tightly associated with cohesin.

4. Defective cohesin dynamics slows down DNA replication

The fact that cohesion is established at the time of DNA replication suggests an intimate relationship between the replication machinery and the cohesin ring. Indeed, there are a number of replication-related factors that contribute to cohesion establishment (Bermudez et al., 2003; Hanna et al., 2001; Moldovan et al., 2006;

Samora et al., 2016; Sherwood et al., 2010). Once origins are fired and DNA replication is initiated, the replication fork progresses through chromatin and the MCM helicase opens the DNA helix to allow copying of each strands (Deegan and Diffley, 2016). What happens when the replisome encounters cohesin is unknown. It was initially proposed that the replisome might simply slide through the cohesin ring (Lengronne et al., 2006). Although the diameter of the cohesin has been estimated to be 30–40 nm based on EM images of DNA free cohesin (Huis in 't Veld et al., 2014), data on reconstituted cohesin complexes diffusing along DNA past obstacles of increasing size reveal that the actual size of the pore is considerably smaller (Stigler et al., 2016). If the same is true in vivo, it is difficult to envision the bulky replisome sliding through cohesin. Instead, upon passage of the replisome, cohesin may be pushed or unloaded and reloaded behind, and eventually bound by Sororin (Kanke et al., 2016). Pds5 proteins participate in all these processes by facilitating Smc3 acetylation, Wapl-mediated cohesin unloading and Sororin binding (Carretero et al., 2013; Chan et al., 2013; Minamino et al., 2015; Nishiyama et al., 2010; Vaur et al., 2012; this study). Using DNA fiber analysis, we have observed a reduction in replication fork speed in Pds5 deficient cells. The same phenotype was also observed after downregulation of Wapl by siRNA in Pds5 lox (wild type) MEFs. We hypothesize that in the absence of either Pds5 or Wapl, defective cohesin release might physically block, or at least hinder, the advancement of the replication fork. We are currently trying to further test this hypothesis by depleting cohesin in Pds5 deficient cells, which should restore fork speed.

Our finding of similar defects in fork progression in either Pds5 or Wapl deficient cells suggests that defective cohesin unloading, and not cohesin acetylation as reported before, is most relevant for the phenotype. However, it is also possible that cohesin acetylation becomes important only in the presence of Pds5-Wapl. In vitro, unacetylated cohesin is rendered immobile when Pds5-Wapl are added, and mobility is restored by acetylation (Kanke et al., 2016). Although acetylated Smc3 is not quantitatively detected in immunoblots of chromatin fractions from Pds5 DKO MEFs, Esco2-driven cohesin acetylation may take place at the fork even without Pds5 (Minamino et al., 2015). Simultaneous staining of acetylated Smc3 and EdU could be useful to better assess the presence of Smc3 acetylation in Pds5 DKO cells traversing S phase. We also note that Terret et al., 2009 did not find fork progression defects upon downregulation of Wapl or Pds5A in HeLa cells and instead showed that Wapl or Pds5A depletion rescued the slow fork progression caused by either Esco1 or Esco2 depletion. The relative abundance of Wapl, Pds5A/B and cohesin or different DNA

replication kinetics in the two cell types (HeLa versus primary MEFs) may account for these differences.

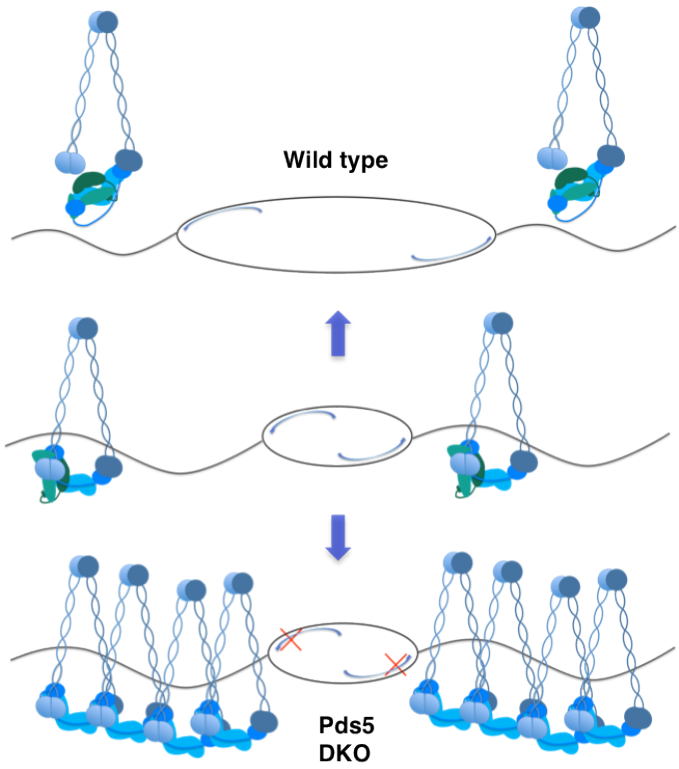

Figure D4. Defective cohesin release hinders replication fork progression.

A model to explain the reduced fork rates observed in cells lacking Pds5 proteins. While in wild type cells cohesin is released to allow passage of the replication fork, Pds5 DKO cells retain cohesin on chromatin, hindering the progression of the fork.

Our results suggest that the fine regulation of cohesin stabilization and release is key to ensure proper DNA replication. We are interested in assessing additional parameters of the DNA replication process such as origin activation. Cohesin has been proposed to enhance the efficiency of origin firing through an architectural role in the organization of replication factories (Guillou et al., 2010). The relevance of cohesin dynamics in this regard is not known.

In summary, taken together our in vivo results with those from recent in vitro studies, we propose that the role of Pds5 proteins in cohesin dynamics is distinct from that of Wapl. While both proteins work together to promote cohesin unloading, Pds5

facilitates cohesin acetylation, which affects cohesin translocation. Although not investigated here in detail, it is also possible that Pds5 contributes to efficient cohesin loading (Kikuchi et al., 2016; Murayama and Uhlmann, 2015). This could explain why cohesin does not accumulate on chromatin in Pds5 DKO cells to the same extent as in Wapl KO cells, in which the soluble population of cohesin is dramatically reduced. Defective cohesin translocation in the absence of Pds5 proteins alters the genome wide distribution of cohesin differently from the absence of Wapl, and results in different changes in gene expression. Thus, our results highlight the importance of Pds5 proteins for cohesin dynamics beyond the regulation of Wapl activity in non-cohesion related functions. Chromosome conformation analyses will have to address how chromatin loops and TADs change in the absence of Wapl and Pds5. Given the importance of cohesin dynamics for genome organization, we suspect that the changes will not be the same after depletion of Pds5 or Wapl.

Conclusions

1. Pds5 proteins are required for maintaining proper levels of acetylated cohesin, Wapl and Sororin on chromatin, confirming an important contribution of Pds5 to cohesin dynamics.

2. The dynamic association of cohesin with chromatin is significantly decreased in cells lacking both Pds5A and Pds5B, leading to aberrant localization of cohesin in axial structures known as *vermicelli.* This phenotype does not require accumulation of cohesin on chromatin to the high levels detected in Wapl deficient cells, in which it was initially observed.

3. Cells lacking only Pds5A or Pds5B show mild defects in cohesin dynamics, which suggests an overlapping contribution of both Pds5 proteins to bulk cohesin unloading throughout the genome.

4. Pds5 proteins do not dictate cohesin localization at particular genomic locations, since either Pds5A or Pds5B can be found at most cohesin positions. However, cohesin distribution is clearly restricted in the absence of both Pds5A and Pds5B.

5. Pds5 depletion changes cohesin distribution in a manner different from Wapl depletion. This could result from a lack of acetylated cohesin in Pds5 deficient cells and not in Wapl deficient cells, since acetylation promotes cohesin translocation.

6. Pds5 proteins contribute to cohesin-mediated regulation of gene expression. Single elimination of Pds5A or Pds5B results in different transcriptional deregulation, although the underlying reasons remain unknown.

7. Starved Pds5 deficient cells show delayed entry in S phase after serum stimulation due to impaired synthesis and assembly of DNA replication initiators on chromatin. Milder defects are observed in cells lacking Pds5A or Pds5B.

8. Replication fork rate is reduced to similar extent in the absence of the two Pds5 proteins or after downregulation of Wapl. This suggests that cohesin unloading is required to allow replication fork progression.

Conclusiones

1. Las proteínas Pds5 son necesarias para mantener niveles apropiados en cromatina de cohesina acetilada, así como de Wapl y Sororina, lo que confirma su importancia en la regulación de la dinámica de la cohesina,

2. La dinámica de disociación de la cohesina de cromatina se ve comprometida en ausencia de Pds5A y Pds5B, lo que provoca una acumulación anormal de la cohesina en estructuras axiales conocidas como *vermicelli*. Este fenotipo no requiere un aumento de la cantidad de cohesina en cromatina tan grande como el que se observa en células sin Wapl, en las que el fenotipo se describió por primera vez.

3. La eliminación individual de Pds5A o Pds5B causa defectos leves en la dinámica de la cohesina, lo que sugiere una contribución redundante de ambas proteínas Pds5.

4. Dado que tanto Pds5A como Pds5B aparecen en la mayoría de las posiciones de cohesina, concluimos que las proteínas Pds5 no dictan la localización de ésta en lugares concretos del genoma.

5. La eliminación simultánea de Pds5A y Pds5B restringe la distribución genómica, lo que no ocurre en células sin Wapl. Esto puede ser debido a la falta de acetilación en células sin Wapl, pues esta modificación parece facilitar el desplazamiento del complejo a lo largo del DNA.

6. Las proteínas Pds5 contribuyen a la regulación de la expresión génica mediada por cohesina. La eliminación de sólo Pds5A o Pds5B ocasiona alteraciones diferentes en la expresión génica, aunque aún no conocemos el mecanismo responsable.

7. Las células deficientes en Pds5 muestran un retraso en la entrada en fase S después de ser liberadas de una parada en G0 debido a defectos en la síntesis y ensamblaje de los complejos iniciadores de la replicación de ADN. La eliminación individual de Pds5A o Pds5B causa defectos más leves.

8. La velocidad de la horquilla replicativa se reduce de forma similar tanto en ausencia de las dos proteínas Pds5 como en ausencia de Wapl, lo que sugiere que la disociación de cohesina mediada por Pds5-Wapl permite el avance del replisoma.

Bibliography

Alvarez, S., Díaz, M., Flach, J., Rodriguez-Acebes, S., López-Contreras, A.J., Martínez, D., Cañamero, M., Fernández-Capetillo, O., Isern, J., Passegué, E., et al. (2015). Replication stress caused by low MCM expression limits fetal erythropoiesis and hematopoietic stem cell functionality. Nat. Commun. *6*, 8548.

Anderson, D.E., Losada, A., Erickson, H.P., and Hirano, T. (2002). Condensin and cohesin display different arm conformations with characteristic hinge angles. J. Cell Biol. *156*, 419–424.

Arumugam, P., Nishino, T., Haering, C.H., Gruber, S., and Nasmyth, K. (2006). Cohesin's ATPase activity is stimulated by the C-terminal Winged-Helix domain of its kleisin subunit. Curr. Biol. CB *16*, 1998–2008.

Barrington, C., Finn, R., and Hadjur, S. (2017). Cohesin biology meets the loop extrusion model. Chromosome Res. Int. J. Mol. Supramol. Evol. Asp. Chromosome Biol. *25*, 51–60.

Beckouët, F., Hu, B., Roig, M.B., Sutani, T., Komata, M., Uluocak, P., Katis, V.L., Shirahige, K., and Nasmyth, K. (2010). An Smc3 Acetylation Cycle Is Essential for Establishment of Sister Chromatid Cohesion. Mol. Cell *39*, 689–699.

Beckouët, F., Srinivasan, M., Roig, M.B., Chan, K.-L., Scheinost, J.C., Batty, P., Hu, B., Petela, N., Gligoris, T., Smith, A.C., et al. (2016). Releasing Activity Disengages Cohesin's Smc3/Scc1 Interface in a Process Blocked by Acetylation. Mol. Cell *61*, 563–574.

Bermudez, V.P., Maniwa, Y., Tappin, I., Ozato, K., Yokomori, K., and Hurwitz, J. (2003). The alternative Ctf18-Dcc1-Ctf8-replication factor C complex required for sister chromatid cohesion loads proliferating cell nuclear antigen onto DNA. Proc. Natl. Acad. Sci. U. S. A. *100*, 10237–10242.

Borges, V., Smith, D.J., Whitehouse, I., and Uhlmann, F. (2013). An Eco1-independent sister chromatid cohesion establishment pathway in S. cerevisiae. Chromosoma *122*, 121–134.

Brough, R., Bajrami, I., Vatcheva, R., Natrajan, R., Reis-Filho, J.S., Lord, C.J., and Ashworth, A. (2012). APRIN is a cell cycle specific BRCA2-interacting protein required for genome integrity and a predictor of outcome after chemotherapy in breast cancer. EMBO J. *31*, 1160–1176.

Buheitel, J., and Stemmann, O. (2013). Prophase pathway-dependent removal of cohesin from human chromosomes requires opening of the Smc3-Scc1 gate. EMBO J. *32*, 666–676.

Busslinger, G.A., Stocsits, R.R., van der Lelij, P., Axelsson, E., Tedeschi, A., Galjart, N., and Peters, J.-M. (2017). Cohesin is positioned in mammalian genomes by transcription, CTCF and Wapl. Nature.

Cadoret, J.-C., Meisch, F., Hassan-Zadeh, V., Luyten, I., Guillet, C., Duret, L., Quesneville, H., and Prioleau, M.-N. (2008). Genome-wide studies highlight indirect links between human replication origins and gene regulation. Proc. Natl. Acad. Sci. U.

S. A. *105*, 15837–15842.

Canudas, S., and Smith, S. (2009). Differential regulation of telomere and centromere cohesion by the Scc3 homologues SA1 and SA2, respectively, in human cells. J. Cell Biol. *187*, 165–173.

Carretero, M., Ruiz-Torres, M., Rodríguez-Corsino, M., Barthelemy, I., and Losada, A. (2013). Pds5B is required for cohesion establishment and Aurora B accumulation at centromeres. EMBO J. *32*, 2938–2949.

Cayrou, C., Ballester, B., Peiffer, I., Fenouil, R., Coulombe, P., Andrau, J.-C., van Helden, J., and Méchali, M. (2015). The chromatin environment shapes DNA replication origin organization and defines origin classes. Genome Res. *25*, 1873–1885.

Chan, K.-L., Roig, M.B., Hu, B., Beckouët, F., Metson, J., and Nasmyth, K. (2012). Cohesin's DNA exit gate is distinct from its entrance gate and is regulated by acetylation. Cell *150*, 961–974.

Chan, K.-L., Gligoris, T., Upcher, W., Kato, Y., Shirahige, K., Nasmyth, K., and Beckouët, F. (2013). Pds5 promotes and protects cohesin acetylation. Proc. Natl. Acad. Sci. U. S. A. *110*, 13020–13025.

Cuadrado, A., Remeseiro, S., Graña, O., Pisano, D.G., and Losada, A. (2015). The contribution of cohesin-SA1 to gene expression and chromatin architecture in two murine tissues. Nucleic Acids Res. *43*, 3056–3067.

Cunningham, M.D., Gause, M., Cheng, Y., Noyes, A., Dorsett, D., Kennison, J.A., and Kassis, J.A. (2012). Wapl antagonizes cohesin binding and promotes Polycomb-group silencing in Drosophila. Dev. Camb. Engl. *139*, 4172–4179.

Davidson, I.F., Goetz, D., Zaczek, M.P., Molodtsov, M.I., Huis In 't Veld, P.J., Weissmann, F., Litos, G., Cisneros, D.A., Ocampo-Hafalla, M., Ladurner, R., et al. (2016). Rapid movement and transcriptional re-localization of human cohesin on DNA. EMBO J. *35*, 2671–2685.

Deardorff, M.A., Bando, M., Nakato, R., Watrin, E., Itoh, T., Minamino, M., Saitoh, K., Komata, M., Katou, Y., Clark, D., et al. (2012). HDAC8 mutations in Cornelia de Lange syndrome affect the cohesin acetylation cycle. Nature *489*, 313–317.

Deegan, T.D., and Diffley, J.F.X. (2016). MCM: one ring to rule them all. Curr. Opin. Struct. Biol. *37*, 145–151.

Denison, S.H., Käfer, E., and May, G.S. (1993). Mutation in the bimD gene of Aspergillus nidulans confers a conditional mitotic block and sensitivity to DNA damaging agents. Genetics *134*, 1085–1096.

Dixon, J.R., Selvaraj, S., Yue, F., Kim, A., Li, Y., Shen, Y., Hu, M., Liu, J.S., and Ren, B. (2012). Topological Domains in Mammalian Genomes Identified by Analysis of Chromatin Interactions. Nature *485*, 376–380.

Dorsett, D., Eissenberg, J.C., Misulovin, Z., Martens, A., Redding, B., and McKim, K.

(2005). Effects of sister chromatid cohesion proteins on cut gene expression during wing development in Drosophila. Dev. Camb. Engl. *132*, 4743–4753.

Dreier, M.R., Bekier, M.E., and Taylor, W.R. (2011). Regulation of sororin by Cdk1-mediated phosphorylation. J. Cell Sci. *124*, 2976–2987.

Dundr, M., Hoffmann-Rohrer, U., Hu, Q., Grummt, I., Rothblum, L.I., Phair, R.D., and Misteli, T. (2002). A kinetic framework for a mammalian RNA polymerase in vivo. Science *298*, 1623–1626.

Eichinger, C.S., Kurze, A., Oliveira, R.A., and Nasmyth, K. (2013). Disengaging the Smc3/kleisin interface releases cohesin from Drosophila chromosomes during interphase and mitosis. EMBO J. *32*, 656–665.

Elbatsh, A.M.O., Haarhuis, J.H.I., Petela, N., Chapard, C., Fish, A., Celie, P.H., Stadnik, M., Ristic, D., Wyman, C., Medema, R.H., et al. (2016). Cohesin Releases DNA through Asymmetric ATPase-Driven Ring Opening. Mol. Cell *61*, 575–588.

Fudenberg, G., Imakaev, M., Lu, C., Goloborodko, A., Abdennur, N., and Mirny, L.A. (2016). Formation of Chromosomal Domains by Loop Extrusion. Cell Rep. *15*, 2038–2049.

Gandhi, R., Gillespie, P.J., and Hirano, T. (2006). Human Wapl is a cohesin-binding protein that promotes sister-chromatid resolution in mitotic prophase. Curr. Biol. CB *16*, 2406–2417.

Gause, M., Misulovin, Z., Bilyeu, A., and Dorsett, D. (2010). Dosage-sensitive regulation of cohesin chromosome binding and dynamics by Nipped-B, Pds5, and Wapl. Mol. Cell. Biol. *30*, 4940–4951.

Gerlich, D., Koch, B., Dupeux, F., Peters, J.-M., and Ellenberg, J. (2006). Live-cell imaging reveals a stable cohesin-chromatin interaction after but not before DNA replication. Curr. Biol. CB *16*, 1571–1578.

Gillespie, P.J., and Hirano, T. (2004). Scc2 couples replication licensing to sister chromatid cohesion in Xenopus egg extracts. Curr. Biol. CB *14*, 1598–1603.

Gilson, E., and Géli, V. (2007). How telomeres are replicated. Nat. Rev. Mol. Cell Biol. *8*, 825–838.

Giménez-Abián, J.F., Sumara, I., Hirota, T., Hauf, S., Gerlich, D., de la Torre, C., Ellenberg, J., and Peters, J.-M. (2004). Regulation of sister chromatid cohesion between chromosome arms. Curr. Biol. CB *14*, 1187–1193.

Gligoris, T.G., Scheinost, J.C., Bürmann, F., Petela, N., Chan, K.-L., Uluocak, P., Beckouët, F., Gruber, S., Nasmyth, K., and Löwe, J. (2014). Closing the cohesin ring: structure and function of its Smc3-kleisin interface. Science *346*, 963–967.

Glynn, E.F., Megee, P.C., Yu, H.-G., Mistrot, C., Unal, E., Koshland, D.E., DeRisi, J.L., and Gerton, J.L. (2004). Genome-wide mapping of the cohesin complex in the yeast Saccharomyces cerevisiae. PLoS Biol. *2*, E259.

Goloborodko, A., Marko, J.F., and Mirny, L.A. (2016). Chromosome Compaction by Active Loop Extrusion. Biophys. J. *110*, 2162–2168.

Gruber, S. (2017). Shaping chromosomes by DNA capture and release: gating the SMC rings. Curr. Opin. Cell Biol. *46*, 87–93.

Gruber, S., Haering, C.H., and Nasmyth, K. (2003). Chromosomal cohesin forms a ring. Cell *112*, 765–777.

Gruber, S., Arumugam, P., Katou, Y., Kuglitsch, D., Helmhart, W., Shirahige, K., and Nasmyth, K. (2006). Evidence that loading of cohesin onto chromosomes involves opening of its SMC hinge. Cell *127*, 523–537.

Guacci, V., Koshland, D., and Strunnikov, A. (1997). A direct link between sister chromatid cohesion and chromosome condensation revealed through the analysis of MCD1 in S. cerevisiae. Cell *91*, 47–57.

Guillou, E., Ibarra, A., Coulon, V., Casado-Vela, J., Rico, D., Casal, I., Schwob, E., Losada, A., and Méndez, J. (2010). Cohesin organizes chromatin loops at DNA replication factories. Genes Dev. *24*, 2812–2822.

Haarhuis, J.H.I., Elbatsh, A.M.O., van den Broek, B., Camps, D., Erkan, H., Jalink, K., Medema, R.H., and Rowland, B.D. (2013). WAPL-mediated removal of cohesin protects against segregation errors and aneuploidy. Curr. Biol. CB *23*, 2071–2077.

Haarhuis, J.H.I., van der Weide, R.H., Blomen, V.A., Yáñez-Cuna, J.O., Amendola, M., van Ruiten, M.S., Krijger, P.H.L., Teunissen, H., Medema, R.H., van Steensel, B., et al. (2017). The Cohesin Release Factor WAPL Restricts Chromatin Loop Extension. Cell *169*, 693–707.e14.

Hadjur, S., Williams, L.M., Ryan, N.K., Cobb, B.S., Sexton, T., Fraser, P., Fisher, A.G., and Merkenschlager, M. (2009). Cohesins form chromosomal cis-interactions at the developmentally regulated IFNG locus. Nature *460*, 410–413.

Haering, C.H., Farcas, A.-M., Arumugam, P., Metson, J., and Nasmyth, K. (2008). The cohesin ring concatenates sister DNA molecules. Nature *454*, 297–301.

Hanna, J.S., Kroll, E.S., Lundblad, V., and Spencer, F.A. (2001). Saccharomyces cerevisiae CTF18 and CTF4 are required for sister chromatid cohesion. Mol. Cell. Biol. *21*, 3144–3158.

Hara, K., Zheng, G., Qu, Q., Liu, H., Ouyang, Z., Chen, Z., Tomchick, D.R., and Yu, H. (2014). Structure of cohesin subcomplex pinpoints direct shugoshin-Wapl antagonism in centromeric cohesion. Nat. Struct. Mol. Biol. *21*, 864–870.

Hartman, T., Stead, K., Koshland, D., and Guacci, V. (2000). Pds5p is an essential chromosomal protein required for both sister chromatid cohesion and condensation in Saccharomyces cerevisiae. J. Cell Biol. *151*, 613–626.

Hauf, S., Waizenegger, I.C., and Peters, J.M. (2001). Cohesin cleavage by separase required for anaphase and cytokinesis in human cells. Science *293*, 1320–1323.

Hauf, S., Roitinger, E., Koch, B., Dittrich, C.M., Mechtler, K., and Peters, J.-M. (2005). Dissociation of cohesin from chromosome arms and loss of arm cohesion during early mitosis depends on phosphorylation of SA2. PLoS Biol. *3*, e69.

van Heemst, D., James, F., Pöggeler, S., Berteaux-Lecellier, V., and Zickler, D. (1999). Spo76p is a conserved chromosome morphogenesis protein that links the mitotic and meiotic programs. Cell *98*, 261–271.

van Heemst, D., Kafer, E., John, T., Heyting, C., van Aalderen, M., and Zickler, D. (2001). BimD/SPO76 is at the interface of cell cycle progression, chromosome morphogenesis, and recombination. Proc. Natl. Acad. Sci. U. S. A. *98*, 6267–6272.

Higashi, T.L., Ikeda, M., Tanaka, H., Nakagawa, T., Bando, M., Shirahige, K., Kubota, Y., Takisawa, H., Masukata, H., and Takahashi, T.S. (2012). The prereplication complex recruits XEco2 to chromatin to promote cohesin acetylation in Xenopus egg extracts. Curr. Biol. CB *22*, 977–988.

Holt, C.L., and May, G.S. (1996). An extragenic suppressor of the mitosis-defective bimD6 mutation of Aspergillus nidulans codes for a chromosome scaffold protein. Genetics *142*, 777–787.

Hou, F., and Zou, H. (2005). Two human orthologues of Eco1/Ctf7 acetyltransferases are both required for proper sister-chromatid cohesion. Mol. Biol. Cell *16*, 3908–3918.

Hu, B., Itoh, T., Mishra, A., Katoh, Y., Chan, K.-L., Upcher, W., Godlee, C., Roig, M.B., Shirahige, K., and Nasmyth, K. (2011). ATP Hydrolysis Is Required for Relocating Cohesin from Sites Occupied by Its Scc2/4 Loading Complex. Curr. Biol. CB *21*, 12–24.

Huis in ’t Veld, P.J., Herzog, F., Ladurner, R., Davidson, I.F., Piric, S., Kreidl, E., Bhaskara, V., Aebersold, R., and Peters, J.-M. (2014). Characterization of a DNA exit gate in the human cohesin ring. Science *346*, 968–972.

Jeppsson, K., Carlborg, K.K., Nakato, R., Berta, D.G., Lilienthal, I., Kanno, T., Lindqvist, A., Brink, M.C., Dantuma, N.P., Katou, Y., et al. (2014). The chromosomal association of the Smc5/6 complex depends on cohesion and predicts the level of sister chromatid entanglement. PLoS Genet. *10*, e1004680.

Kagey, M.H., Newman, J.J., Bilodeau, S., Zhan, Y., Orlando, D.A., van Berkum, N.L., Ebmeier, C.C., Goossens, J., Rahl, P.B., Levine, S.S., et al. (2010). Mediator and cohesin connect gene expression and chromatin architecture. Nature *467*, 430–435.

Kanke, M., Tahara, E., Huis In’t Veld, P.J., and Nishiyama, T. (2016). Cohesin acetylation and Wapl-Pds5 oppositely regulate translocation of cohesin along DNA. EMBO J. *35*, 2686–2698.

Kikuchi, S., Borek, D.M., Otwinowski, Z., Tomchick, D.R., and Yu, H. (2016). Crystal structure of the cohesin loader Scc2 and insight into cohesinopathy. Proc. Natl. Acad. Sci. U. S. A. *113*, 12444–12449.

Kueng, S., Hegemann, B., Peters, B.H., Lipp, J.J., Schleiffer, A., Mechtler, K., and Peters, J.-M. (2006). Wapl controls the dynamic association of cohesin with chromatin.

Cell *127*, 955–967.

Ladurner, R., Bhaskara, V., Huis in 't Veld, P.J., Davidson, I.F., Kreidl, E., Petzold, G., and Peters, J.-M. (2014). Cohesin's ATPase activity couples cohesin loading onto DNA with Smc3 acetylation. Curr. Biol. CB *24*, 2228–2237.

Ladurner, R., Kreidl, E., Ivanov, M.P., Ekker, H., Idarraga-Amado, M.H., Busslinger, G.A., Wutz, G., Cisneros, D.A., and Peters, J.-M. (2016). Sororin actively maintains sister chromatid cohesion. EMBO J. *35*, 635–653.

Lafont, A.L., Song, J., and Rankin, S. (2010). Sororin cooperates with the acetyltransferase Eco2 to ensure DNA replication-dependent sister chromatid cohesion. Proc. Natl. Acad. Sci. U. S. A. *107*, 20364–20369.

Lengronne, A., Katou, Y., Mori, S., Yokobayashi, S., Kelly, G.P., Itoh, T., Watanabe, Y., Shirahige, K., and Uhlmann, F. (2004). Cohesin relocation from sites of chromosomal loading to places of convergent transcription. Nature *430*, 573–578.

Lengronne, A., McIntyre, J., Katou, Y., Kanoh, Y., Hopfner, K.-P., Shirahige, K., and Uhlmann, F. (2006). Establishment of sister chromatid cohesion at the S. cerevisiae replication fork. Mol. Cell *23*, 787–799.

Li, H., and Durbin, R. (2009). Fast and accurate short read alignment with Burrows-Wheeler transform. Bioinforma. Oxf. Engl. *25*, 1754–1760.

Liu, H., Rankin, S., and Yu, H. (2013). Phosphorylation-enabled binding of SGO1-PP2A to cohesin protects sororin and centromeric cohesion during mitosis. Nat. Cell Biol. *15*, 40–49.

Lopez-Serra, L., Lengronne, A., Borges, V., Kelly, G., and Uhlmann, F. (2013). Budding yeast Wapl controls sister chromatid cohesion maintenance and chromosome condensation. Curr. Biol. CB *23*, 64–69.

Losada, A., and Hirano, T. (2005). Dynamic molecular linkers of the genome: the first decade of SMC proteins. Genes Dev. *19*, 1269–1287.

Losada, A., Hirano, M., and Hirano, T. (1998). Identification of Xenopus SMC protein complexes required for sister chromatid cohesion. Genes Dev. *12*, 1986–1997.

Losada, A., Yokochi, T., Kobayashi, R., and Hirano, T. (2000). Identification and characterization of SA/Scc3p subunits in the Xenopus and human cohesin complexes. J. Cell Biol. *150*, 405–416.

Losada, A., Hirano, M., and Hirano, T. (2002). Cohesin release is required for sister chromatid resolution, but not for condensin-mediated compaction, at the onset of mitosis. Genes Dev. *16*, 3004–3016.

Losada, A., Yokochi, T., and Hirano, T. (2005). Functional contribution of Pds5 to cohesin-mediated cohesion in human cells and Xenopus egg extracts. J. Cell Sci. *118*, 2133–2141.

Lupiáñez, D.G., Kraft, K., Heinrich, V., Krawitz, P., Brancati, F., Klopocki, E., Horn, D.,

Kayserili, H., Opitz, J.M., Laxova, R., et al. (2015). Disruptions of Topological Chromatin Domains Cause Pathogenic Rewiring of Gene-Enhancer Interactions. Cell *161*, 1012–1025.

MacAlpine, H.K., Gordân, R., Powell, S.K., Hartemink, A.J., and MacAlpine, D.M. (2010). Drosophila ORC localizes to open chromatin and marks sites of cohesin complex loading. Genome Res. *20*, 201–211.

McGuinness, B.E., Hirota, T., Kudo, N.R., Peters, J.-M., and Nasmyth, K. (2005). Shugoshin prevents dissociation of cohesin from centromeres during mitosis in vertebrate cells. PLoS Biol. *3*, e86.

Méndez, J., and Stillman, B. (2000). Chromatin association of human origin recognition complex, cdc6, and minichromosome maintenance proteins during the cell cycle: assembly of prereplication complexes in late mitosis. Mol. Cell. Biol. *20*, 8602–8612.

Michaelis, C., Ciosk, R., and Nasmyth, K. (1997). Cohesins: chromosomal proteins that prevent premature separation of sister chromatids. Cell *91*, 35–45.

Minamino, M., Ishibashi, M., Nakato, R., Akiyama, K., Tanaka, H., Kato, Y., Negishi, L., Hirota, T., Sutani, T., Bando, M., et al. (2015). Esco1 Acetylates Cohesin via a Mechanism Different from That of Esco2. Curr. Biol. CB *25*, 1694–1706.

Moldovan, G.-L., Pfander, B., and Jentsch, S. (2006). PCNA controls establishment of sister chromatid cohesion during S phase. Mol. Cell *23*, 723–732.

Mourón, S., Rodriguez-Acebes, S., Martínez-Jiménez, M.I., García-Gómez, S., Chocrón, S., Blanco, L., and Méndez, J. (2013). Repriming of DNA synthesis at stalled replication forks by human PrimPol. Nat. Struct. Mol. Biol. *20*, 1383–1389.

Murayama, Y., and Uhlmann, F. (2014). Biochemical reconstitution of topological DNA binding by the cohesin ring. Nature *505*, 367–371.

Murayama, Y., and Uhlmann, F. (2015). DNA Entry into and Exit out of the Cohesin Ring by an Interlocking Gate Mechanism. Cell *163*, 1628–1640.

Musacchio, A., and Salmon, E.D. (2007). The spindle-assembly checkpoint in space and time. Nat. Rev. Mol. Cell Biol. *8*, 379–393.

Nasmyth, K. (2011). Cohesin: a catenase with separate entry and exit gates? Nat. Cell Biol. *13*, 1170–1177.

Nasmyth, K., and Haering, C.H. (2005). The structure and function of SMC and kleisin complexes. Annu. Rev. Biochem. *74*, 595–648.

Nasmyth, K., and Haering, C.H. (2009). Cohesin: its roles and mechanisms. Annu. Rev. Genet. *43*, 525–558.

Natsume, T., Müller, C.A., Katou, Y., Retkute, R., Gierliński, M., Araki, H., Blow, J.J., Shirahige, K., Nieduszynski, C.A., and Tanaka, T.U. (2013). Kinetochores coordinate pericentromeric cohesion and early DNA replication by Cdc7-Dbf4 kinase recruitment. Mol. Cell *50*, 661–674.

Nichols, M.H., and Corces, V.G. (2015). A CTCF Code for 3D Genome Architecture. Cell *162*, 703–705.

Nishiyama, T., Ladurner, R., Schmitz, J., Kreidl, E., Schleiffer, A., Bhaskara, V., Bando, M., Shirahige, K., Hyman, A.A., Mechtler, K., et al. (2010). Sororin mediates sister chromatid cohesion by antagonizing Wapl. Cell *143*, 737–749.

Nishiyama, T., Sykora, M.M., Huis in 't Veld, P.J., Mechtler, K., and Peters, J.-M. (2013). Aurora B and Cdk1 mediate Wapl activation and release of acetylated cohesin from chromosomes by phosphorylating Sororin. Proc. Natl. Acad. Sci. U. S. A. *110*, 13404–13409.

Nora, E.P., Lajoie, B.R., Schulz, E.G., Giorgetti, L., Okamoto, I., Servant, N., Piolot, T., van Berkum, N.L., Meisig, J., Sedat, J., et al. (2012). Spatial partitioning of the regulatory landscape of the X-inactivation center. Nature *485*, 381–385.

Ocampo-Hafalla, M.T., and Uhlmann, F. (2011). Cohesin loading and sliding. J. Cell Sci. *124*, 685–691.

Ocampo-Hafalla, M., Muñoz, S., Samora, C.P., and Uhlmann, F. (2016). Evidence for cohesin sliding along budding yeast chromosomes. Open Biol. *6*.

Ouyang, Z., Zheng, G., Song, J., Borek, D.M., Otwinowski, Z., Brautigam, C.A., Tomchick, D.R., Rankin, S., and Yu, H. (2013a). Structure of the human cohesin inhibitor Wapl. Proc. Natl. Acad. Sci. U. S. A. *110*, 11355–11360.

Ouyang, Z., Zheng, G., Song, J., Borek, D.M., Otwinowski, Z., Brautigam, C.A., Tomchick, D.R., Rankin, S., and Yu, H. (2013b). Structure of the human cohesin inhibitor Wapl. Proc. Natl. Acad. Sci. U. S. A. *110*, 11355–11360.

Ouyang, Z., Zheng, G., Tomchick, D.R., Luo, X., and Yu, H. (2016). Structural Basis and IP6 Requirement for Pds5-Dependent Cohesin Dynamics. Mol. Cell *62*, 248–259.

Panizza, S., Tanaka, T., Hochwagen, A., Eisenhaber, F., and Nasmyth, K. (2000). Pds5 cooperates with cohesin in maintaining sister chromatid cohesion. Curr. Biol. CB *10*, 1557–1564.

Parelho, V., Hadjur, S., Spivakov, M., Leleu, M., Sauer, S., Gregson, H.C., Jarmuz, A., Canzonetta, C., Webster, Z., Nesterova, T., et al. (2008). Cohesins functionally associate with CTCF on mammalian chromosome arms. Cell *132*, 422–433.

Pope, B.D., Ryba, T., Dileep, V., Yue, F., Wu, W., Denas, O., Vera, D.L., Wang, Y., Hansen, R.S., Canfield, T.K., et al. (2014). Topologically associating domains are stable units of replication-timing regulation. Nature *515*, 402–405.

Quinlan, A.R., and Hall, I.M. (2010). BEDTools: a flexible suite of utilities for comparing genomic features. Bioinforma. Oxf. Engl. *26*, 841–842.

Rahman, S., Jones, M.J.K., and Jallepalli, P.V. (2015). Cohesin recruits the Esco1 acetyltransferase genome wide to repress transcription and promote cohesion in somatic cells. Proc. Natl. Acad. Sci. U. S. A. *112*, 11270–11275.

Ran, F.A., Hsu, P.D., Lin, C.-Y., Gootenberg, J.S., Konermann, S., Trevino, A.E., Scott, D.A., Inoue, A., Matoba, S., Zhang, Y., et al. (2013). Double Nicking by RNA-Guided CRISPR Cas9 for Enhanced Genome Editing Specificity. Cell *154*, 1380–1389.

Rankin, S., Ayad, N.G., and Kirschner, M.W. (2005). Sororin, a substrate of the anaphase-promoting complex, is required for sister chromatid cohesion in vertebrates. Mol. Cell *18*, 185–200.

Rao, S.S.P., Huntley, M.H., Durand, N.C., Stamenova, E.K., Bochkov, I.D., Robinson, J.T., Sanborn, A.L., Machol, I., Omer, A.D., Lander, E.S., et al. (2014). A 3D map of the human genome at kilobase resolution reveals principles of chromatin looping. Cell *159*, 1665–1680.

Remeseiro, S., Cuadrado, A., Carretero, M., Martínez, P., Drosopoulos, W.C., Cañamero, M., Schildkraut, C.L., Blasco, M.A., and Losada, A. (2012a). Cohesin-SA1 deficiency drives aneuploidy and tumourigenesis in mice due to impaired replication of telomeres. EMBO J. *31*, 2076–2089.

Remeseiro, S., Cuadrado, A., Gómez-López, G., Pisano, D.G., and Losada, A. (2012b). A unique role of cohesin-SA1 in gene regulation and development. EMBO J. *31*, 2090–2102.

Rolef Ben-Shahar, T., Heeger, S., Lehane, C., East, P., Flynn, H., Skehel, M., and Uhlmann, F. (2008). Eco1-dependent cohesin acetylation during establishment of sister chromatid cohesion. Science *321*, 563–566.

Rowland, B.D., Roig, M.B., Nishino, T., Kurze, A., Uluocak, P., Mishra, A., Beckouët, F., Underwood, P., Metson, J., Imre, R., et al. (2009). Building sister chromatid cohesion: smc3 acetylation counteracts an antiestablishment activity. Mol. Cell *33*, 763–774.

Rubio, E.D., Reiss, D.J., Welcsh, P.L., Disteche, C.M., Filippova, G.N., Baliga, N.S., Aebersold, R., Ranish, J.A., and Krumm, A. (2008). CTCF physically links cohesin to chromatin. Proc. Natl. Acad. Sci. U. S. A. *105*, 8309–8314.

Salic, A., and Mitchison, T.J. (2008). A chemical method for fast and sensitive detection of DNA synthesis in vivo. Proc. Natl. Acad. Sci. U. S. A. *105*, 2415–2420.

Salic, A., Waters, J.C., and Mitchison, T.J. (2004). Vertebrate shugoshin links sister centromere cohesion and kinetochore microtubule stability in mitosis. Cell *118*, 567–578.

Samora, C.P., Saksouk, J., Goswami, P., Wade, B.O., Singleton, M.R., Bates, P.A., Lengronne, A., Costa, A., and Uhlmann, F. (2016). Ctf4 Links DNA Replication with Sister Chromatid Cohesion Establishment by Recruiting the Chl1 Helicase to the Replisome. Mol. Cell *63*, 371–384.

Sanborn, A.L., Rao, S.S.P., Huang, S.-C., Durand, N.C., Huntley, M.H., Jewett, A.I., Bochkov, I.D., Chinnappan, D., Cutkosky, A., Li, J., et al. (2015). Chromatin extrusion explains key features of loop and domain formation in wild-type and engineered genomes. Proc. Natl. Acad. Sci. U. S. A. *112*, E6456-6465.

Schindelin, J., Arganda-Carreras, I., Frise, E., Kaynig, V., Longair, M., Pietzsch, T., Preibisch, S., Rueden, C., Saalfeld, S., Schmid, B., et al. (2012). Fiji: an open-source platform for biological-image analysis. Nat. Methods *9*, 676–682.

Schlacher, K., Christ, N., Siaud, N., Egashira, A., Wu, H., and Jasin, M. (2011). Double-strand break repair-independent role for BRCA2 in blocking stalled replication fork degradation by MRE11. Cell *145*, 529–542.

Schmidt, D., Schwalie, P.C., Ross-Innes, C.S., Hurtado, A., Brown, G.D., Carroll, J.S., Flicek, P., and Odom, D.T. (2010). A CTCF-independent role for cohesin in tissue-specific transcription. Genome Res. *20*, 578–588.

Schmitz, J., Watrin, E., Lénárt, P., Mechtler, K., and Peters, J.-M. (2007). Sororin is required for stable binding of cohesin to chromatin and for sister chromatid cohesion in interphase. Curr. Biol. CB *17*, 630–636.

Seitan, V.C., Hao, B., Tachibana-Konwalski, K., Lavagnolli, T., Mira-Bontenbal, H., Brown, K.E., Teng, G., Carroll, T., Terry, A., Horan, K., et al. (2011). A role for cohesin in T-cell-receptor rearrangement and thymocyte differentiation. Nature *476*, 467–471.

Sfeir, A., Kosiyatrakul, S.T., Hockemeyer, D., MacRae, S.L., Karlseder, J., Schildkraut, C.L., and de Lange, T. (2009). Mammalian telomeres resemble fragile sites and require TRF1 for efficient replication. Cell *138*, 90–103.

Sherwood, R., Takahashi, T.S., and Jallepalli, P.V. (2010). Sister acts: coordinating DNA replication and cohesion establishment. Genes Dev. *24*, 2723–2731.

Shintomi, K., and Hirano, T. (2009). Releasing cohesin from chromosome arms in early mitosis: opposing actions of Wapl-Pds5 and Sgo1. Genes Dev. *23*, 2224–2236.

Song, J., Lafont, A., Chen, J., Wu, F.M., Shirahige, K., and Rankin, S. (2012). Cohesin acetylation promotes sister chromatid cohesion only in association with the replication machinery. J. Biol. Chem. *287*, 34325–34336.

Stedman, W., Kang, H., Lin, S., Kissil, J.L., Bartolomei, M.S., and Lieberman, P.M. (2008). Cohesins localize with CTCF at the KSHV latency control region and at cellular c-myc and H19/Igf2 insulators. EMBO J. *27*, 654–666.

Stigler, J., Çamdere, G.Ö., Koshland, D.E., and Greene, E.C. (2016). Single-Molecule Imaging Reveals a Collapsed Conformational State for DNA-Bound Cohesin. Cell Rep. *15*, 988–998.

Subramanian, A., Tamayo, P., Mootha, V.K., Mukherjee, S., Ebert, B.L., Gillette, M.A., Paulovich, A., Pomeroy, S.L., Golub, T.R., Lander, E.S., et al. (2005). Gene set enrichment analysis: a knowledge-based approach for interpreting genome-wide expression profiles. Proc. Natl. Acad. Sci. U. S. A. *102*, 15545–15550.

Sumara, I., Vorlaufer, E., Gieffers, C., Peters, B.H., and Peters, J.M. (2000). Characterization of vertebrate cohesin complexes and their regulation in prophase. J. Cell Biol. *151*, 749–762.

Sutani, T., Kawaguchi, T., Kanno, R., Itoh, T., and Shirahige, K. (2009). Budding yeast

Wpl1(Rad61)-Pds5 complex counteracts sister chromatid cohesion-establishing reaction. Curr. Biol. CB *19*, 492–497.

Takahashi, T.S., Basu, A., Bermudez, V., Hurwitz, J., and Walter, J.C. (2008). Cdc7-Drf1 kinase links chromosome cohesion to the initiation of DNA replication in Xenopus egg extracts. Genes Dev. *22*, 1894–1905.

Tanaka, K., Yonekawa, T., Kawasaki, Y., Kai, M., Furuya, K., Iwasaki, M., Murakami, H., Yanagida, M., and Okayama, H. (2000). Fission yeast Eso1p is required for establishing sister chromatid cohesion during S phase. Mol. Cell. Biol. *20*, 3459–3469.

Tanaka, K., Hao, Z., Kai, M., and Okayama, H. (2001). Establishment and maintenance of sister chromatid cohesion in fission yeast by a unique mechanism. EMBO J. *20*, 5779–5790.

Técher, H., Koundrioukoff, S., Azar, D., Wilhelm, T., Carignon, S., Brison, O., Debatisse, M., and Le Tallec, B. (2013). Replication dynamics: biases and robustness of DNA fiber analysis. J. Mol. Biol. *425*, 4845–4855.

Tedeschi, A., Wutz, G., Huet, S., Jaritz, M., Wuensche, A., Schirghuber, E., Davidson, I.F., Tang, W., Cisneros, D.A., Bhaskara, V., et al. (2013). Wapl is an essential regulator of chromatin structure and chromosome segregation. Nature *501*, 564–568.

Terret, M.-E., Sherwood, R., Rahman, S., Qin, J., and Jallepalli, P.V. (2009). Cohesin acetylation speeds the replication fork. Nature *462*, 231–234.

Tittel-Elmer, M., Lengronne, A., Davidson, M.B., Bacal, J., François, P., Hohl, M., Petrini, J.H.J., Pasero, P., and Cobb, J.A. (2012). Cohesin association to replication sites depends on rad50 and promotes fork restart. Mol. Cell *48*, 98–108.

Uhlmann, F., and Nasmyth, K. (1998). Cohesion between sister chromatids must be established during DNA replication. Curr. Biol. CB *8*, 1095–1101.

Uhlmann, F., Lottspeich, F., and Nasmyth, K. (1999). Sister-chromatid separation at anaphase onset is promoted by cleavage of the cohesin subunit Scc1. Nature *400*, 37–42.

Unal, E., Heidinger-Pauli, J.M., Kim, W., Guacci, V., Onn, I., Gygi, S.P., and Koshland, D.E. (2008). A molecular determinant for the establishment of sister chromatid cohesion. Science *321*, 566–569.

Vaur, S., Feytout, A., Vazquez, S., and Javerzat, J.-P. (2012). Pds5 promotes cohesin acetylation and stable cohesin-chromosome interaction. EMBO Rep. *13*, 645–652.

Waizenegger, I.C., Hauf, S., Meinke, A., and Peters, J.M. (2000). Two distinct pathways remove mammalian cohesin from chromosome arms in prophase and from centromeres in anaphase. Cell *103*, 399–410.

Wang, F., Yoder, J., Antoshechkin, I., and Han, M. (2003). Caenorhabditis elegans EVL-14/PDS-5 and SCC-3 are essential for sister chromatid cohesion in meiosis and mitosis. Mol. Cell. Biol. *23*, 7698–7707.

Wang, S.-W., Read, R.L., and Norbury, C.J. (2002). Fission yeast Pds5 is required for accurate chromosome segregation and for survival after DNA damage or metaphase arrest. J. Cell Sci. *115*, 587–598.

Watrin, E., Schleiffer, A., Tanaka, K., Eisenhaber, F., Nasmyth, K., and Peters, J.-M. (2006). Human Scc4 is required for cohesin binding to chromatin, sister-chromatid cohesion, and mitotic progression. Curr. Biol. CB *16*, 863–874.

Wendt, K.S., Yoshida, K., Itoh, T., Bando, M., Koch, B., Schirghuber, E., Tsutsumi, S., Nagae, G., Ishihara, K., Mishiro, T., et al. (2008). Cohesin mediates transcriptional insulation by CCCTC-binding factor. Nature *451*, 796–801.

Whelan, G., Kreidl, E., Wutz, G., Egner, A., Peters, J.-M., and Eichele, G. (2012). Cohesin acetyltransferase Esco2 is a cell viability factor and is required for cohesion in pericentric heterochromatin. EMBO J. *31*, 71–82.

Ye, T., Krebs, A.R., Choukrallah, M.-A., Keime, C., Plewniak, F., Davidson, I., and Tora, L. (2011). seqMINER: an integrated ChIP-seq data interpretation platform. Nucleic Acids Res. *39*, e35.

Zhang, J., Shi, X., Li, Y., Kim, B.-J., Jia, J., Huang, Z., Yang, T., Fu, X., Jung, S.Y., Wang, Y., et al. (2008a). Acetylation of Smc3 by Eco1 is required for S phase sister chromatid cohesion in both human and yeast. Mol. Cell *31*, 143–151.

Zhang, Y., Liu, T., Meyer, C.A., Eeckhoute, J., Johnson, D.S., Bernstein, B.E., Nusbaum, C., Myers, R.M., Brown, M., Li, W., et al. (2008b). Model-based analysis of ChIP-Seq (MACS). Genome Biol. *9*, R137.

Zuin, J., Franke, V., van Ijcken, W.F.J., van der Sloot, A., Krantz, I.D., van der Reijden, M.I.J.A., Nakato, R., Lenhard, B., and Wendt, K.S. (2014). A cohesin-independent role for NIPBL at promoters provides insights in CdLS. PLoS Genet. *10*, e1004153.